CHAPTER 4: TEST RESULTS AND DISCUSSION

4.1 Introduction

The results obtained from the experiments of the nine tested slabs are discussed in this chapter. All slabs had the same cross section, concrete cover, average cube compressive strength, diameter of tension reinforcement, reinforcement percentage, and loading arrangement. The investigated parameters were: length of the lap splice, confinement at the splice zone, effect the debonding of bars in the splice zone, and effect of applying repeated loading. The results obtained from tests are presented in Figures (4-1) to (4-78) and Tables (4-1) to (4-7). The spliced bars in seven slabs were provided with heads at the ends .The slabs were classified according to the studied variables into four groups. In Group 1, the effect of lap splice length was studied. The effect of confinement at the splice zone on the behavior of lap splices was studied in Group 2, while in Group 3, effect of the debonding of bars in the splice zone is investigated. In Group 4, effect of applying repeated cyclic loading on the behavior of slabs with lap splices was studied. Before testing, all slabs were painted with white paint to facilitate cracks detection and detailing the reinforcement layout within the lap zone was drawn on the surface of the slabs to facilitate the interpretation of the cracking behavior and recording the position and propagation of cracks.

4.2 Group 1: Effect of Lap Splice Length

Four slabs were tested to study the effect of lap splice length: Slab **AS-1** was without splices. Slab **AS-2** with 45 d_b lap splice length (450 mm) was without head for the spliced bars. In the case of headed bars, slab **AS-3** was with 15 d_b lap splice length (150 mm) and slab **AS-7** was with 27 d_b lap splice length (270 mm).

4.2.1 Crack Patterns and Mode of Failure

For the reference slab **AS-1**, with no splice, flexural cracks appeared at the constant moment zone at a load of 30 kN (about 55% of the ultimate load; P_u). As the load was increased, flexural cracks propagated upward towards the compression zone. Yield of bottom longitudinal steel occurred at a load of 50 kN (about 91% of the ultimate load; P_u), with load increase, cracks became wider and extended upward to about 95% of the slab height and increased along the span to cover the constant moment zone. Failure of the slab occurred by crushing of compression zone at a load of 55 kN, as shown in Figure (4-1).

For specimens with lap splice, the first crack within the lap zone occurred along the line of heads at each end of the lap. Cracks of slabs were marked at each load increment up to failure. Figures (4-2) to (4-5) show the crack patterns of slabs **AS-2**, **AS-3**, and **AS-7** respectively.

For slab **AS-2**, with 45 d_b lap splice length (450 mm) and without any special reinforcement at lap splice zone, the spliced bars were without head, flexural cracks initiated at the constant moment zone at a load of 25 kN (about 46% of the ultimate load; P_u). As the load was increased, flexural cracks appeared at the lap-splice zone at a load of 35 kN (about 64% of the ultimate load; P_u). As the load was increased, flexural cracks propagated upward towards the compression zone. With the load increase, cracks became wider and extended upward to about 97% of the slab height and extended along the span to cover all the constant moment zone. Yielding of bottom longitudinal tension steel occurred at a load of 52.5 kN (about 96%

of the ultimate load; P_u). Failure of the slab occurred by crushing of concrete in compression at a load of 55 kN, as shown in Figure (4-2).

Slab **AS-3**, with 15 d_b lap splice joint provided with headed bars (150 mm) and without any special reinforcement at the splice area, flexural cracks initiated at the constant moment zone at a load of 15 kN (about 35% of the ultimate load; P_u). As the load was increased, flexural cracks formed and appeared along the position of the heads at each end of the lap-spliced bar at a load of 20 kN (about 47% of the ultimate load; P_u). As the load was increased, cracks propagate further across the length of the lap zone and flexural cracks propagated upward towards the compression zone. With load increase, cracks became wider and extended upward to about 97% of the slab thickness and spread along the span to cover the constant moment zone. No yield of steel reinforcement was recorded at the bottom longitudinal steel bars up to failure. Failure of the slab was a brittle one with failure of bond between concrete and the bars with pushing down the bottom cover causing the brittle failure at a load of 42.5 kN. According to ACI 318-14, the calculated development length for spliced bars with head is 15 d_b as the length used in slab **AS-3**. The results indicate that this splice length is not sufficient for developing the forces in the bars. Figures (4-3) and (4-4) show the crack pattern and failure at the lap splice joint in slab **AS-3**, respectively.

For slab **AS-7**, with 27 d_b lap splice length (270 mm) as recommended by Yassin[28] for headed deformed bar in wide beams. No confinement at lap splice connection zone was introduced. Flexural cracks initiated at the constant moment zone at a load of 25 kN (about 42% of the ultimate load; P_u). As the load was increased, flexural cracks appeared at the lap-splice zone at a load of 27.5 kN (about 46% of the ultimate load; P_u) and appeared close to position of the head of the spliced bar at a load of 37.5 kN (about 63% of the ultimate load; P_u). As the load was increased, flexural cracks propagated upward to the compression zone and cracks became wider extending upward to about 97% of the slab thickness in the constant moment zone. Yielding of bottom longitudinal tension steel occurred at a load of 48 kN (about 80% of the ultimate load; P_u). Failure of the slab occurred by flexure at a load of 60 kN.

Figure (4-6) shows the first cracking load and lap splice length for the slabs in Group (1). In slabs, **AS-2** and **AS-7** the first crack appeared at a load 17% less than that of the reference slab without splice. While slab **AS-3**, the first crack appeared at a load 50% of reference slab **AS-1** due to small length of the splice.

4.2.2 Ultimate Load

Figure (4-7) shows the failure load and lap splice length of the tested slabs **AS-1**, **AS-2**, **AS-3**, and **AS-7**. The failure loads were 55, 55, 42.5, and 60 kN respectively. Slabs **AS-2**, **AS-3**, and **AS-7** achieved ultimate load of 100%, 77%, and 109%, of that of slab **AS-1** respectively. The results indicate that the failure load of slab **AS-7** (with headed bar and lap splice length = 27 d_b) increased by 9% of that of the reference specimen **AS-1** (without splice). Using lap length of 45 d_b in slab **AS-2** (without headed bars) did not cause a reduction in the failure load comparing with the reference specimen **AS-1**. With a further reduction in lap splice length to 15 d_b (slab **AS-3**) the failure load reduced to 23% the failure load of the reference specimen **AS-1**. The theoretical ultimate load was calculated according to the Egyptian code ECP (203-2007), considering the actual material properties; f_y, f_{cu} and taking the reduction factors as unity, and it is equal to 41.5 kN. Figure (4-8) shows the relation between the ratio of experimental ultimate (failure) load to the calculated ultimate load and lap splice length.

According to test results, increasing lap splice from 15 d_b in slab **AS-3** to 27 d_b in slab **AS-7** with headed bars in lap splice increased the ultimate load value by 41%.

4.2.3 Load – Deflection Relationship

Figure (4-9) shows the relationship between the applied load and mid-span deflection (dial No.2) of the tested slabs **AS-1**, **AS-2**, **AS-3**, and **AS-7**, while Table (4-2) contains the values of the measured deflection at mid-span of these slabs. As shown in Table (4-2), the maximum-recorded deflection at mid span of slab **AS-3** at failure was less than of those of the other slabs in this group due to small lap splice length (15 d_b). At failure load, the maximum deflection at mid-span of slab **AS-7** (with 27 d_b lap splice) was about 360% higher than that of slab **AS-3** (with 15 d_b lap splice). As shown in Fig (4-9), the load deflection curve for slab **AS-1** (without splice) was close to that of slab **AS-2** (with 45 d_b lap splice) while slab **AS-7** (with 27 d_b lap splice) showed higher values of deflection. However, the behavior of slab **AS-3** was less ductile than other slabs **AS-1**, **AS-2** and **AS-7**. These results indicate that increasing lap splice from 15 d_b in slab **AS-3** to 27 d_b in slab **AS-7** caused an increase of the maximum deflection at failure.

Figures (4-10) and (4-11) show the relationship between the applied load and deflection under the left and right concentrated load respectively, for the tested slabs in this group. The behavior at these two positions was almost the same as that at the mid- span.

4.2.4 Ductility and Strain Energy

Most researches used maximum deflection at mid- span as a measure for ductility. Figure (4-12) shows the maximum deflection at failure load and lap splice length for the slabs in this group. Slabs **AS-2**, **AS-3**, and **AS-7** achieved maximum deflection at failure load of 81%, 60%, and 217% of that of the reference slab **AS-1** respectively. The area under the load-deflection curve is termed strain energy or toughness. It was calculated and plotted to measure the maximum energy absorbed by the tested slabs. Figure (4-13) shows the relation between strain energy and lap splice length. The strain energy achieved by the tested slabs was 1.748, 1.423, 0.696, and 4.255 kN.m for slabs **AS-1**, **AS-2**, **AS-3**, and **AS-7** respectively. One can conclude that the use of lap splices without headed bars and with length of 45 d_b (slab **AS-2**) gave close results to those of the reference slab **AS-1**, but slab **AS-3** (with 15 d_b lap splice) showed reduction in strain energy while slab **AS-7** (with 27 d_b lap splice) showed higher strain energy than the reference slab **AS-1**.

4.2.5 Steel Strains

Steel strains were measured at several locations within the lap splice zone. Figure (3-11-a) shows the distribution of strain gauges in tested specimens. For slab **AS-1** (without splice), yield occurred near mid span (gauge B) at 50 kN (about 91% of the ultimate load; P_u) and at gauge A at 53 kN (about 96% of the ultimate load; P_u) as shown in Fig (4-14). While for slab **AS-2** with 45 d_b lap splice length (without head), yield occurred at the position of start lap splice (gauge C) at 52.5 kN (about 96% of the ultimate load; P_u) as shown in Fig (4-15). No yield was recorded in slabs **AS-3** and **AS-7** with different splice lengths as shown in Figs (4-16) and (4-17). It should be noted that strains in these slabs were measured at both mid-length of splice (gauge B), and at end of splice near head (gauge A), while gauge C was placed at start of splice. This indicates that the force carried by the spliced bar is maximum at the start of the splice length then reduced to about half of its value at mid-length of splice. For gauge C in slab **AS-7** no reading was recorded on the strain and it may be damaged during casting or during welding the wires to strain gauge. Figures (4-21) to (4-23) show the relation between

steel strains and strain positions along the splice zone of slabs **AS-1**, **AS-2** and **AS-3** respectively.
For slab **AS-1,** at failure load, strain reading of gauge A equals to 92% of that of gauge B. For slab **AS-2**, at failure load, strain reading of gauge A equals to 8% of that of gauge C. For slab **AS-3**, at failure load, strain reading of gauge A and B equal to 12% and 67% of that of gauge C, respectively.

4.3 Group 2: Effect of using confinement in the splice zone

This group consisted of four slabs: Slab **AS-1** was a reference slab without splices, slab **AS-3** had a splice of length 15 d_b while the other two slabs **AS-5** and **AS-6** had a splice of length 15 d_b but with a confinement of the splice zone. Slab **AS-5** was confined with two transverse embedded beams perpendicular to the splice zone, as shown in Fig. (3-7-a), while in slab **AS-6**, circular spiral stirrups around spliced bars were applied, as shown in Fig. (3-7-b).

4.3.1 Crack Patterns and Mode of Failure

Cracks of slabs were traced and marked at each load increment up to failure. Figures (4-24) to (4-27) show the crack patterns and shape of failure of slabs **AS-5**, and **AS-6** respectively.

Slab **AS-5**, confined with two transverse embedded beams at splice zone, first flexural crack appeared at the constant moment zone outside edge of the embedded beams, and extend to the head of the spliced bar at a load of 32.5 kN (about 52% of the ultimate load; P_u). As the load was increased, cracks initiated outside of the lap zone at a location close to transverse embedded beams, and flexural cracks propagated toward the compression zone. First crack inside the lap zone initiated near from the heads and at the bottom of the transverse embedded beams at a load of 47.5 kN (about 76% of the ultimate load; P_u). Figure (4-24) shows the crack patterns of slab **AS-5**. With load increase, the longitudinal cracks formed outside the end of the lap zone. This type of cracks did not propagate between transverses embedded beams in the lap zone, as cracks propagated and formed just outside of the lap zone. These cracks became wider and extended to cover the constant moment zone. Yield of bottom longitudinal steel occurred at a load of 48 kN (about 77% of the ultimate load; P_u). Failure of the slab occurred by crushing of concrete in compression zone at load of 62.5 kN. Figure (4-25-a) shows crushing of compression zone just after this load and Fig (4-25-c) shows the shape of slab **AS-5,** after testing and removal of the concrete cover around the embedded beam in lap zone.

For slab **AS-6**, confined with circular spiral stirrup around the lap splice joint, flexural cracks appeared in the constant moment zone and near the head of the spliced bar at a load of 32.5 kN (about 50% of the ultimate load; P_u). As the load was increased, the first cracking in the lap zone initiated near the heads and close to the edge of the spiral stirrup around lap splice. This behavior was observed in slab **AS-5** in this group; and flexural cracks propagated upward to the compression zone. Then with the gradual increased of load, additional transverse cracks outside of the lap zone were formed. Only one crack appeared between opposing headed bars in lap zone. Just before failure, some cracks formed within the lap zone. These cracks became wider and extended in the lap zone. Yield of bottom longitudinal steel occurred at a load of 57.5 kN (about 88% of the ultimate load; P_u). Failure of the slab occurred by crushing of concrete in compression zone at load of 65 kN. Figure (4-26) shows the crack patterns of slab **AS-6,** and Fig (4-27) shows the photos of slab **AS-6,** after testing and removing the bottom cover over circular spiral stirrup in the lap zone. Figure (4-26-c) shows the cracks in the lap zone with no splitting after the occurrence of excessive deflection.

Figure (4-28) shows the cracking load of this group. Slab **AS-1**, reference specimen without splice, had first flexural cracking load at 30 kN. Slab **AS-3**, without confinement in lap splice zone, had first cracking load at 15 kN. For slabs, **AS-5,** and **AS-6** had first cracking load at 30 kN, and 25 kN respectively. This indicates that confinement of the lap splice delayed the cracking of the slabs.

4.3.2 Ultimate Load

Figure (4-29) shows the failure load and effect of confinement in lap splice zone of the tested slabs in this group. The failure loads of slabs **AS-3**, **AS-5**, and **AS-6** were 42.5, 62.5, and 65 kN respectively. These slabs achieved ultimate load of 77%, 114%, and 118%, respectively, of that of slab **AS-1** (reference slab). These results indicate that the failure load of slab **AS-3** (without confinement) was reduced by only 23% of that of the reference slab **AS-1**. Using confinement with embedded beams around the bar heads for slab **AS-5**, and spiral stirrups around lap splice for slab **AS-6**, respectively increased the failure load by 14%, and 18% than that of the reference slab **AS-1**, respectively. Figure (4-30) shows the relation between the ratios of experimental ultimate (failure) load to the calculated ultimate load (calculated as 41.5kN). Slab **AS-3**, without confinement at lap splice zone, showed 2.4% increase in its ultimate load than the calculated value, while for slab **AS-5** confined with embedded beams around the bar heads, the ultimate load was higher than the calculated value by 51%. For slab **AS-6** confined with spiral stirrups around lap splice zone, the ultimate load was higher than the calculated value by 57%. This indicates that confinement of the lap splice improved the load capacity of the slabs.

4.3.3 Load – Deflection Relationship

Figure (4-31) shows the relationship between the applied load and mid-span deflection for the tested slabs **AS-1**, **AS-3**, **AS-5**, and **AS-6**, while Table (4-2) contains the values of the measured deflection at mid-span of these slabs. At any load level, the recorded deflection at mid-span of slabs provided with confinement at the splice zone was less than that of slab **AS-3** without confinement.

Figures (4-32) and (4-33) show the relationship between the applied load and deflection under the point of the left and right concentrated load respectively, for the tested slabs **AS-1**, **AS-3**, **AS-5**, and **AS-6**. The behavior of these tested slabs at the two positions was almost the same as that at the mid- span point.

4.3.4 Ductility and Strain Energy

Figure (4-34) shows the maximum deflection at mid-span at failure load and effect of confinement in the lap splice zone. Slabs **AS-3**, **AS-5**, and **AS-6** achieved maximum deflection at failure load of 60%, 362%, and 241% respectively of that of slab **AS-1** (reference slab). The area under the load-deflection curve is calculated and plotted to measure the maximum energy absorbed by these slabs. Figure (4-35) shows the values of the calculated strain energy. Strain energy achieved by the tested slabs was 1.748, 0.696, 7.229, and 4.956 kN.m for slabs **AS-1**(reference slab), **AS-3**, **AS-5**, and **AS-6** respectively. One can conclude that strain energy absorbed by the slab, increased when the confinement in the splice zone was provided.

4.3.5 Steel Strains

As mentioned before, steel strains were measured at four locations for slab **AS-3** as shown in Figure (3-11-a-iii) and Fig. (3-11-a-iv) for slabs **AS-5**, and **AS-6**, respectively. No yield was recorded in slabs **AS-3** (without confinement). While for slabs **AS-5** (confined with

embedded beams around the bar heads) and slab **AS-6** (confined with a spiral stirrups around lap splice) yielding was recorded at the start of splice (gauge C) at 48 kN (77% of ultimate load; P_u) and at 57.5 kN (88% of ultimate load; P_u). Also, for slab **AS-6** yield was recorded near the head (gauge A) at 62.5 kN (about 96% of ultimate load; P_u) as shown in Figures (4-16), (4-36) and (4-37) respectively. It should be noted that reading of strain gauge C in slab **AS-3** (without confinement) was comparable for reading of strain gauge C in another specimens with confinement in lap splice zone. For specimens **AS-6**, no reading was recorded for strain gauge S in stirrups it may be damaged during casting. Figures (4-36) to (4-39) show load-steel strains relationship of slabs in this group. Figures (4-40), and (4-41) show the relation between steel strains and strain positions along the splice zone of slabs **AS-5**, and **AS-6** respectively. For slab **AS-6**, at failure load, strain reading of gauge A was equal to 63% of that of gauge C.

4.4 Group 3: Effect of debonding

Only one slab was tested to study the role of the head in lap splice by eliminating the bond of the bars within the lap joint. Slab **AS-4**, provided with headed bars and 15 d_b lap splice length (150 mm). The bond between concrete and steel bars in the splice zone was eliminated by wrapping an elastic tape around the bars in this zone. For slab **AS-3** with headed bars 15 d_b lap splice length (150 mm) and bonded lap splice was compared with slab **AS-4**.

4.4.1 Crack Patterns and Mode of Failure

Cracks of slabs were marked at each load increment up to failure. Figures (4-3) and (4-43) show the crack patterns of slabs **AS-3** and **AS-4** respectively. Crack patterns for slab **AS-3** was previously discussed in section 4.2.1.

For slab **AS-4**, with debonded headed bars in the splice zone, 15 d_b lap splice length (150 mm) and with no confinement at lap zone , flexural cracks appeared at the constant moment zone near the head of the spliced bar at a load of 12.5 kN (about 31% of the ultimate load; P_u). This value was less than that recorded in the bonded specimen **AS-3**. The width of cracks was much wider than the bonded specimen (**AS-3**). Transverse cracking in the slab (**AS-4**) occurred close to the position of the bar head. Distinct longitudinal cracks formed between two sets of opposing heads. These cracks appeared at a load of 37.5 kN (about 94% of the ultimate load; P_u). Cracking around the heads of bonded slabs was more propagation at the lap zone with indications of bond stress between headed bars and the surrounding concrete. This behavior was not evident in the debonded slab (**AS-4**) because there was no contribution from bond. As the load was increased, flexural cracks propagated upward towards the compression zone. With the load increase, cracks along the line of heads at each end of the lap became wider and extended upward to about 97% of the slab height and covered the lap zone. No yield was recorded in the tension steel up to failure. Failure of the slab was a brittle (pushed down the bottom cover by the heads of bars and cover separated from the slab) at a load of 40 kN, as shown in Fig (4-43). Figure (4-44) shows the first cracking load for the slabs in Group (3).

4.4.2 Ultimate Load

Figure (4-45) shows the failure load for bonded and debonded lap splice zone of the tested slabs **AS-1**, **AS-3**, and **AS-4**, respectively .The failure loads of these slabs were 55.0, 42.5, and 40.0 kN respectively. Slabs **AS-3**, and **AS-4** achieved a load of 77%, and 73%, respectively, of that of slab **AS-1**(reference slab). Figure (4-46) shows the ratio of

experimental ultimate (failure) load to the calculated ultimate load for bonded, debonded splice bar in slabs in this group. Slab **AS-3**, showed 2.4% increase in its ultimate load above the calculated value, while for slab **AS-4** with debonding in the lap splice zone, a 3.6% reduction in its ultimate load below the calculated value was obtained .This indicates the role of head in transferring the bar force in the spliced bars.

4.4.3 Load – Deflection Relationship

Figure (4-47) shows the relationship between the applied load and mid-span deflection of the tested slabs **AS-1**, **AS-3**, and **AS-4**, respectively, while Table (4-2) contains the values of the measured deflection at mid-span of these slabs. The maximum-recorded deflection at mid span of slab **AS-4** at failure was about 58% of that of slab **AS-3**. These results indicate that the elimination of bond in the lap splice zone decreased the maximum deflection at failure load and decreased the ductility and the lap splice joint, with a brittle failure in this case.
Figures (4-48) and (4-49) show the relationship between the applied load and deflection under the left and right concentrated load respectively for the tested slabs **AS-3**, and **AS-4**.

4.4.4 Ductility and Strain Energy

Figure (4-50) shows the maximum deflections at mid-span at failure load of the slabs of this group. Slabs **AS-3**, and **AS-4** achieved maximum deflection at failure load equal to 60%, and 35% respectively of that of slab **AS-1** (reference slab). The area under the load-deflection curve is calculated and plotted to measure the maximum energy absorbed by these slabs. Figure (4-51) shows strain energy for the slabs in this group. The strain energy achieved by the tested slabs was 0.696, and 0.412 kN.m for slabs **AS-3**, and **AS-4** respectively. One can conclude that strain energy that can be absorbed by the slab decreased when debonding at the splice zone was used and the behavior is brittle.

4.4.5 Steel Strains

As mentioned before, steel strains were measured at four locations for slab **AS-3** and slab **AS-4** as shown in Figure (3-11-a-iii). No yield was recorded in slabs **AS-3**, and **AS-4** as shown in Figs. (4-16) and (4-52). It should be noted that, the force carried by the spliced bar is maximum at the start of the splice length then reduced to about half of its value at mid-length of splice. Figures (4-53) to (4-56) show load-steel strains relationship of slabs in this group. Figures (4-23) and (4-57) show the relation between steel strains and strain positions along the splice zone of slabs **AS-3**, and **AS-4** respectively. For slab **AS-3,** at failure load, strain reading of gauges A and B equal to 12% and 67% of that of gauge C, respectively. For slab **AS-4**, at failure load, strain reading of gauges A and B equal to 13% and 76% of that of gauge C, respectively. This behavior was not expected for slab **AS-4** with debonded bars in the lap splice zone, because the expected distribution of strain along the splice length is uniform, this may be due to improper installation of strain gauge.

4.5 Group4: Effect of applying repeated loading

In this group, the effect of applying repeated cyclic loading on two specimens, with confinement in the splice zone was studied. Slab **AS-8** was confined with embedded beams around the bar heads with the same details for slab **AS-5**, and slab **AS-9** was confined with circular spiral stirrups around spliced bars similar to slab **AS-6**. All specimens in this group had the same lap splice length (15 d_b = 150 mm).The main objective of this group was to examine the integrity of lap splice joint and the ability of the lap splice joint to maintain its strength when subjected to repeated loading. The load was increased gradually in cycles. At the end of each cycle, the load was removed completely, then another load cycle was started

by increasing the loading again. Figures (4-65) and (4-66) show the load cycles for slabs **AS-8** and **AS-9** respectively.

4.5.1 Crack Patterns and Mode of Failure

Cracks of slabs were marked with different colors at each load increment up to failure. Figures (4-58) and (4-60) show the crack patterns of slabs **AS-8**, and **AS-9** in all cycles respectively.

Slab **AS-8** confined with embedded beams around the bar heads, with the same details of slab **AS-5** and the applied loads were repeated up to failure. Flexural crack appeared in the first cycle at a load of 20 kN (about 33% of the ultimate load; P_u) at the constant moment zone, near the leg of the transverse stirrups cage of the embedded beam located at the head. In the second cycle, the crack occurred near at the other head in the lap zone at a load of 25 kN (about 42% of the ultimate load; P_u) and began to extend transversely near the edge of the embedded beam. In the third cycle, the cracks were extended outside the embedded beams at a load of 30 kN (about 50% of the ultimate load; P_u). With increase the applied repeated cycles, the cracks initiated outside the lap zone at a location close to embedded beams. At the seventh cycle, cracks were extensive and adjacent to the right and left of the embedded beam. Also, at the seventh cycle, yield of longitudinal headed bars occurred at a load of 42.5 kN (about 71% of the ultimate load; P_u). During removing the applied load, width of some cracks decreased. In the eighth cycle, the cracks parallel to the embedded beams also became wider with load increase, after this cycle, flexural cracks propagated upward to the compression zone. Failure of the slab occurred in the tenth cycle by crushing of concrete in compression zone at load of 60 kN. Figure (4-58) shows crack patterns of slab **AS-8**, and Fig. (4-59) shows the shape of slab **AS-8** after testing and removing the cover over the embedded beams.

For slab **AS-9**, provided with circular spiral stirrups around the lap splice, with the same reinforcement details of slab **AS-6** but with repeated loading up to failure. Flexural crack appeared at the constant moment zone adjacent of the end of circular spiral stirrup in the first cycle at a load of 25 kN (about 37% of the ultimate load; P_u). In the second cycle, the cracks occurred outside the confined zone and extended up ward at a load of 27.5 kN (about 40% of the ultimate load; P_u). In the third cycle, cracks began to form near the head of bars at the bottom of the specimen at a load of 30 kN (about 44% of the ultimate load; P_u). In the fourth cycle, cracks appeared and extended within the lap zone on the side face of the specimen at a load of 40 kN (about 59% of the ultimate load; P_u). With applying repeated cycles, the cracks formed and initiated outside of the lap zone close to the end of the spiral stirrups. Also, some cracks started near the head of the bar. In the fifth cycle, yield in longitudinal headed bars occurred at a load of 50.7 kN (about 75% of the ultimate load; P_u).The behavior of this specimen was similar to that of slab **AS-8** provided with embedded beams around the bar heads. In the sixth cycle, flexural cracks propagated upward to the compression zone. Failure of this slab occurred by crushing of concrete in compression zone at load of 68 kN. Figure (4-60) shows the crack patterns of slab **AS-9**, and Fig. (4-61) shows the shape of slab **AS-9**, after testing and removing the concrete cover of the spiral stirrups around the lap zone. It is clear that concrete inside the spiral stirrups zone was not damaged and concrete cover did not spilt off. Figure (4-62) shows the first cracking load for slabs in this group.

4.5.2 Ultimate Load

Figure (4-63) shows the failure load for the slabs in this group with confinement in lap splice zone. The failure loads of slabs **AS-1** (reference slab), **AS-3** (without confinement), **AS-5**, **AS-6**, **AS-8** and **AS-9** were 55.0, 42.5, 62.5, 65.0, 60.0, and 68.0 kN respectively. These slabs

achieved ultimate load of 77%, 114%, 118%, 109%, and 124%, respectively, of that of slab **AS-1** (reference slab). The results indicate that the failure load of slab **AS-3** (without confinement and monotonic loading) reduced by only 23% of that of the reference slab **AS-1**. While using the confinement in the lap splice joint for the specimens, **AS-5**, **AS-6** (with monotonic loading), and **AS-8**, **AS-9** (with repeated loading) increased the ultimate load but the cracks became wider and extensive outside of the confinement lap zone in the specimens **AS-8** and **AS-9** with applying repeated loading. Even though, when repeated loading was applied to slabs **AS-8** and **AS-9**, the ultimate load for these two slabs was higher by 9% and 24% than that of slab **AS-1** (reference slab) respectively. Figure (4-64) shows the ratio of experimental ultimate (failure) load to the calculated ultimate load (calculated as 41.5 kN) for the slabs in this group. Slab **AS-3**, without confinement in lap splice zone and monotonic loading, showed 2.4% increase in its ultimate load above the calculated value, while for slab **AS-5** confined with embedded beams around the bar heads and monotonic loading , the ultimate load was higher than the calculated value by 51%. While specimen **AS-8** with the same reinforcement details of slab **AS-5**, but with the application of repeated load, showed 45% increase in its ultimate load above the calculated value. For slab **AS-6** confined with the spiral stirrups around lap splice zone and monotonic loading, the ultimate load was higher than the calculated value by 57%. While specimen **AS-9** similar to slab **AS-6**, but with the application of repeated load, showed 64% increase in its ultimate load above the calculated value.

4.5.3 Load – Deflection Relationship

Figure (4-67) shows the relationship between the applied load and mid-span deflection of the tested slabs **AS-1**, **AS-3**, **AS-5**, **AS-6** (with monotonic loading), and **AS-8**, **AS-9** (subjected to repeated loading), while Table (4-2) contains the values of the measured deflection at mid-span of these slabs . At any load level, the recorded deflection at mid-span of slabs provided with confinement at the splice zone and subjected to repeated loading was less than that of slab **AS-3** without confinement and monotonic loading.

Figures (4-68) and (4-69) show the relationship between the applied load and deflection under the point of the left and right concentrated load respectively, for the tested slabs in this group. The behavior of these tested slabs at the two positions was almost the same as that at the mid-span point.

4.5.4 Ductility and Strain Energy

Figure (4-70) shows the maximum deflections at mid-span at failure load of the slabs of this group. Slabs **AS-3**, **AS-5**, **AS-6**, **AS-8**, and **AS-9** achieved maximum deflection at failure load equal to 60%, 362%, 241%, 318%, and 377% respectively of that of slab **AS-1** (reference slab). The area under the load-deflection curve is calculated and plotted to measure the maximum energy absorbed by these slabs. Figure (4-71) shows the relation between strain energy and confinement. Strain energy achieved by the tested slabs was 1.748, 0.696, 7.229, 4.956, 7.394, and 8.173 kN.m for slabs **AS-1** (reference slab), **AS-3** (without confinement), **AS-5**, **AS-6**, **AS-8**, and **AS-9** respectively. Specimens **AS-8** and **AS-9** were able to dissipate energy, exhibited good ductility, and showed almost stable hysteric loops. Even though the loading was cyclic one, but it can be concluded that strain energy by the slabs increased when using the confinement in the lap zone.

4.5.5 Steel Strains

As mentioned before, steel strains were measured at four locations for slab **AS-3** as shown in Figure (3-11-a-iii) and figure (3-11-a. iv) for slabs, **AS-5**, **AS-6**, **AS-8**, and **AS-9** respectively. Moreover, one strain gauge S was placed over the stirrup within the confinement splice zone

for slabs in this group. No yield was recorded in slabs **AS-3** (without confinement). While for slabs **AS-5** (confined with embedded beams around the bar heads) and slab **AS-6** (confined with spiral stirrups around lap splice) yielding was recorded at the start of splice (gauge C) at 48 kN (77% of ultimate load; P_u) and at 57.5 kN (88% of ultimate load; P_u), as shown in Figures (4-16), (4-36) and (4-37) respectively. For slab **AS-8** (confined with embedded beams around the bar heads and subjected to repeated loading) yielding was recorded in the seventh cycle at the start of splice (gauge C) at 42.5 kN (71% of ultimate load; P_u) and near the head (gauge A) just before failure at 59 kN (about 98% of the ultimate load; P_u) in the last cycle. While for slab **AS-9** (confined with circular spiral stirrups around lap splice and subjected to repeated loading) yielding was recorded in the fifth cycle at the start of the splice (gauge C) at 50 kN (74% of ultimate load; P_u) and near the head (gauge A) at 61 kN (about 90% of the ultimate load; P_u) in the fifth cycle near failure, as shown in figures (4-72) and (4-73) respectively. For specimens **AS-6**, and **AS-9** no reading was recorded for strain gauge S in stirrups as it may be damaged during casting. Figures (4-74) to (4-76) show load-steel strains relationship of slabs in this group. Figures (4-40) , (4-41), (4-77), and (4-78) show the relation between steel strains and strain positions along the splice zone of slabs **AS-5**, **AS-6**, **AS-8**, and **AS-9** respectively. For slab **AS-6**, at failure load, strain reading of gauges A equal to 63% of that of gauge C. For slab **AS-8**, at failure load, strain reading of gauges A equal to 56% of that of gauge C.

4.6 Conclusions

Nine reinforced concrete slabs of dimensions (2400 mm x 1000 mm x 120 mm) were tested to study the following variables:

1- Lap splices length,
2- Confinement at the lap splice zone,
3- Effect of the debonding in the splice zone,
4-Effect of applying repeated loading on the integrity of the lap joint.

From the results of the tested slabs, the following conclusions were drawn:

1. The use of lap splice with 100% cut off ratio, with lap length equals to 45 times bar diameter (i.e. close to the length recommended by Egyptian code ECP 203-2007), and without headed bars in the lap zone (Slab **AS-2**) resulted in a ductile flexural failure with the same ultimate load of the unspliced slab. The maximum deflection before failure load of such spliced slab was close to that of unspliced slab. Generally, this slab showed identical behavior that of the unspliced slab. The failure was ductile by with crushing concrete in compression zone and tension reinforcement steel reached yield.

2. The use of lap splice with 100% cut off ratio, with lap length 15 times bar diameter (i.e. the length recommended by ACI 318-14 for headed bars), and without any confining reinforcement in the lap spliced zone (Slab **AS-3**) resulted in a brittle failure (bottom split) with a reduction of the ultimate load by 23% compared with the unspliced slab. However, the failure load for this slab was higher than the calculated ultimate load of a slab without splices by 2% .The maximum deflection before failure load of such spliced slab was close to that of unspliced slab. The failure was brittle and tension reinforcement steel did not reach yield.

3. The use of headed bars in lap splice with 100% cut off ratio, with lap length 27 times bar diameter (i.e. 1.80 times the length recommended by ACI 318-14 for headed bars), and

without any confinement (Slab **AS-7**) resulted in a ductile flexural failure with an increase in the ultimate load by only 9% compared with the unspliced slab. The maximum deflection before failure load of spliced slab was higher by 217% than that of the reference slab. The tension steel reached yield at failure.

4. The use of headed bars in lap splice with 100% cut off ratio, and lap length 15 times bar diameter (i.e. The length recommended by ACI 318-14 for head bars), and with debonded bars in the lap spliced zone (Slab **AS-4**) resulted in a fewer number of surface cracks with greater width compared with the similar bonded specimen (Slab **AS-3**). Also, debonding resulted a loss of ductility. Due to the loss of bond contribution in transferring load in the spliced bars, the overall capacity reduced. However, the presence of head substituted the loss of bond and only a reduction 27% of ultimate load was recorded compared with the unspliced slab. The maximum deflection at failure load for debonded specimen was less than that of unspliced specimen by 65%. Generally, this specimen showed less ductility than of the unspliced specimen. The failure was brittle and tension reinforcement steel did not reach yield.

5. In slab **AS-5** with the lap splice length 15 times bar diameter, 100% cut off ratio, and provided with embedded beams around the bar heads, showed higher value of ultimate load when compared to the slab without confinement in lap zone and with the same lap splice length 15 times bar diameter (slab **AS-3**). The gain in ultimate strength was 47%. The concrete cover over the lap zone did not split off even after severe deflection was imposed to the specimen.

6. In slab **AS-6** with the lap splice length 15 times bar diameter, 100% cut off ratio, and provided with circular spiral stirrups around lap splice zone showed higher value of ultimate load when compared to the slab without confinement (slab **AS-3**). This confinement improved the ultimate strength, however, for this slab an increase in the failure load by 18% than that of slab **AS-1** (reference slab) and the ultimate strength increased by 53%, compared with the specimen without confinement (slab **AS-3**) . This type of confinement helped to improve the anchorage performance of the heads; also, increased the ability of the slab to absorb energy, and to sustain excessive deformations after yielding. The strain energy in this slab was greater than that of unspliced specimen (slab **AS-1**). However, the tension reinforcement steel in this slab reached yield at gauge C and gauge A.

7. Slabs **AS-8** and **AS-9** were able to dissipate energy, exhibited good ductility and showed almost stable hysteric loops. Also, the integrity of the lap joint was preserved during all the loading and unloading cycles. The strain energy for these slabs with repeated loading increased when confinement in the lap zone was used. For both slabs yield in the spliced occurred at both start of splice and at bar head. Mode of failure was ductile flexure failure with crushing of concrete in compression zone. However, the number and width of cracks for slab subjected to repeated loading was higher than those without repeated loading and subjected to monotonic loading.
8. Slabs **AS-6**, **AS-8** and **AS-9**, yield was recorded at the end of splice and near the head (gauge A) just before failure, this indicates the effect of confinement in the splice zone on developing very high strain values at bar head.

Table (4-1): Test Results

Specimen	Average concrete strength; f_{cu} (N/mm^2)	(L_o / d_b)	Special reinforcement in the lap zone	Loading	Debonding of lap bars	First crack load P_{cr},(kN)	First crack load at head P_{crh} (kN)	Yield load P_y,(kN)	Ultimate load P_u,(kN)	Strain Energy at failure load (kN.m)	Mode of failure
AS-1	34.7	No splice	----------	Monotonic	Bonded	30.0	-----	50.0	55.0	1.748	Ductile flexural failure
AS-2	36.7	45 (without headed bars)	----------	Monotonic	Bonded	25.0	-----	52.5	55.0	1.423	Ductile flexural failure
AS-3	37.0	15	----------	Monotonic	Bonded	15.0	20.0	NY	42.5	0.696	Brittle bottom cover split
AS-4	34.9	15	----------	Monotonic	Debonded	12.5	12.5	NY	40.0	0.412	Brittle bottom cover split
AS-5	35.9	15	Embedded beams	Monotonic	Bonded	30.0	32.5	48.0 *	62.5	7.229	Ductile flexural failure
AS-6	31.7	15	Spiral stirrups	Monotonic	Bonded	25.0	32.5	57.5	65.0	4.956	Ductile flexural failure
AS-7	42.1	27	----------	Monotonic	Bonded	25.0	37.5	48.0 *	60.0	4.255	Ductile flexural failure
AS-8	30.7	15	Embedded beams	Repeated loading	Bonded	20.0	20.0	42.5	60.0	7.394	Ductile flexural failure
AS-9	31.0	15	Spiral stirrups	Repeated loading	Bonded	25.0	30.0	50.7	68.0	8.173	Ductile flexural failure

L_o: lap splice length.
d_b: bar diameter.
p_{cr}: first visible flexural crack at mid-span.
p_{crh}: first visible flexural crack at head of spliced bar.
p_y: load at which spliced steel yields.
NY: no yield was recorded.
*: from load-deflection relationship figs. (4-9) & (4-32) for slabs AS-7 & AS-5 respectively.
Cut off ratio in all slabs was 100% except AS-1.
Transverse reinforcement in all slabs 5ϕ8/m.

Table (4-2): Values of measured deflection at mid-span for tested slabs

Specimen	Deflection at first crack load Δ_{cr},(mm)	Deflection at load of first crack at head Δ_{cr},(mm)	Deflection at yield load Δ_y,(mm)	Deflection at failure load Δ_u,(mm)	Δ_u/Δ_y	Strain Energy at failure load (kN.m)
AS-1	4.91	-----	12.98	38.25	2.95	1.748
AS-2	1.49	-----	20.27	30.91	1.53	1.423
AS-3	2.25	4.48	NY	23.05	-----	0.696
AS-4	0.72	0.72	NY	13.48	-----	0.412
AS-5	2.79	4.44	27.50	138.56	5.04	7.229
AS-6	3.62	10.06	38.65	92.0	2.38	4.956
AS-7	1.62	7.19	16.07	83.06	5.17	4.255
AS-8	2.01	2.01	12.45	121.45	9.76	7.394
AS-9	3.07	4.86	14.65	144.19	9.84	8.173

NY: no yield was recorded.

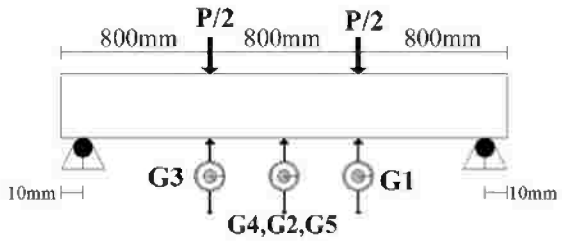

Dial gauges and transducers position.

Table (4-3): values of recorded strains for the tested slabs

Specimen	Strain (A)				Strain (B)				Strain (C)			
	strain at first crack load $\varepsilon_{cr}*10^{-6}$ (mm/mm)	strain at first crack load at head $\varepsilon_{crh}*10^{-6}$ (mm/mm)	strain at yield load ε_y*10^{-6} (mm/mm)	strain at failure load ε_u*10^{-6} (mm/mm)	strain at first crack load $\varepsilon_{cr}*10^{-6}$ (mm/mm)	strain at first crack load at head $\varepsilon_{crh}*10^{-6}$ (mm/mm)	strain at yield load ε_y*10^{-6} (mm/mm)	strain at failure load ε_u*10^{-6} (mm/mm)	strain at first crack load $\varepsilon_{cr}*10^{-6}$ (mm/mm)	strain at first crack load at head $\varepsilon_{crh}*10^{-6}$ (mm/mm)	strain at yield load ε_y*10^{-6} (mm/mm)	strain at failure load ε_u*10^{-6} (mm/mm)
AS-1	610	-----	1880	2280	650	-----	2180	2480	-----	-----	-----	-----
AS-2	130	-----	250	250	-----	-----	-----	-----	200	-----	2190	3310
AS-3	40	80	NY	190	120	310	NY	1080	120	420	NY	1620
AS-4	30	30	NY	180	60	60	NY	1060	100	100	NY	1400
AS-5	136	369	1051	1334	-----	-----	-----	-----	765	910	NR	>> ε_y
AS-6	56	436	1244	4248	-----	-----	-----	-----	52	576	2188	6776
AS-7	146	300	708	1548	-----	-----	-----	-----	267	NR	NR	>> ε_y
AS-8	133	133	1172	2233	-----	-----	-----	-----	442	442	2228	4007
AS-9	197	371	1265	>> ε_y	-----	-----	-----	-----	257	542	2261	>> ε_y

NY: no yield was recorded
NR: not recorded
ε_y = 2175*10 E-6
Gauges (A) and (E): located at the head
Gauge (B): located at mid length of splice
Gauge (C) and (D): located at the start of splice

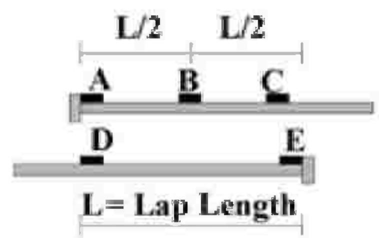

Strain gauge positions

Table (4-4): Results obtained from testing slabs in Group 1

Specimen	Average concrete strength; f_{cu}, (N/mm^2)	(L_d / d_b)	Special reinforcement in the lap zone	Loading	Debonding of lap bars	First crack load P_{cr},(kN)	First crack load at head P_{crh},(kN)	Yield load P_y,(kN)	Ultimate load P_u,(kN)	Strain Energy at failure load (kN.m)	Mode of failure
AS-1	34.7	No splice	———	Monotonic	Bonded	30.0	——	50.0	55.0	1.748	Ductile flexural failure
AS-2	36.7	45 (without headed bars)	———	Monotonic	Bonded	25.0	——	52.5	55.0	1.423	Ductile flexural failure
AS-3	37.0	15	———	Monotonic	Bonded	15.0	20.0	NY	42.5	0.696	Brittle bottom cover split and pullout of the bars at the joint
AS-7	42.1	27	———	Monotonic	Bonded	25.0	37.5	48.0 *	60.0	4.255	Ductile flexural failure

L_d: lap splice length.
d_b: bar diameter.
p_{cr}: first visible flexural crack at mid-span.
p_{crh}: first visible flexural crack at head of spliced bar.
p_y: load at which spliced steel yields.
NY: no yield was recorded.
*: from load-deflection relationship fig. (4-9) for slab AS-7.
Cut off ratio in all slabs was 100% except AS-1.
Transverse reinforcement in all slabs 5ϕ8/m.

Table (4-5): Results obtained from testing slabs in Group 2

Specimen	Average concrete strength; f_{cu}, (N/mm^2)	(L_o / d_b)	Special reinforcement in the lap zone	Loading	Debonding of lap bars	First crack load P_{cr},(kN)	First crack load at head P_{crh}, (kN)	Yield load P_y,(kN)	Ultimate load P_u,(kN)	Strain Energy at failure load (kN.m)	Mode of failure
AS-1	34.7	No splice	———	Monotonic	Bonded	30.0	——	50.0	55.0	1.748	Ductile flexural failure
AS-3	37.0	15	———	Monotonic	Bonded	15.0	20.0	NY	42.5	0.696	Brittle bottom cover split and pullout of the bars at the joint
AS-5	35.9	15	Embedded beams	Monotonic	Bonded	30.0	32.5	48.0 *	62.5	7.229	Ductile flexural failure
AS-6	31.7	15	Spiral stirrups	Monotonic	Bonded	25.0	32.5	57.5	65.0	4.956	Ductile flexural failure

L_o: lap splice length.
d_b: bar diameter.
p_{cr}: first visible flexural crack at mid-span.
p_{crh}: first visible flexural crack at head of spliced bar.
p_y: load at which spliced steel yields.
NY: no yield was recorded.
*: from load-deflection relationship fig. (4-31) for slab AS-5.
Cut off ratio in all slabs was 100% except AS-1.
Transverse reinforcement in all slabs 5ϕ8/m.

Table (4-6): Results obtained from testing slabs in Group 3

Specimen	Average concrete strength; f_{cu}, (N/mm^2)	(L_o / d_b)	Special reinforcement in the lap zone	Loading	Debonding of lap bars	First crack load P_{cr},(kN)	First crack load at head P_{crh}, (kN)	Yield load P_y,(kN)	Ultimate load P_u,(kN)	Strain Energy at failure load (kN.m)	Mode of failure
AS-1	34.7	No splice	———	Monotonic	Bonded	30.0	——	50.0	55.0	1.748	Ductile flexural failure
AS-3	37.0	15	———	Monotonic	Bonded	15.0	20.0	NY	42.5	0.696	Brittle bottom cover split and pullout of the bars at the joint
AS-4	34.9	15	———	Monotonic	Debonded	12.5	12.5	NY	40.0	0.412	Brittle bottom cover split and pullout of the bars at the joint

L_o: lap splice length.
d_b: bar diameter.
p_{cr}: first visible flexural crack at mid-span.
p_{crh}: first visible flexural crack at head of spliced bar.
p_y: load at which spliced steel yields.
NY: no yield was recorded.
Cut off ratio in all slabs was 100% except AS-1.
Transverse reinforcement in all slabs 5ϕ8/m.

Table (4-7): Results obtained from testing slabs in Group 4

Specimen	Average concrete strength; f_{cu}, (N/mm^2)	(L_o / d_b)	Special reinforcement in the lap zone	Loading	Debonding of lap bars	First crack load P_{cr},(kN)	First crack load at head P_{crh}, (kN)	Yield load P_y,(kN)	Ultimate load P_u,(kN)	Strain Energy at failure load (kN.m)	Mode of failure
AS-1	34.7	No splice	———	Monotonic	Bonded	30.0	——	50.0	55.0	1.748	Ductile flexural failure
AS-3	37.0	15	———	Monotonic	Bonded	15.0	20.0	NY	42.5	0.696	Brittle bottom cover split and pullout of the bars at the joint
AS-5	35.9	15	Embedded beams	Monotonic	Bonded	30.0	32.5	48.0 *	62.5	7.229	Ductile flexural failure
AS-6	31.7	15	Spiral stirrups	Monotonic	Bonded	25.0	32.5	57.5	65.0	4.956	Ductile flexural failure
AS-8	30.7	15	Embedded beams	Repeated loading	Bonded	20.0	20.0	42.5	60.0	7.394	Ductile flexural failure
AS-9	31.0	15	Spiral stirrups	Repeated loading	Bonded	25.0	30.0	50.7	68.0	8.173	Ductile flexural failure

L_o: lap splice length.
d_b: bar diameter.
p_{cr}: first visible flexural crack at mid-span.
p_{crh}: first visible flexural crack at head of spliced bar.
p_y: load at which spliced steel yields.
NY: no yield was recorded.
*: from load-deflection relationship fig. (4-32) for slab AS-5.
Cut off ratio in all slabs was 100% except AS-1.
Transverse reinforcement in all slabs 5ϕ8/m.

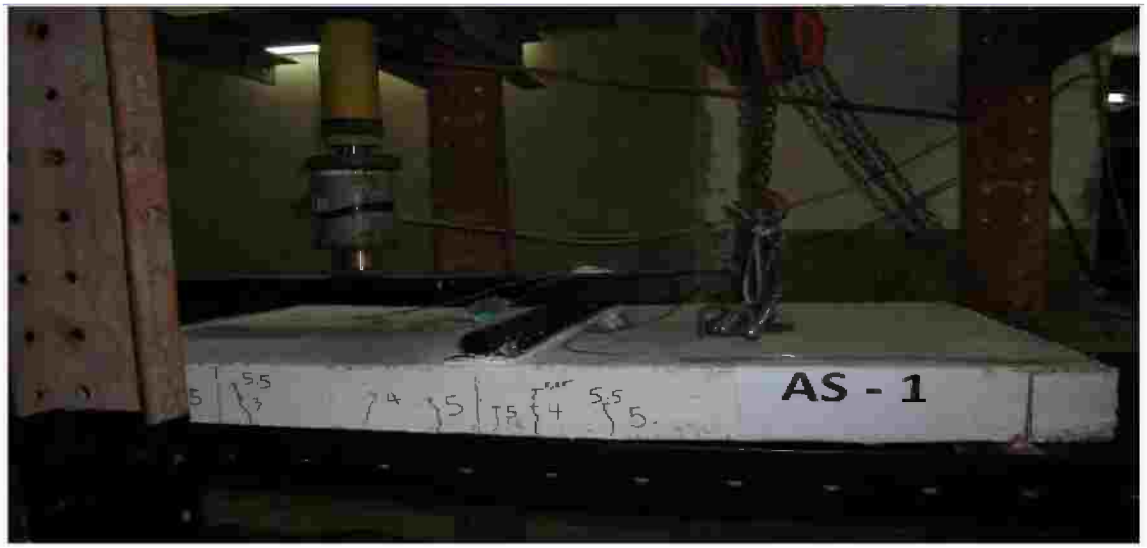

(a): Cracks on the side face at failure.

(b): Cracks on the bottom surface of slab at failure.

Figure (4-1): Crack patterns of **AS-1**(Reference specimen).

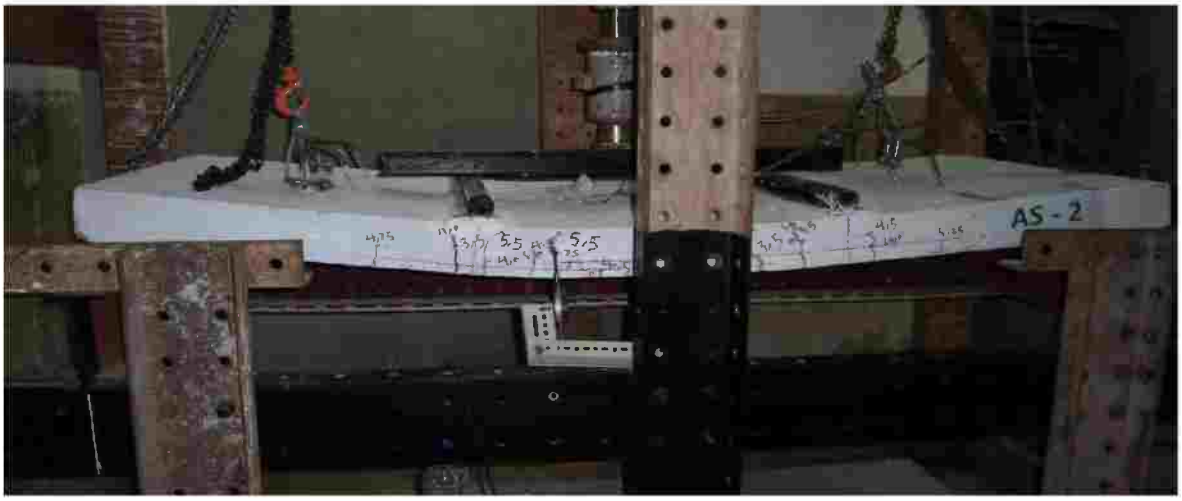

(a): Cracks on the side face at failure.

(b): Cracks close to the end of the lap zone.

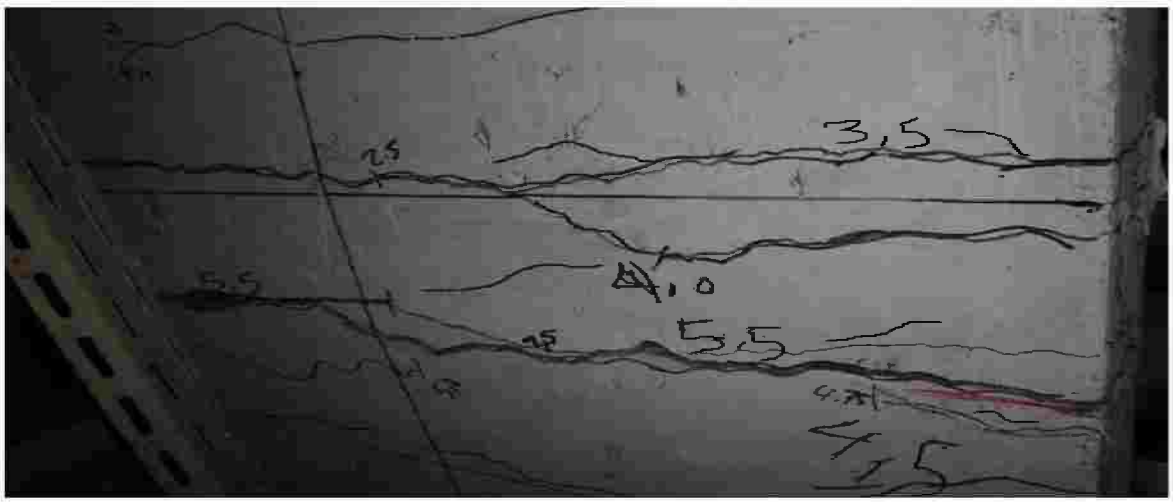

(c): Cracks on the bottom surface of slab inside and outside the lap zone at failure.

Figure (4-2): Crack patterns **AS-2**.

(a): Cracks on the side face.

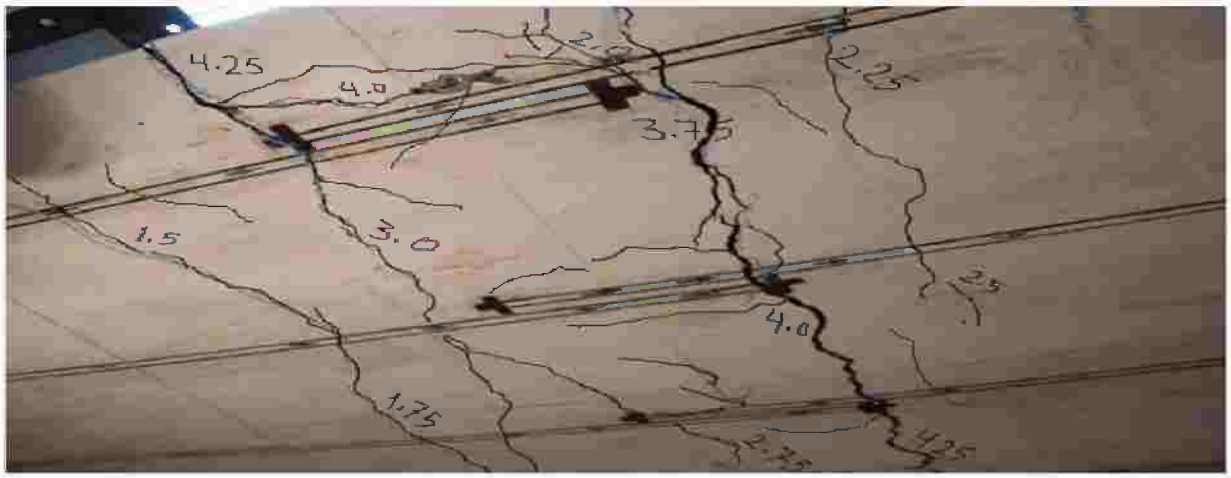

(b): Extensive cracks on the bottom surface of slab inside and outside the lap zone at failure.

(c): Wide cracks at failure of the slab **AS-3**.

Figure (4-3): The crack pattern of **AS-3**.

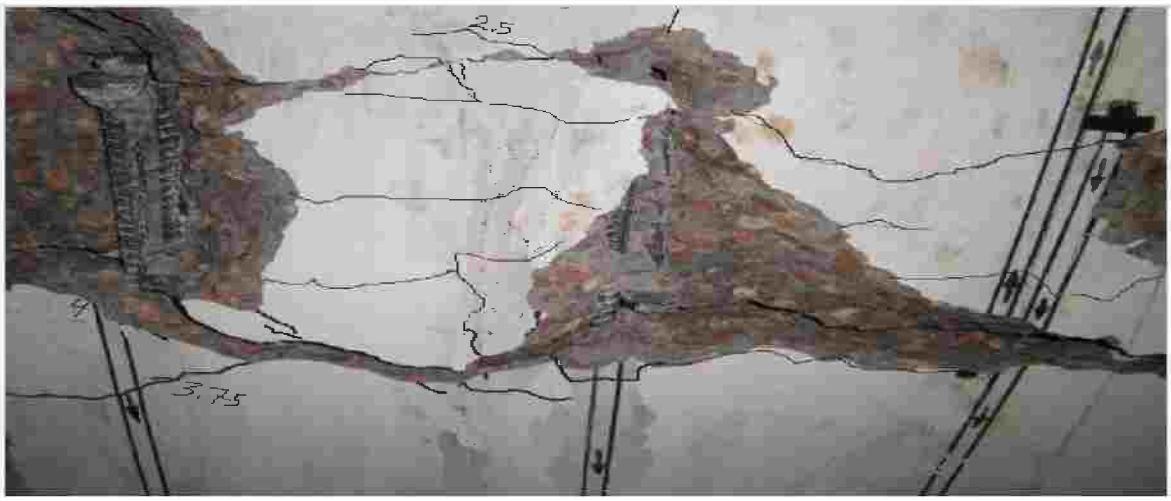

(a): Bottom cover spalling in lap zone just before failure.

(b): Specimen just after the failure.

(c): The specimen after failure.

Figure (4-4): Failure of the lap splice in slab **AS-3**.

(a): Cracks on the side face at failure.

(b): Cracks close to the end of the lap zone.

(c): Wide cracks on the bottom surface of slab inside and outside the lap zone at failure.

Figure (4-5): The crack pattern of **AS-7**.

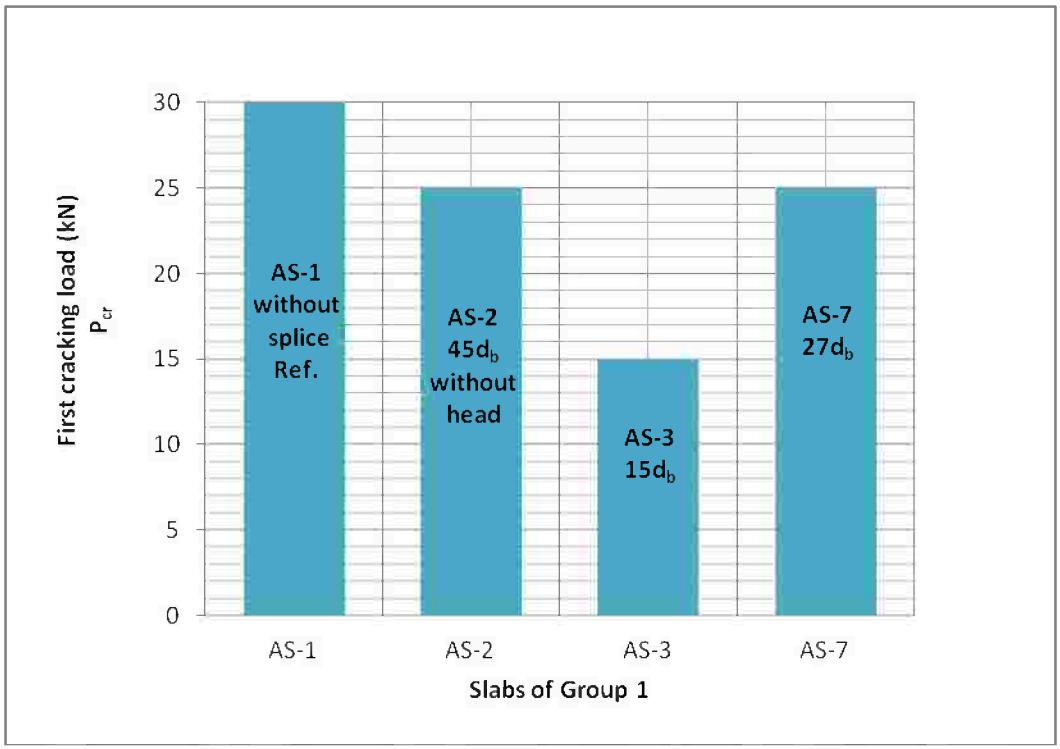

Figure (4-6): First cracking loads for slabs of Group (1).

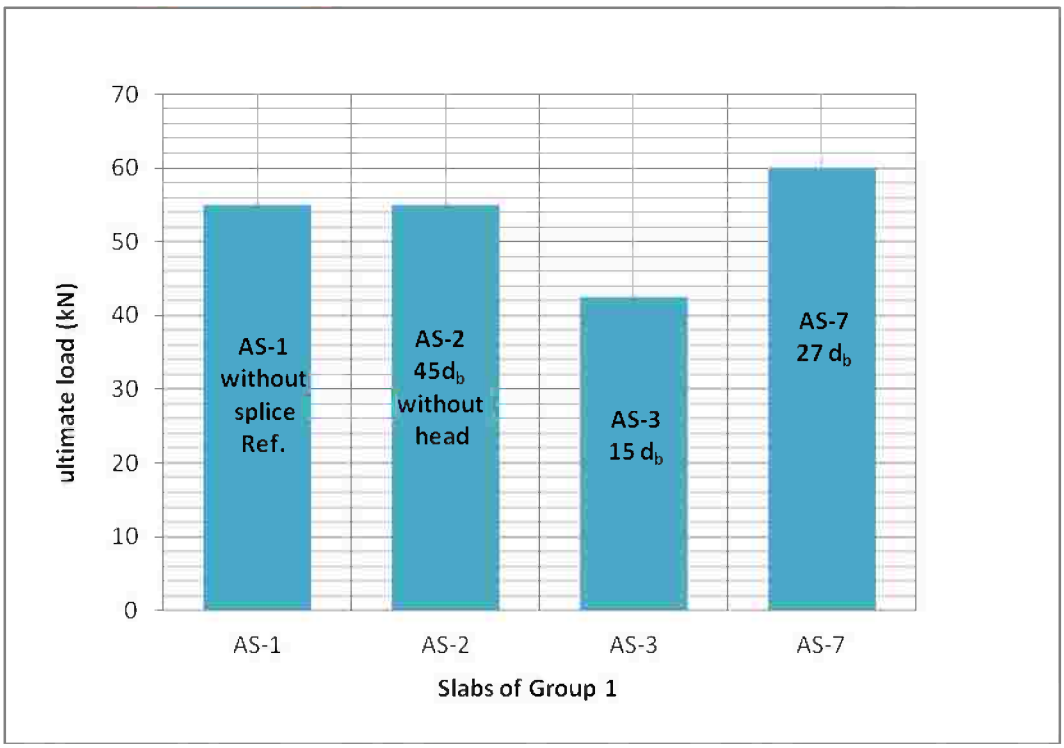

Figure (4-7): Failure loads for slabs of Group (1).

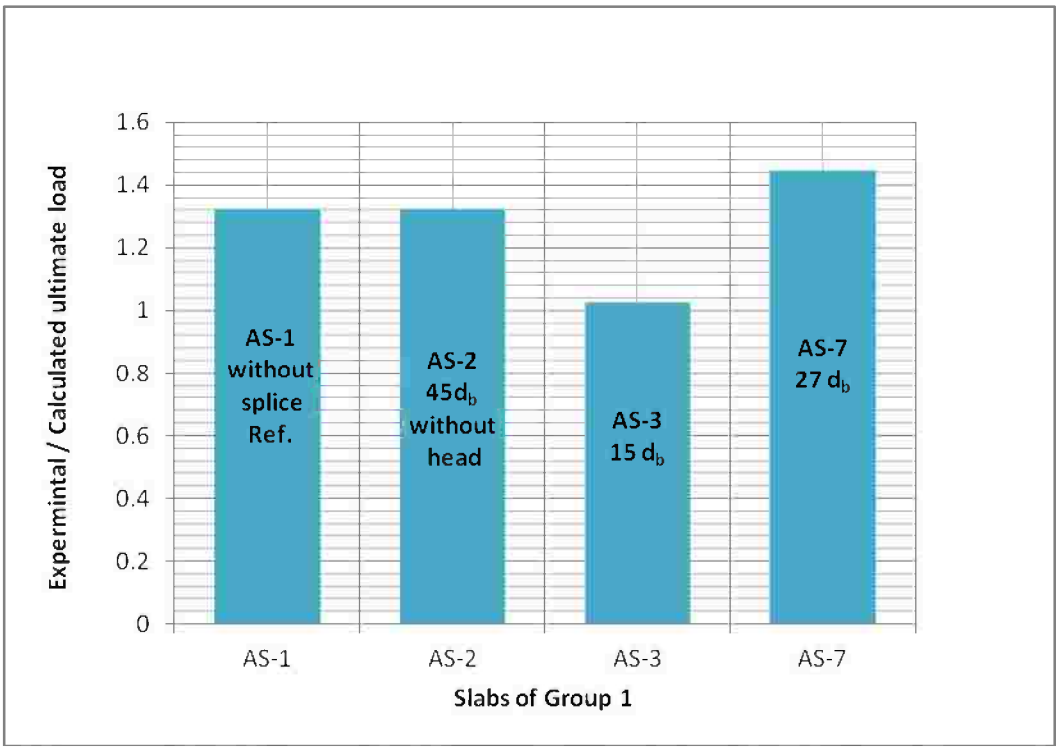

Figure (4-8): (Experimental / Calculated) ultimate loads for slabs of Group (1).

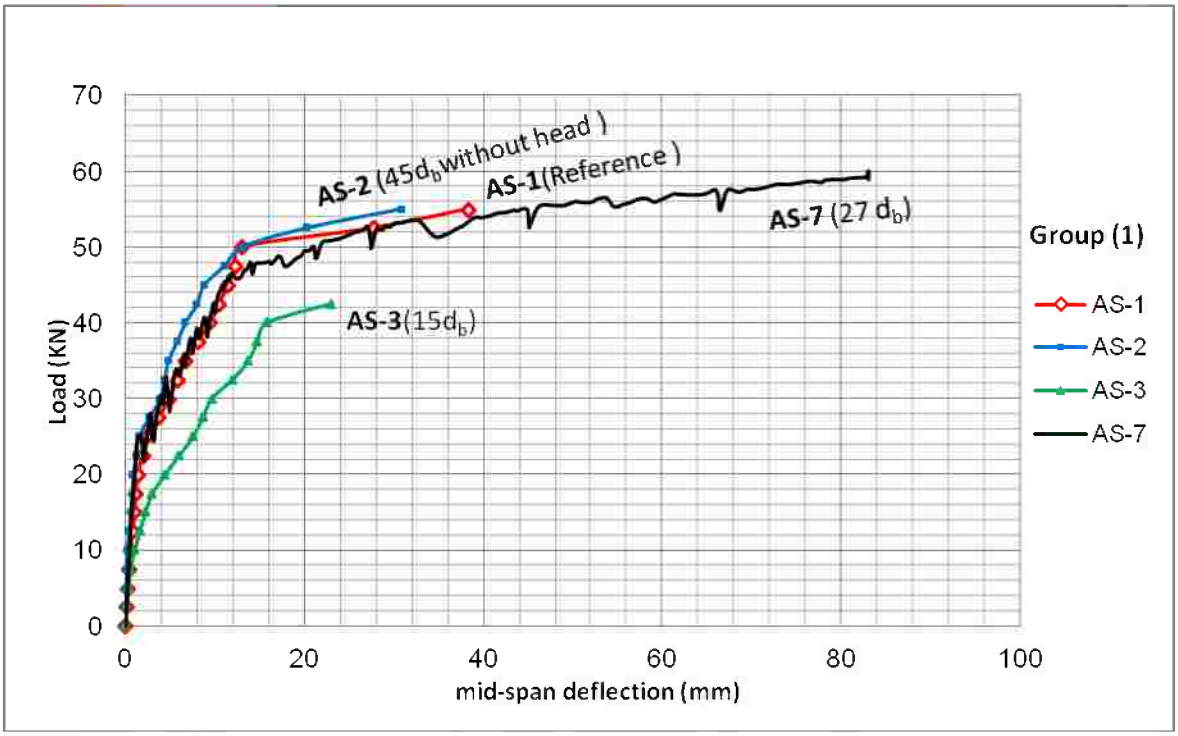

Figure (4-9): Relation between mid-Span deflection and load for slabs of Group (1) (dial No.2).

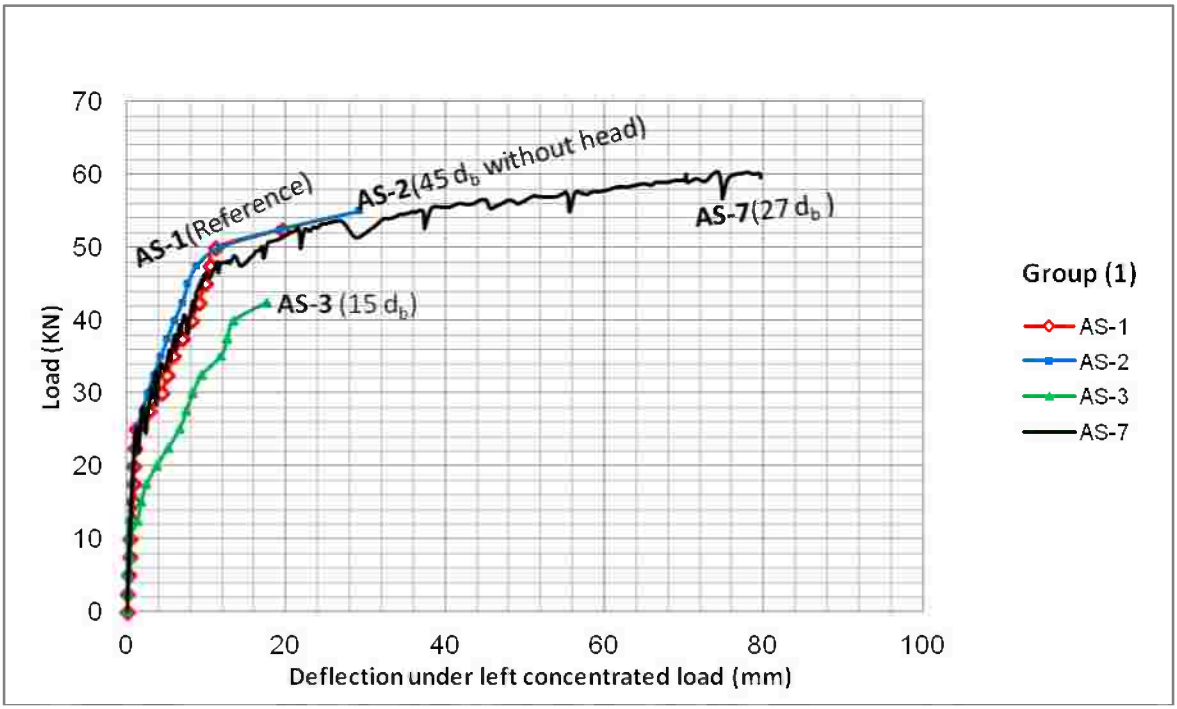

Figure (4-10): Relation between load and deflection under left concentrated load of Group (1) (dial No.1).

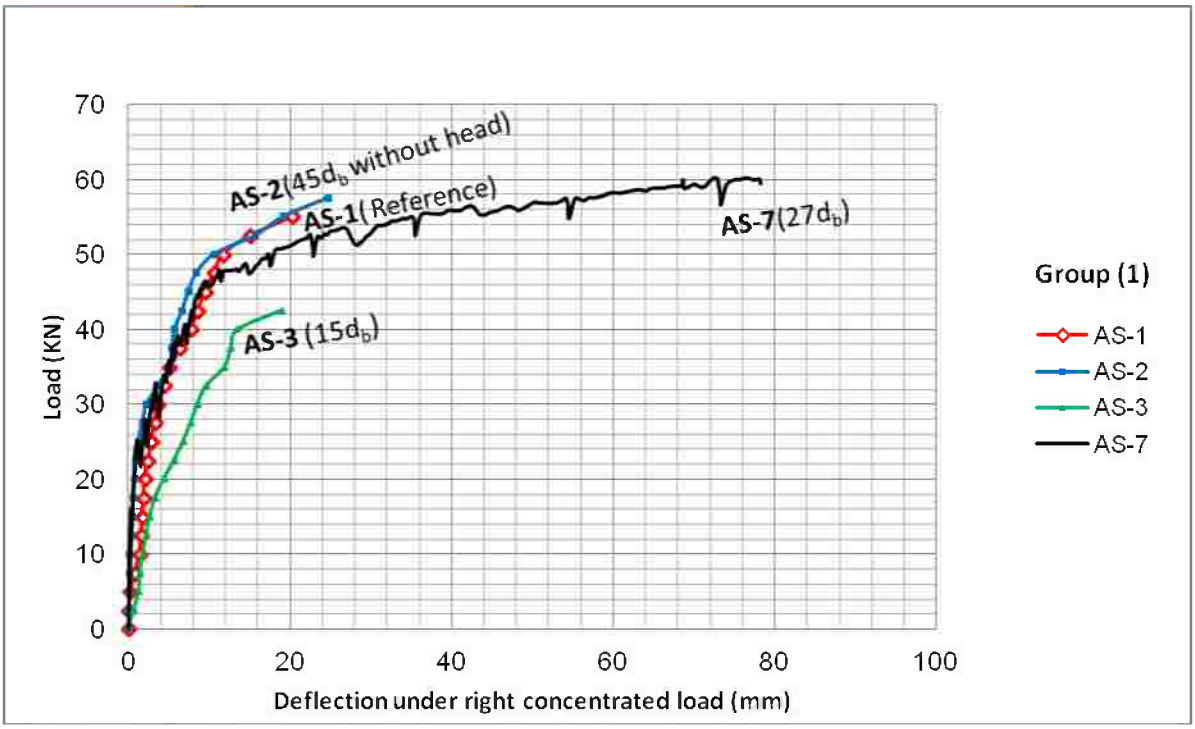

Figure (4-11):Relation between load and deflection under right concentrated load of Group (1) (dial No.3).

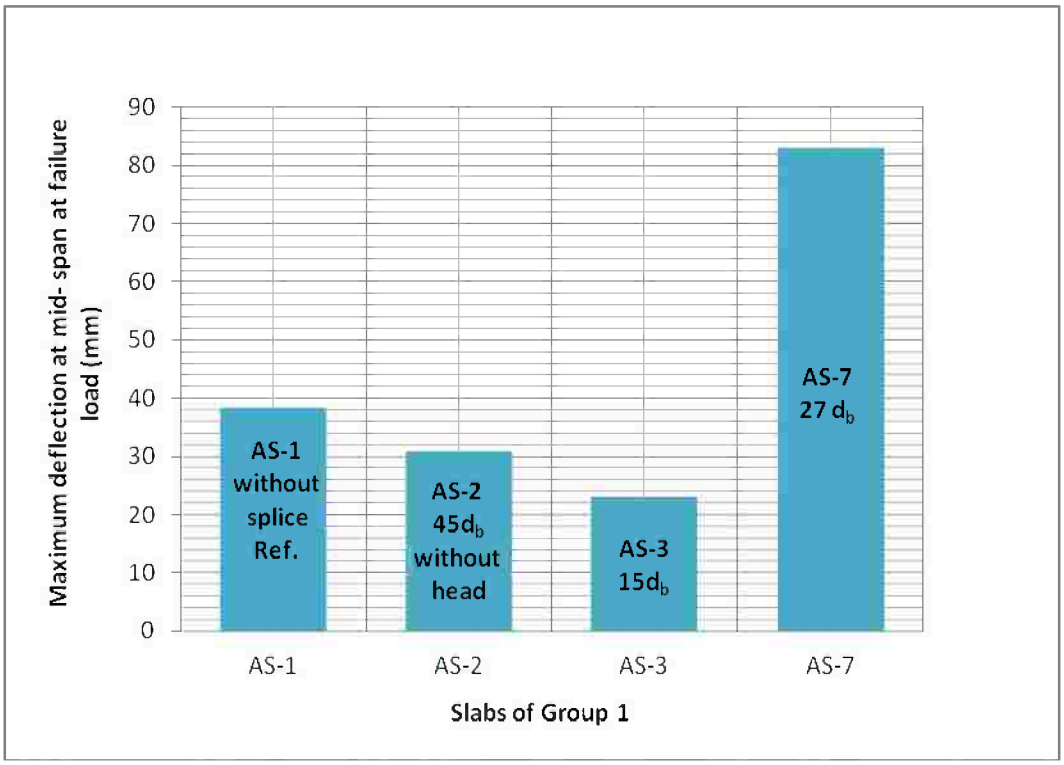

Figure (4-12): Maximum deflection at mid-span at failure load for slabs of Group (1).

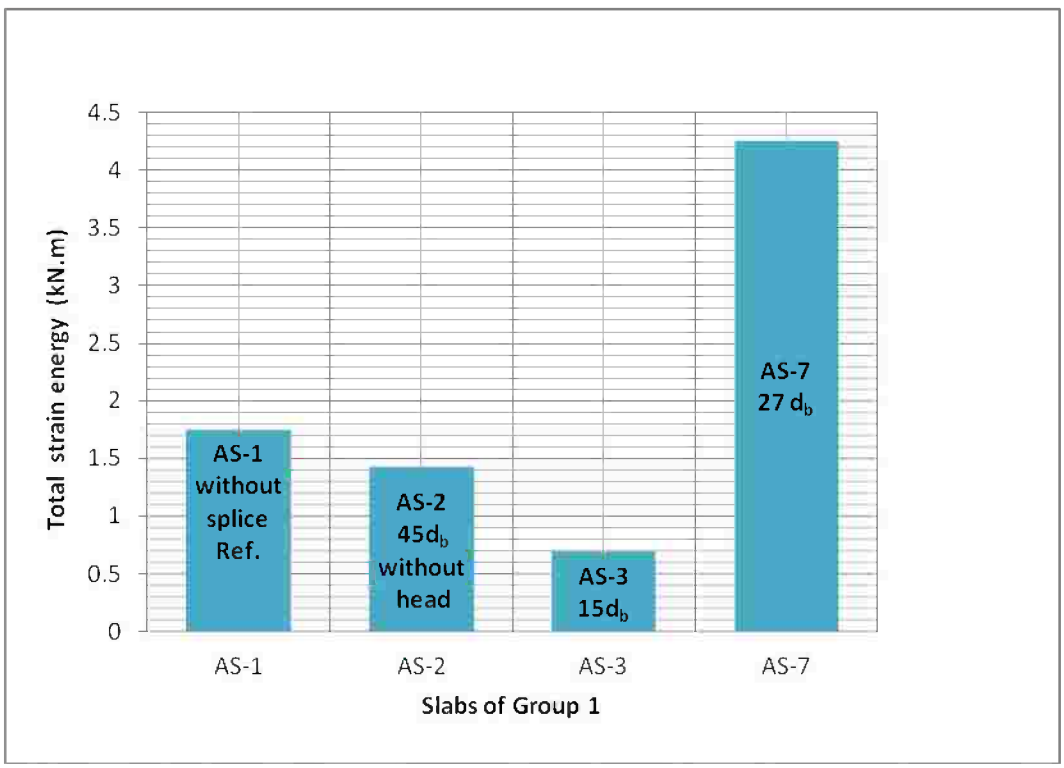

Figure (4-13): Total strain energy for slabs of Group (1).

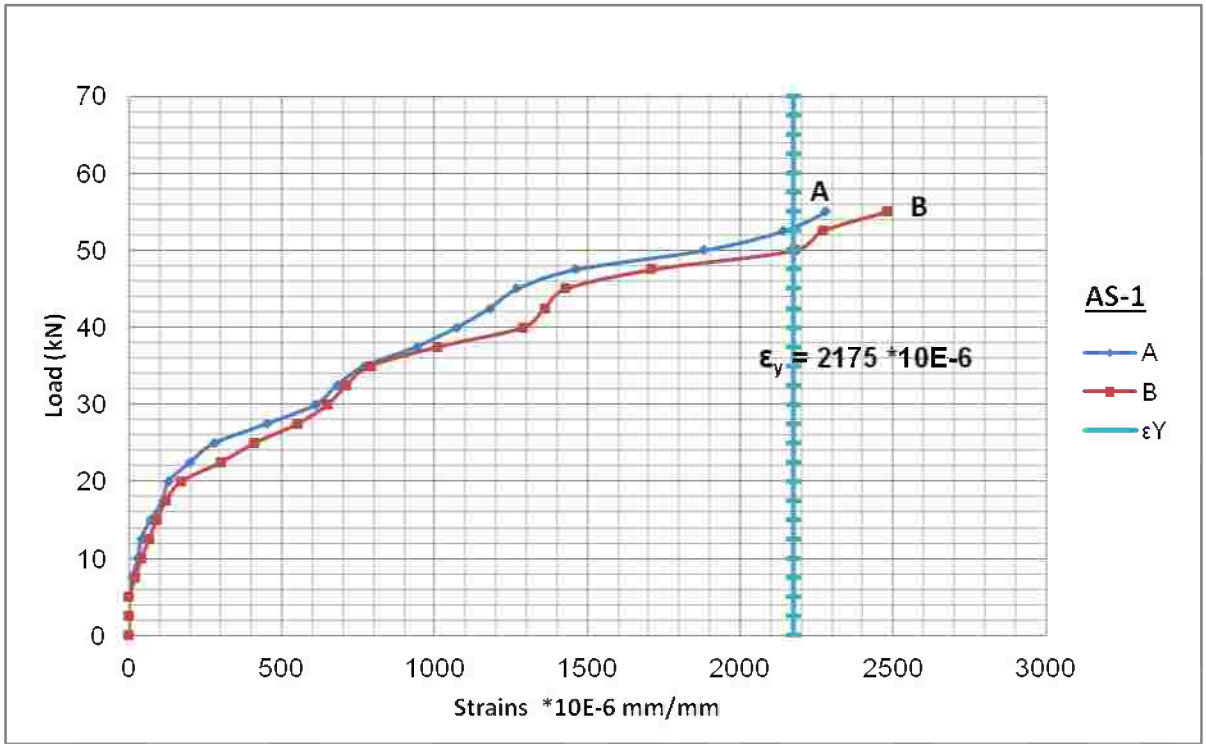

Figure (4-14): Relation between steel strain and load of slab **AS-1** (without splice), Group (1).

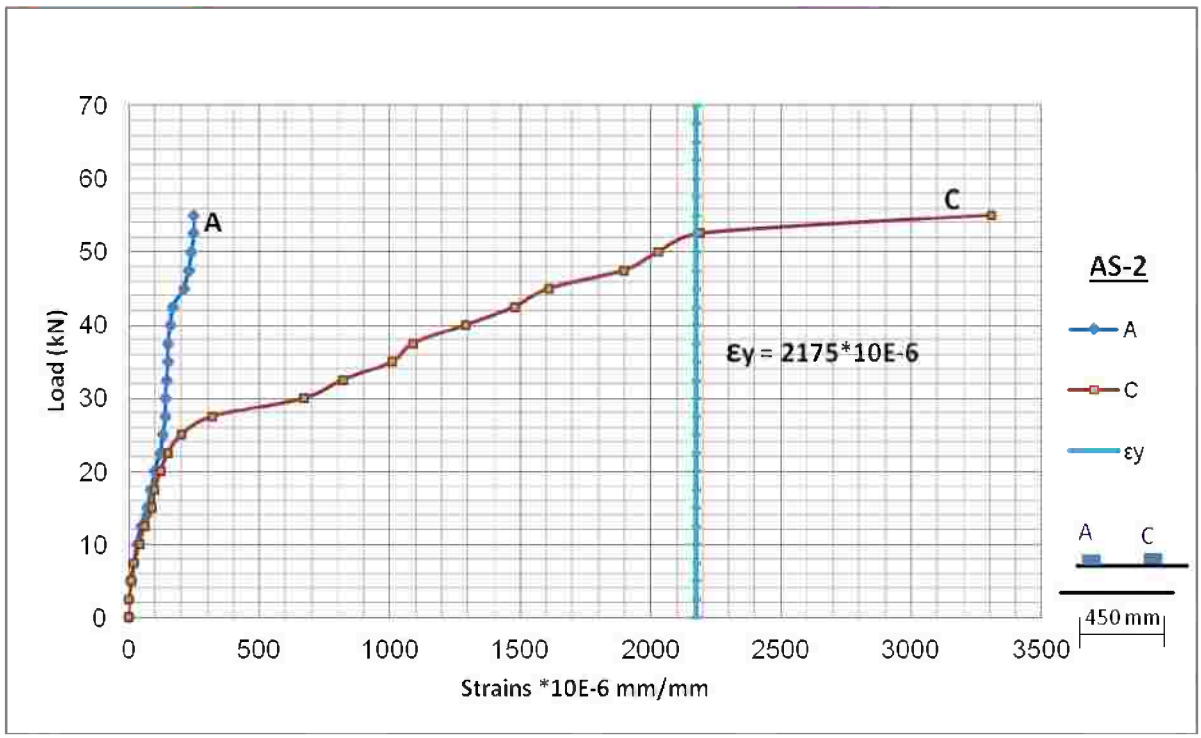

Figure (4-15): Relation between steel strain and load of slab **AS-2** ($45d_b$, without head), Group (1)

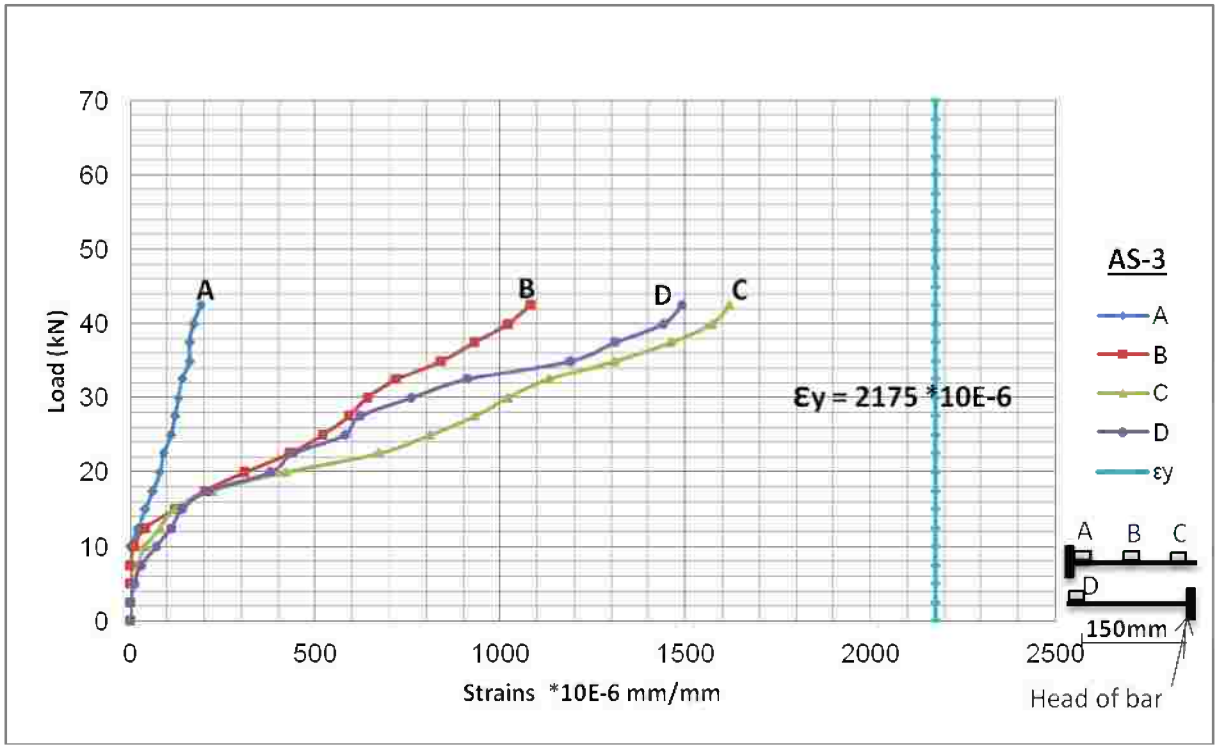

Figure (4-16): Relation between steel strain and load of slab **AS-3** ($15d_b$), Group (1).

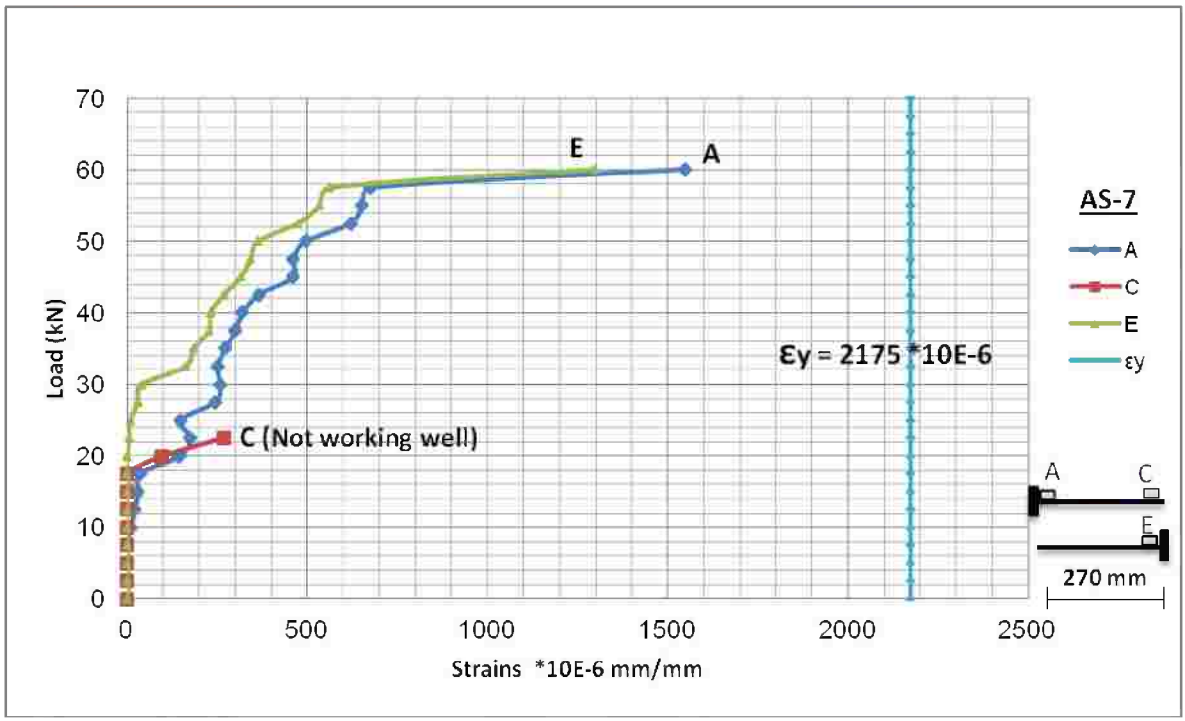

Figure (4-17): Relation between steel strain and load of slab **AS-7** ($27d_b$), Group (1).

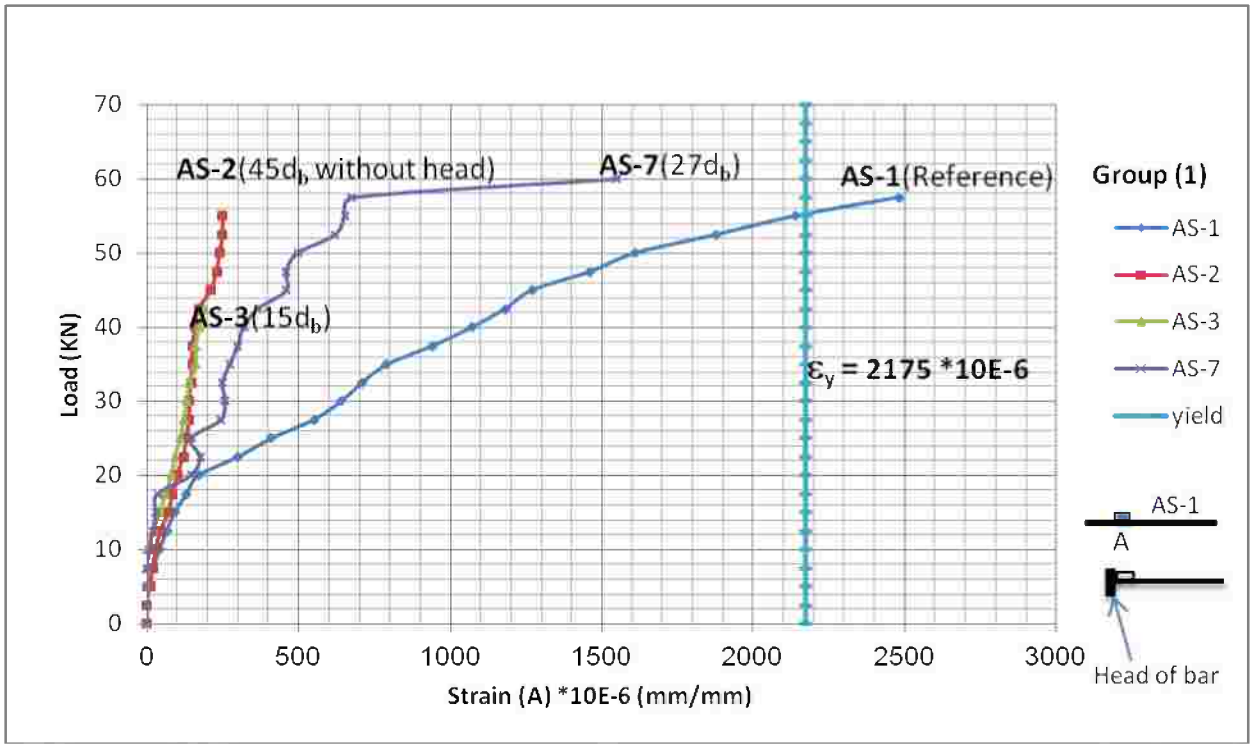

Figure (4-18): Relation between Strain (A) and load for slabs of Group (1).

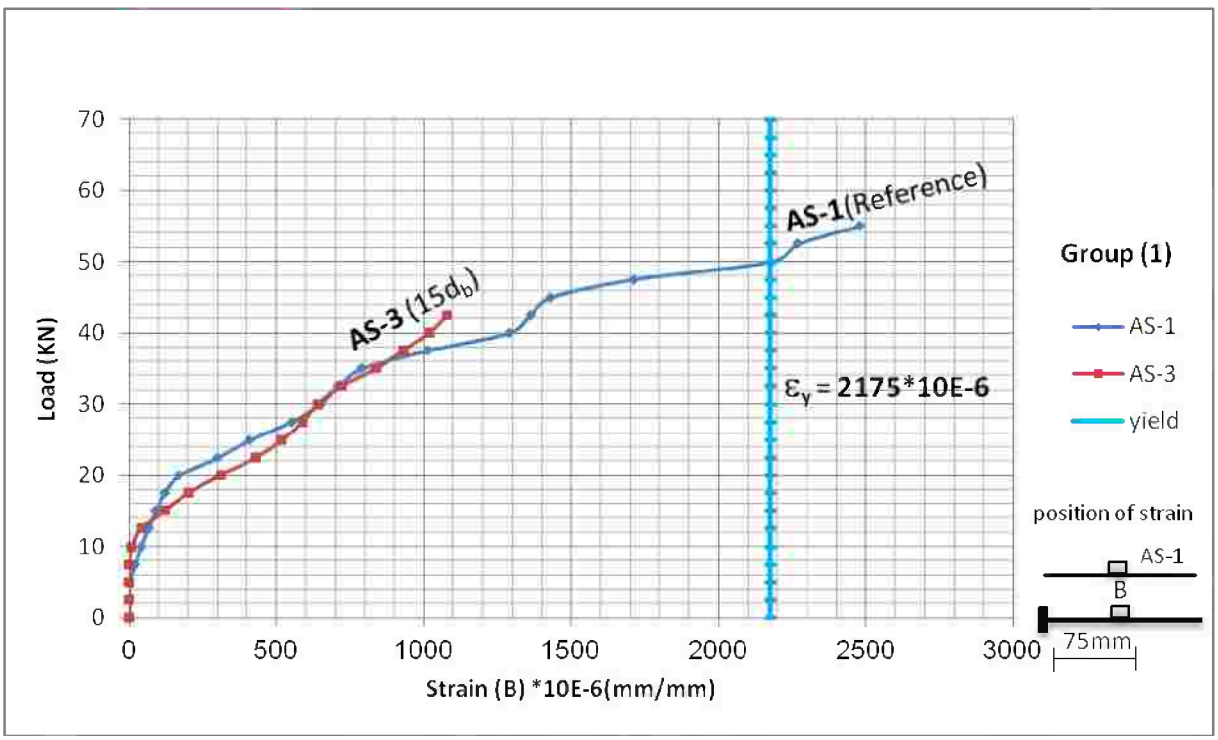

Figure (4-19): Relation between Strain (B) and load for slabs of Group (1).

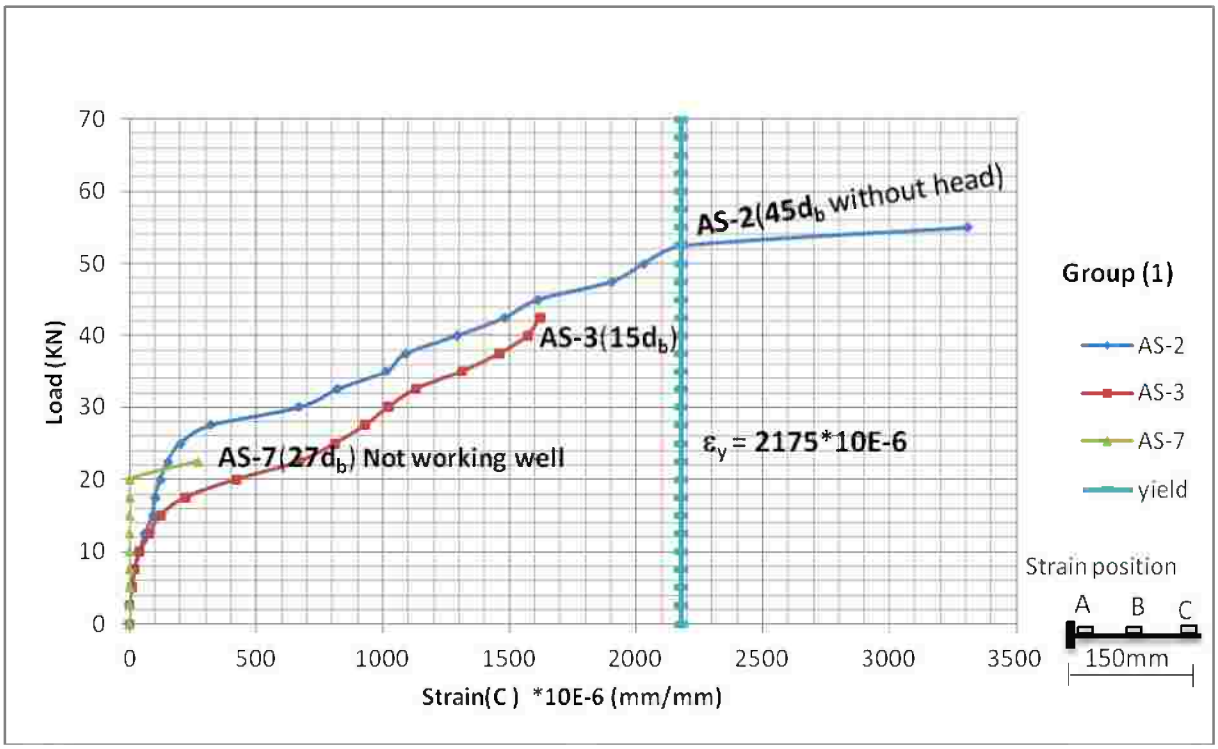

Figure (4-20): Relation between Strain (C) and load for slabs of Group (1).

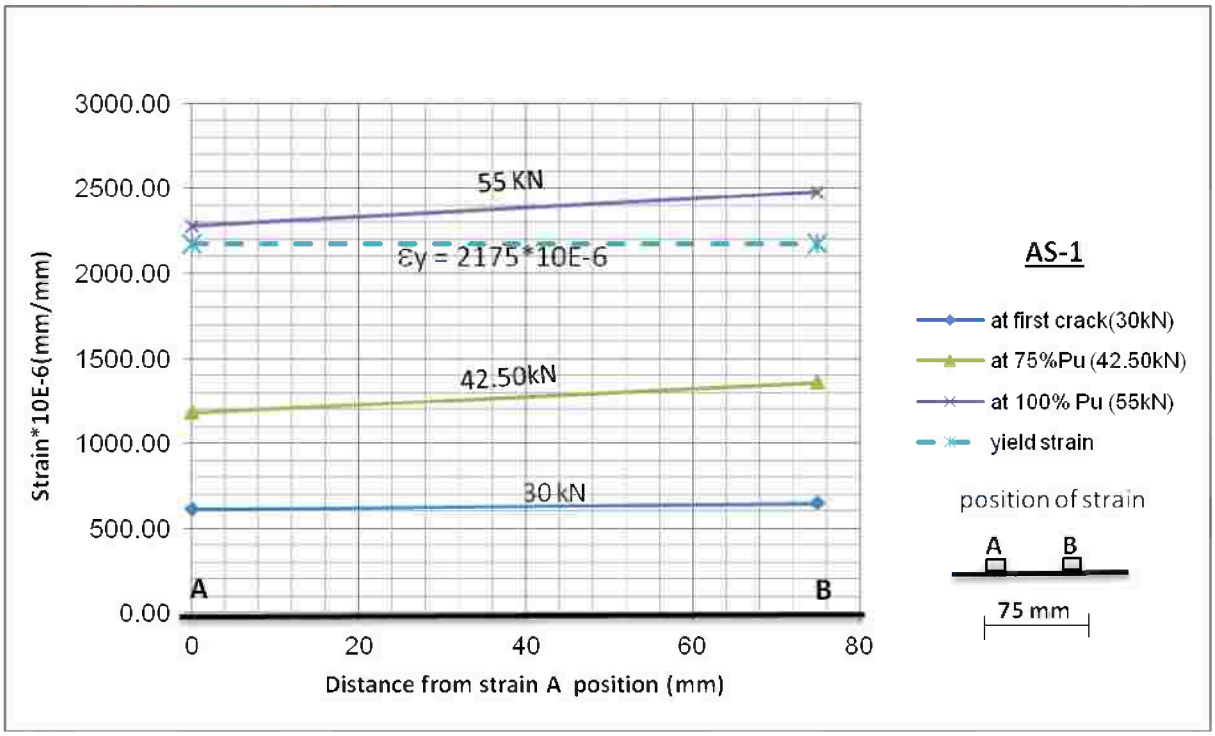

Figure (4-21): Strain distribution along slab **AS-1** at different loads.

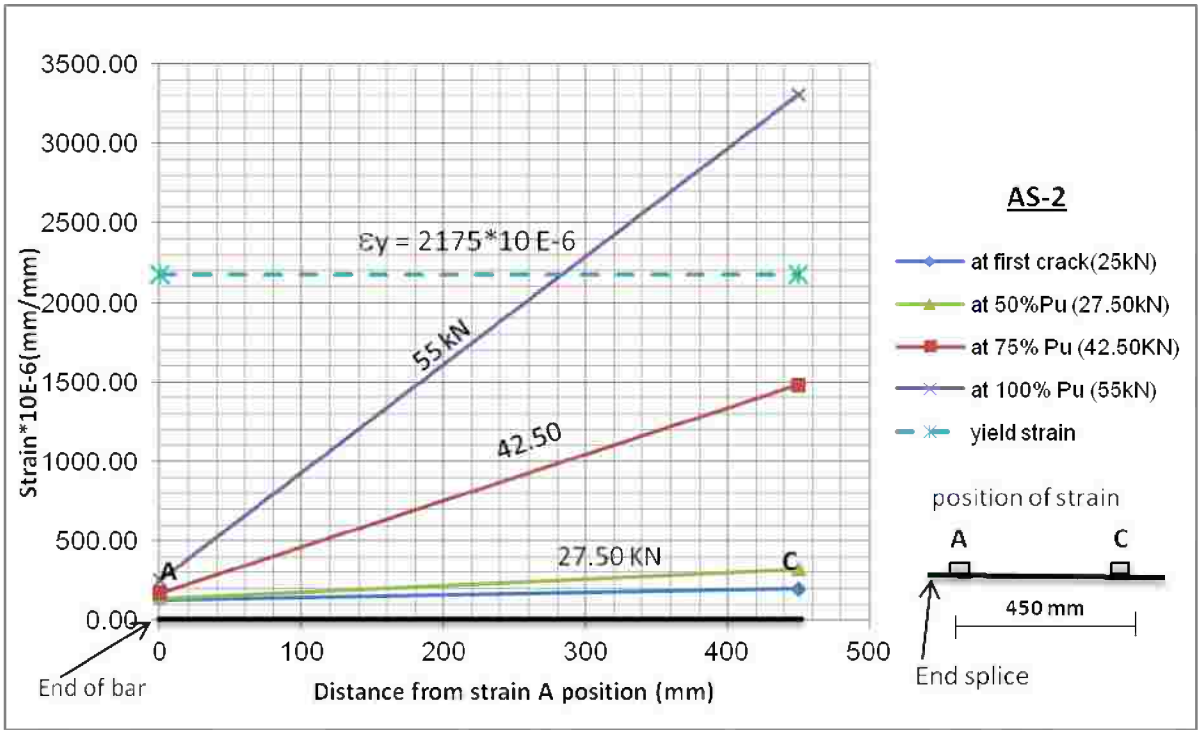

Figure (4-22): Strain distribution along the splice zone of slab **AS-2** at different loads (with no head).

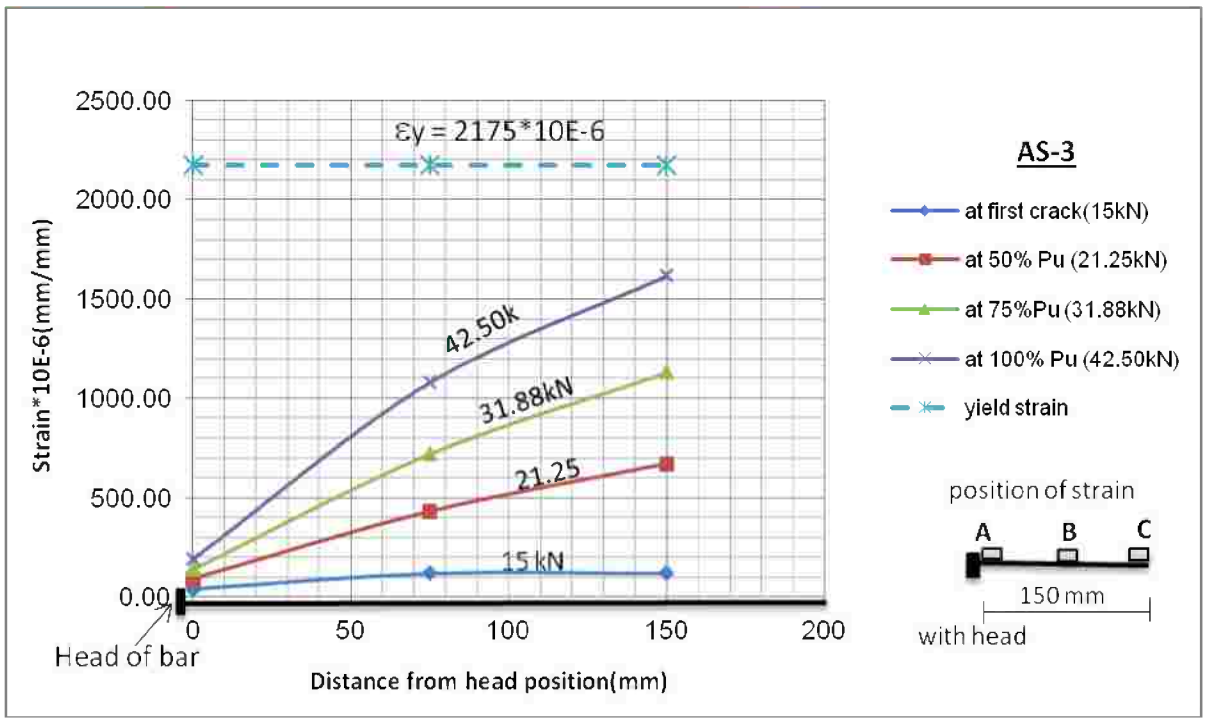

Figure (4-23): Strain distribution along the splice zone of slab **AS-3** at different loads.

(a): Cracks on the side of slab confined with embedded beams in lap zone at failure.

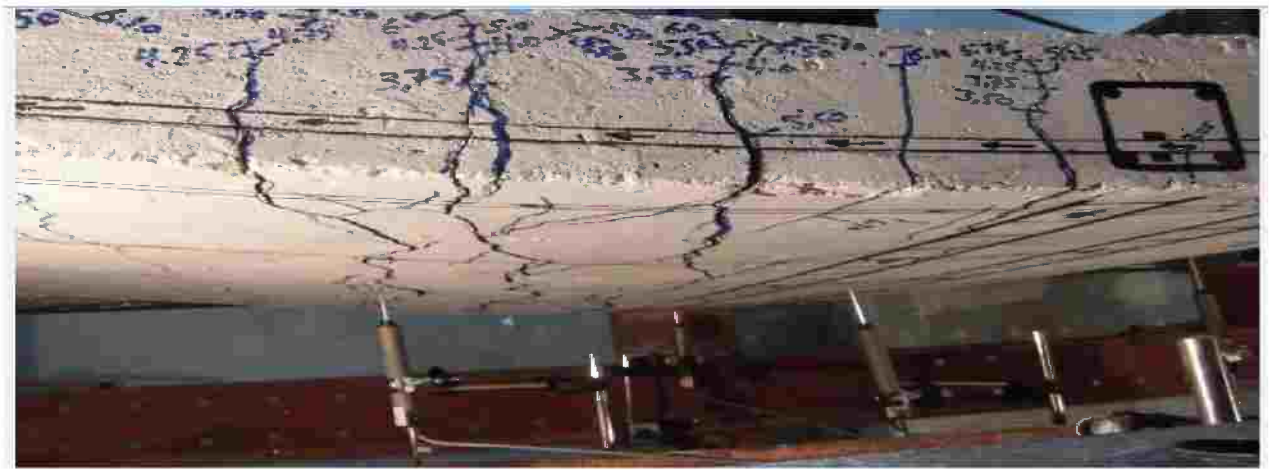

(b): Cracks formation at the edge of the transverse embedded beams confined and outside lap zone.

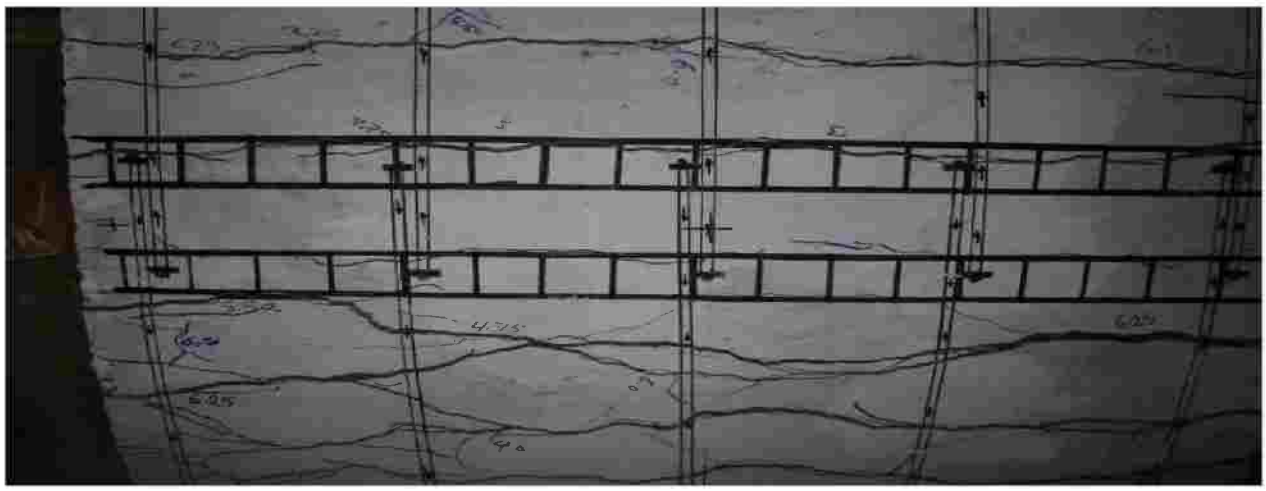

(c):Cracks on the bottom surface of slab confined with embedded beams in lap zone at failure.

Figure (4-24): The crack pattern of **AS-5**.

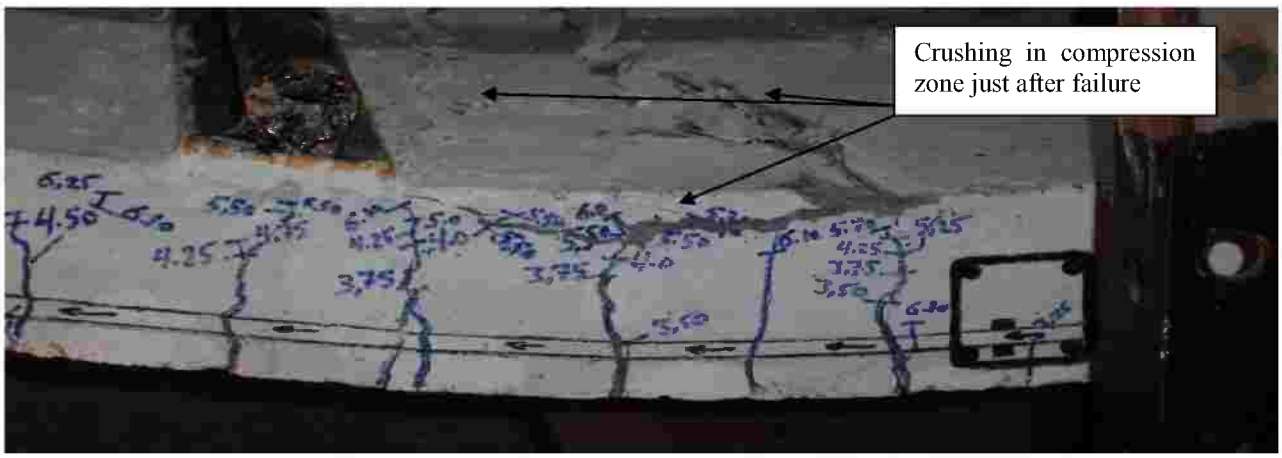

(a): Splitting and crushing compression zone just after failure.

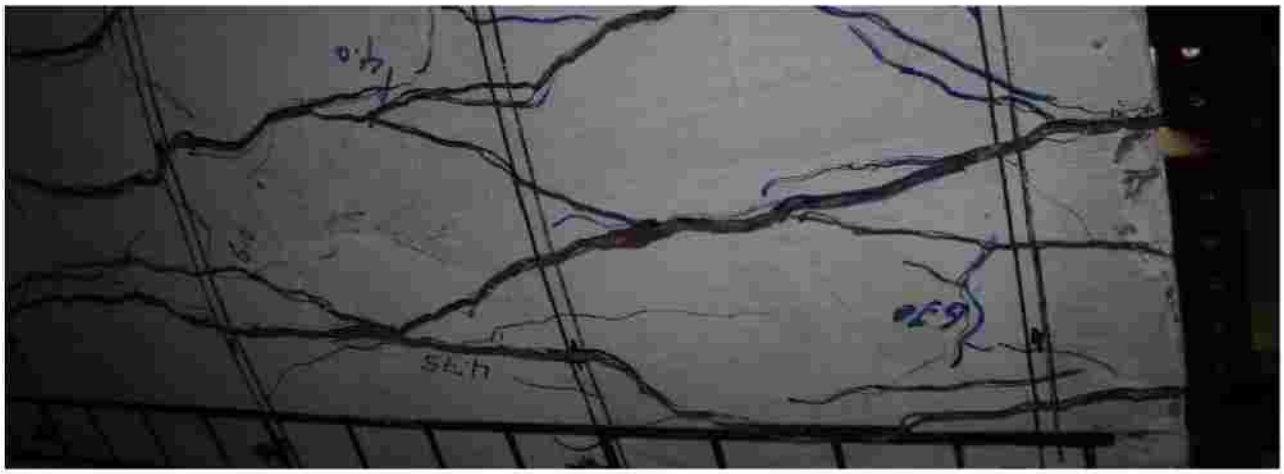

(b) :Cracks became wider and extensive outside the confined lap zone.

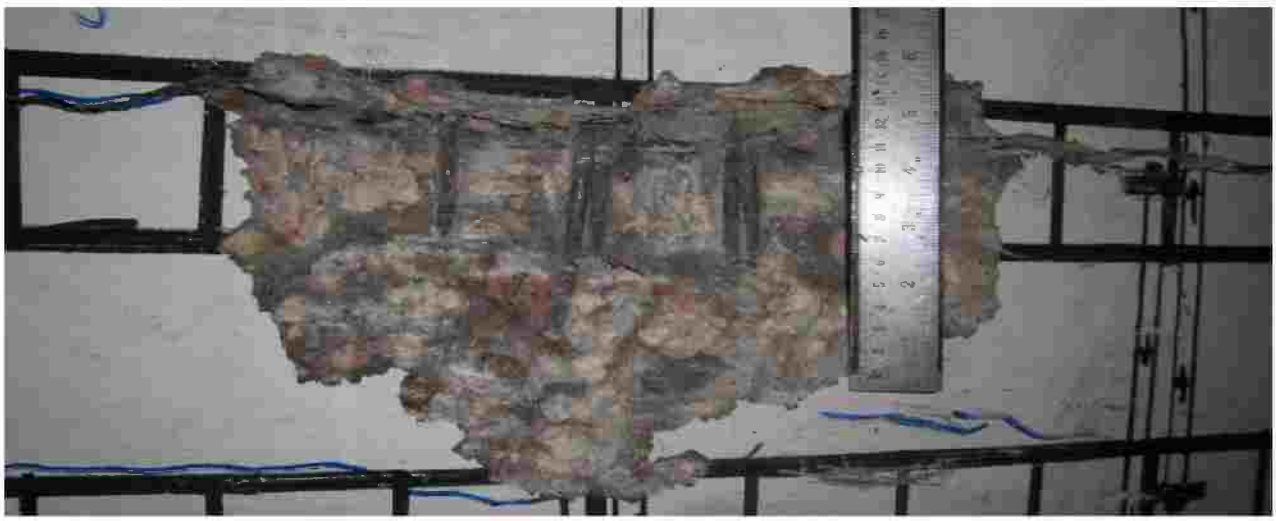

(c): The concrete around confined zone after bottom cover removed from the confined lap zone.

Figure (4-25): Cracks at failure stage of the confined splice slab **AS-5**.

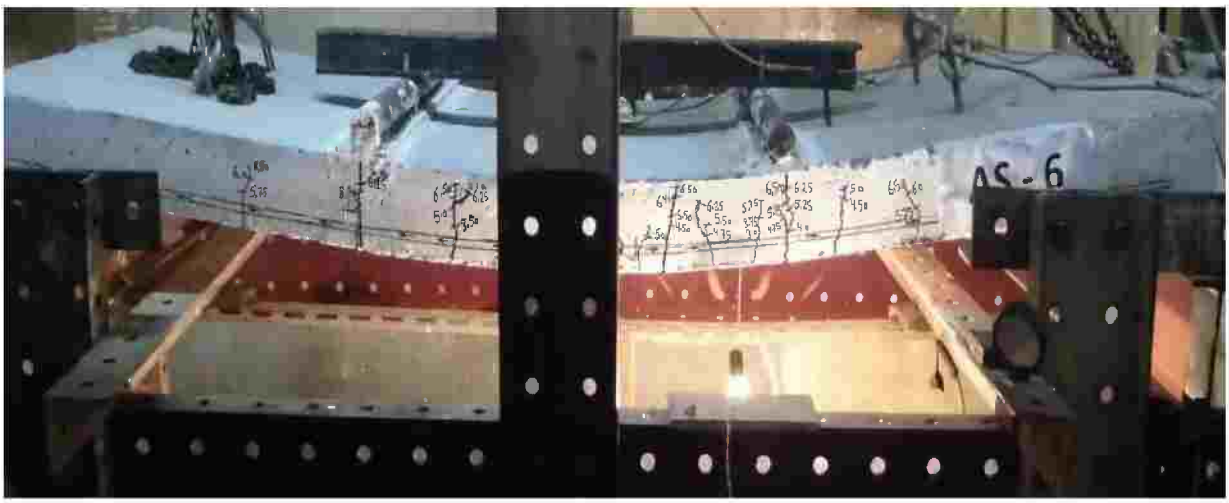

(a): Cracks on side of slab confined with circular spiral stirrups around lap splice at failure.

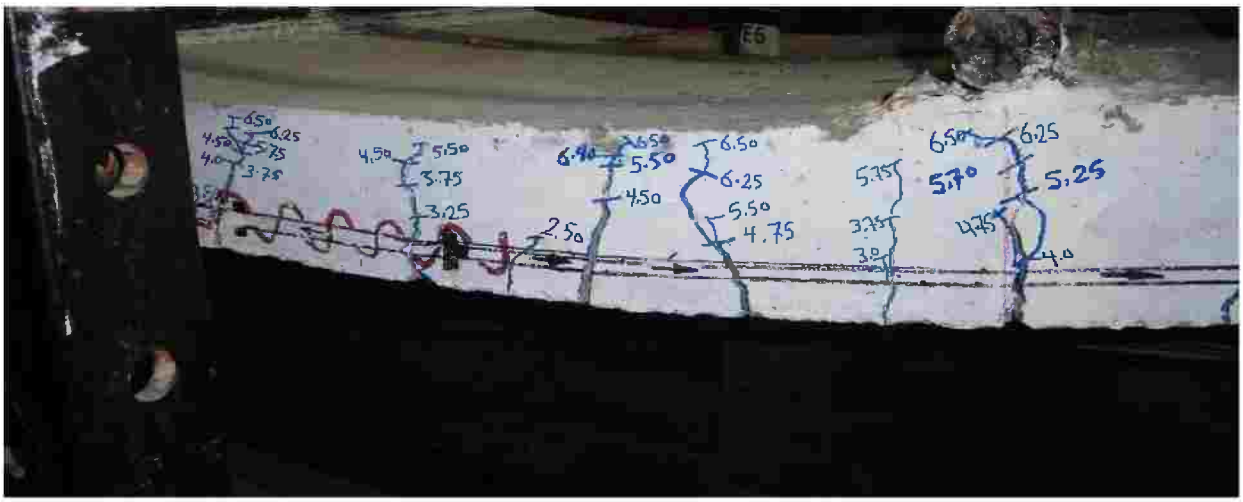

(b): Cracks formation at the lap zone and extensive outside of confined lap zone.

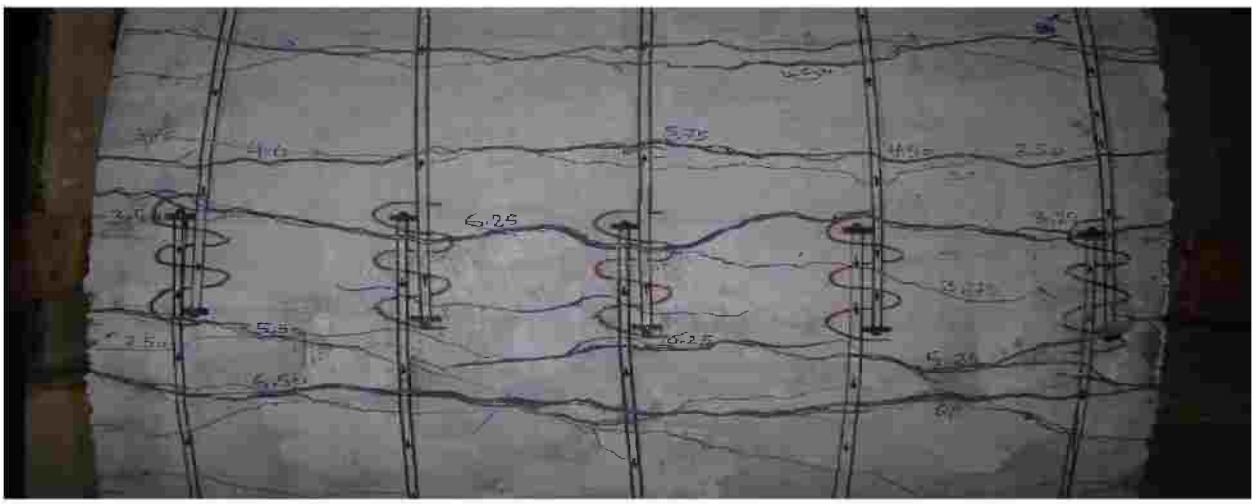

(c): Cracks on the bottom surface of slab after excessive deflection.

Figure (4-26): The crack pattern of **AS-6**.

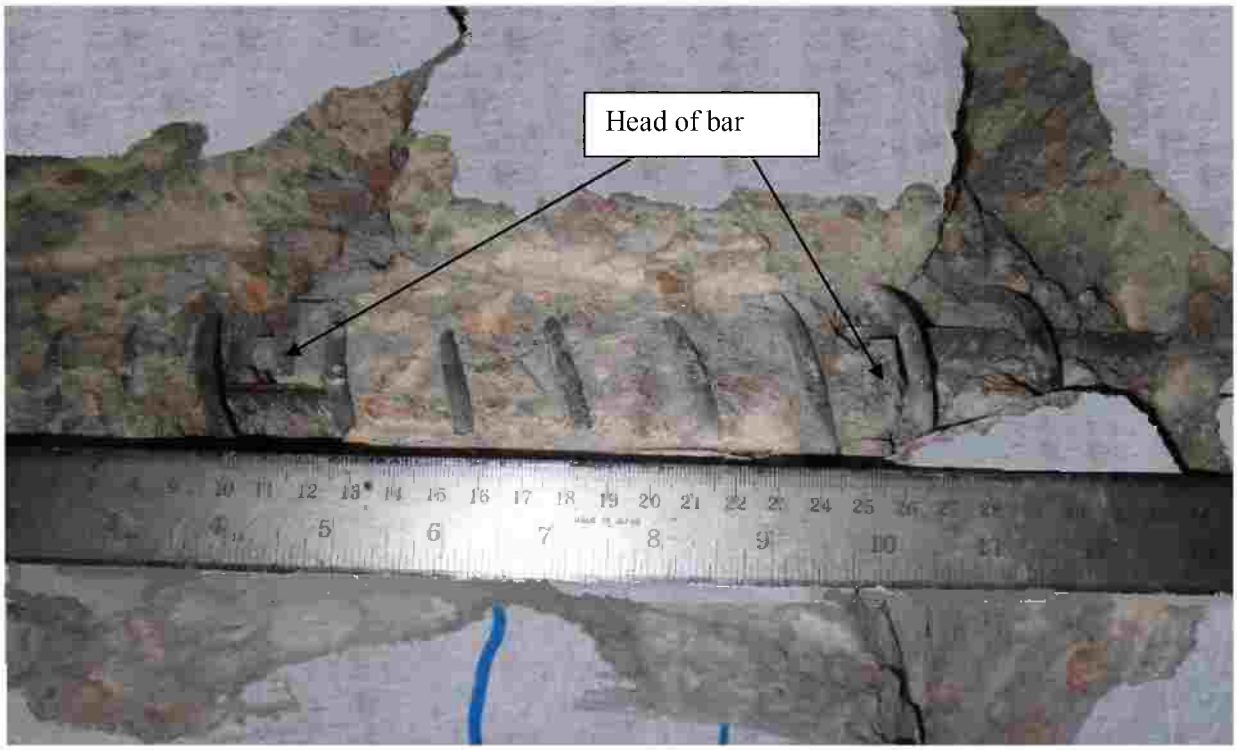

(a): The concrete around spiral stirrups after bottom cover was removed from the lap zone.

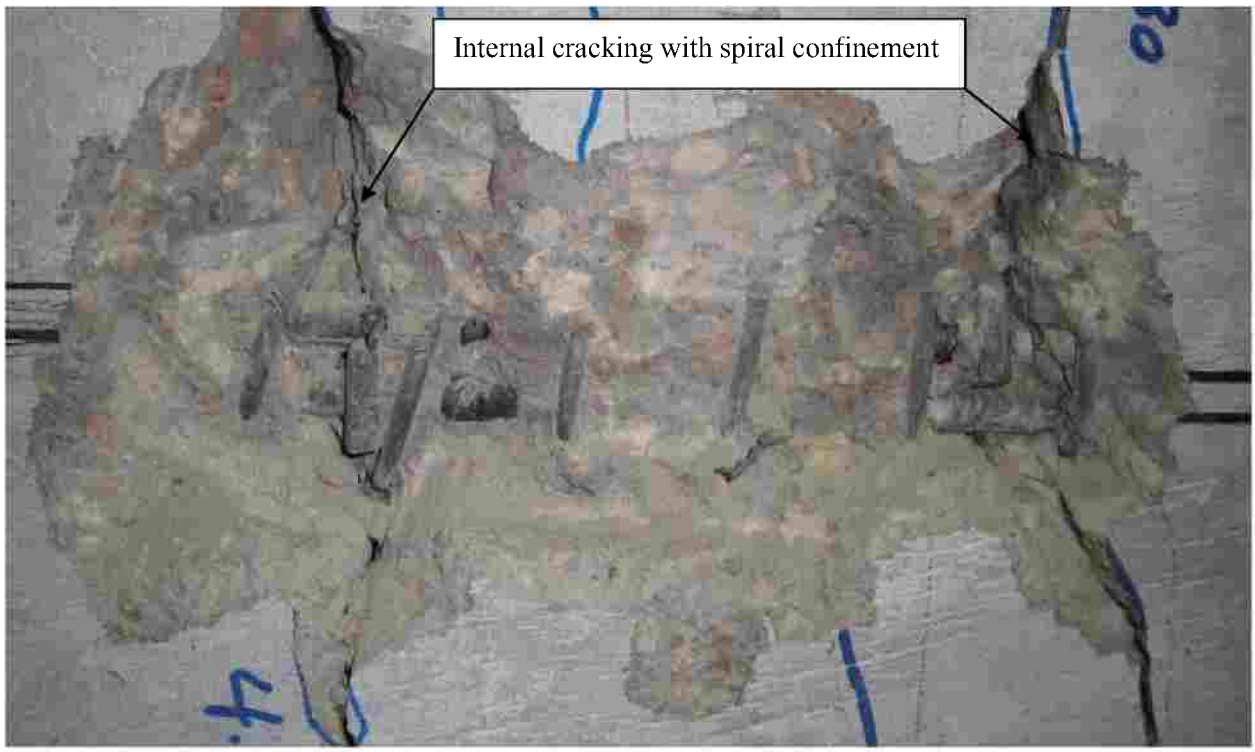

(b): Cracking in the lap zone occurred along the heads.

Figure (4-27): Failure of the confined splice slab **AS-6**, confined with spiral stirrup around the lap joint.

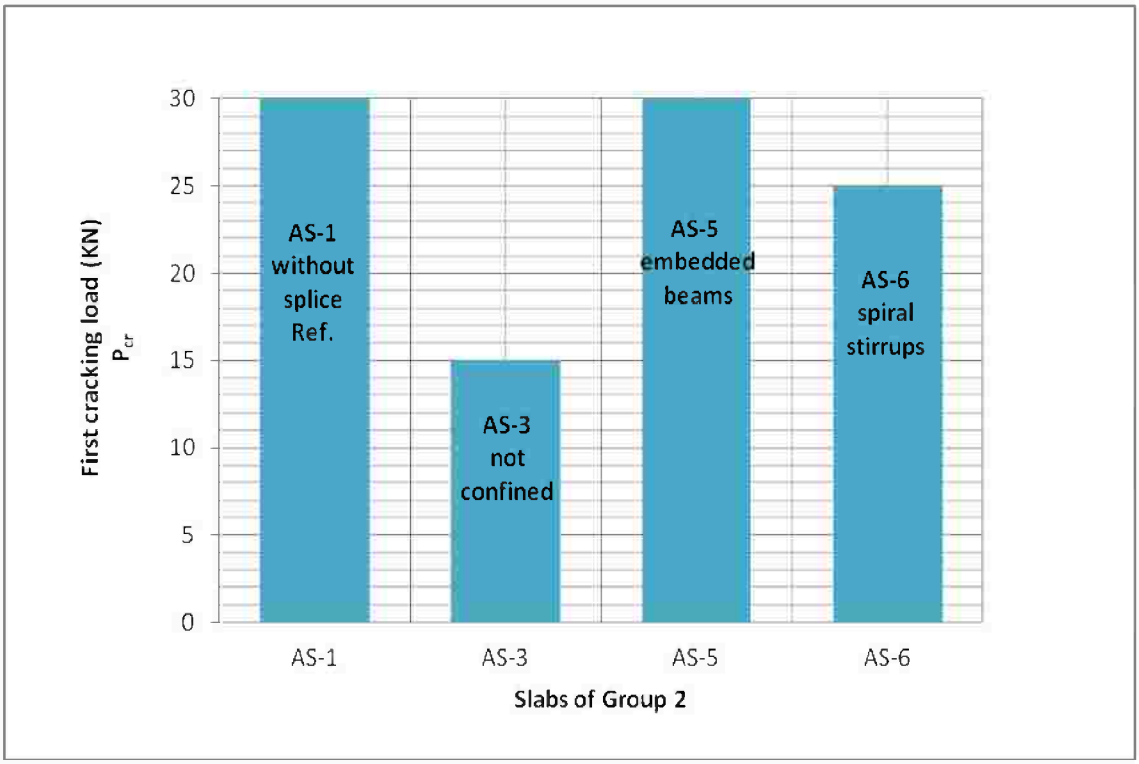

Figure (4-28): First cracking loads for slabs of Group (2).

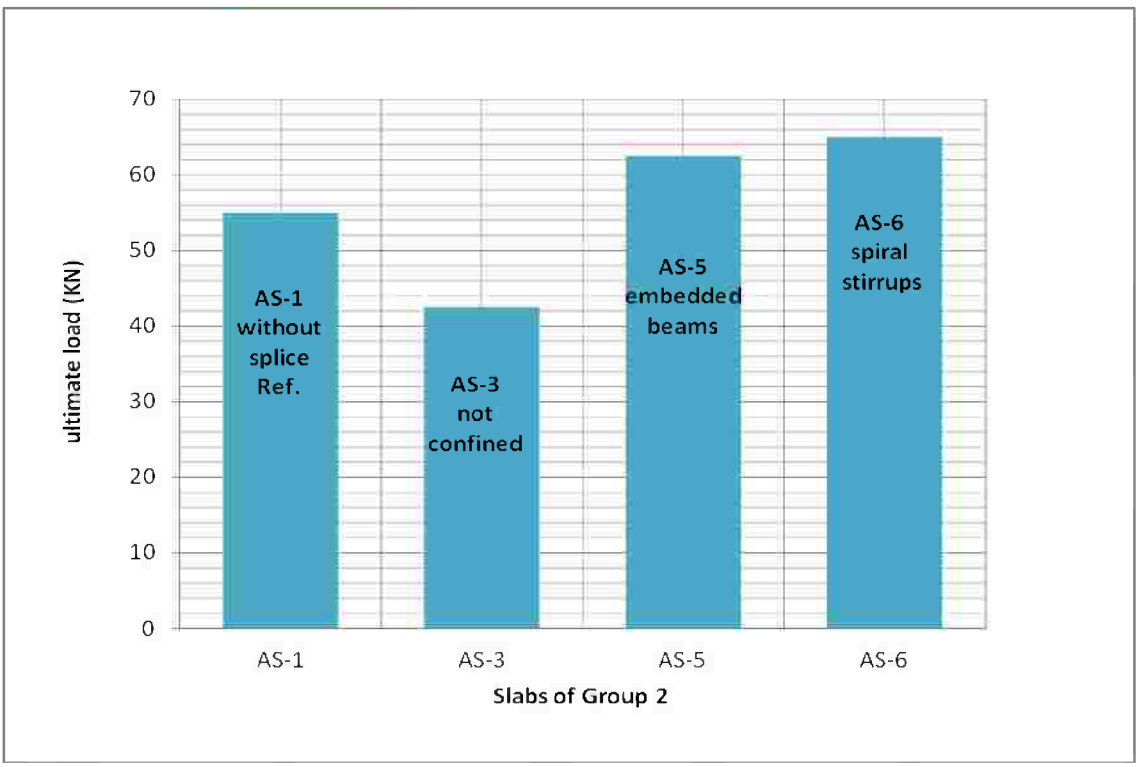

Figure (4-29): Failure loads for slabs of Group (2).

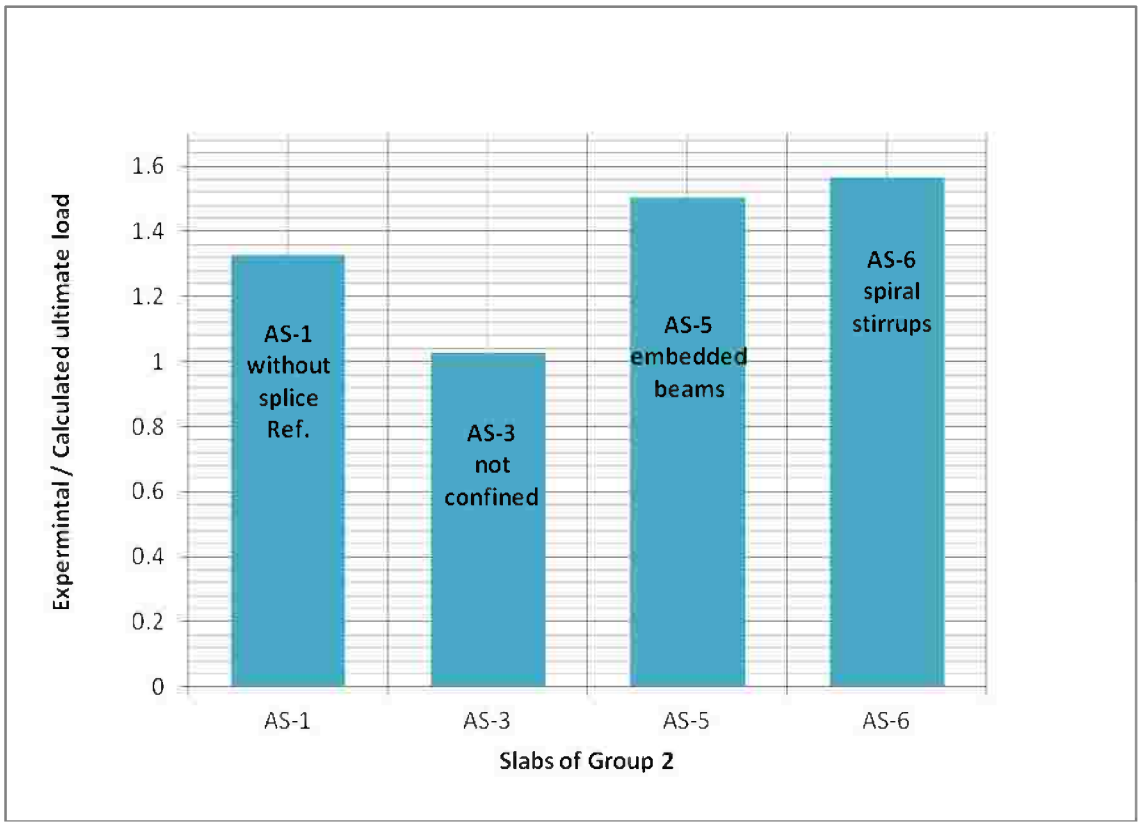

Figure (4-30): (Experimental / Calculated) ultimate loads for slabs of Group (2).

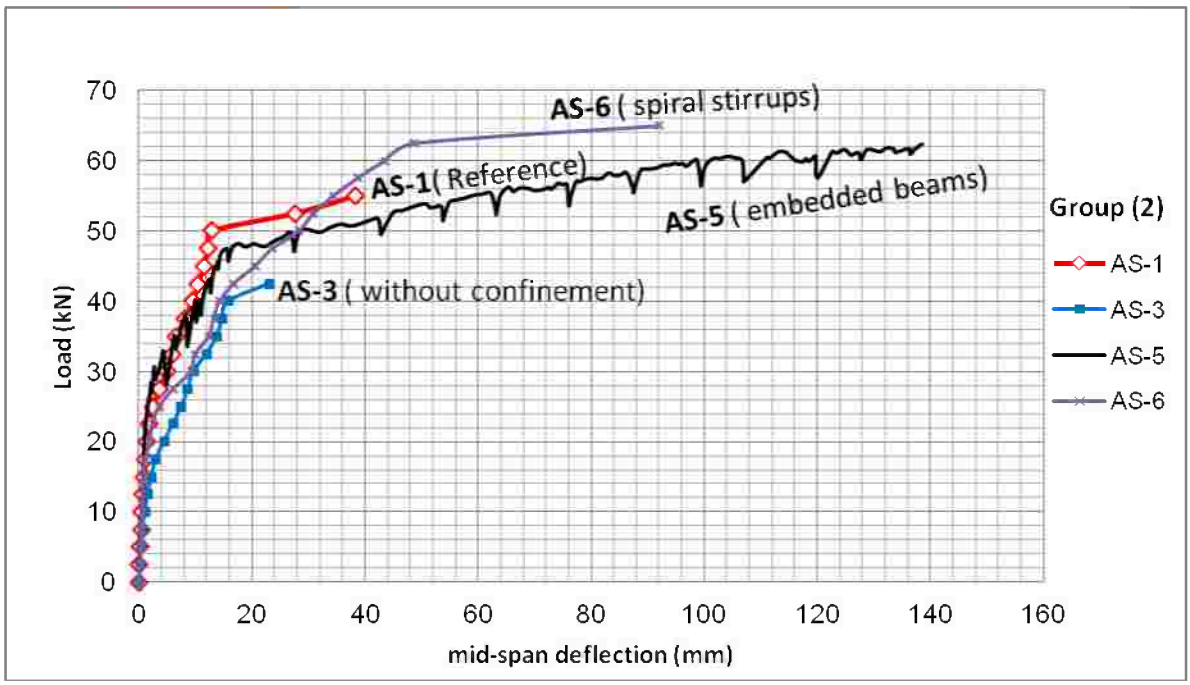

Figure (4-31): Relation between mid-span deflection and load for slabs of Group (2) (dial No.2).

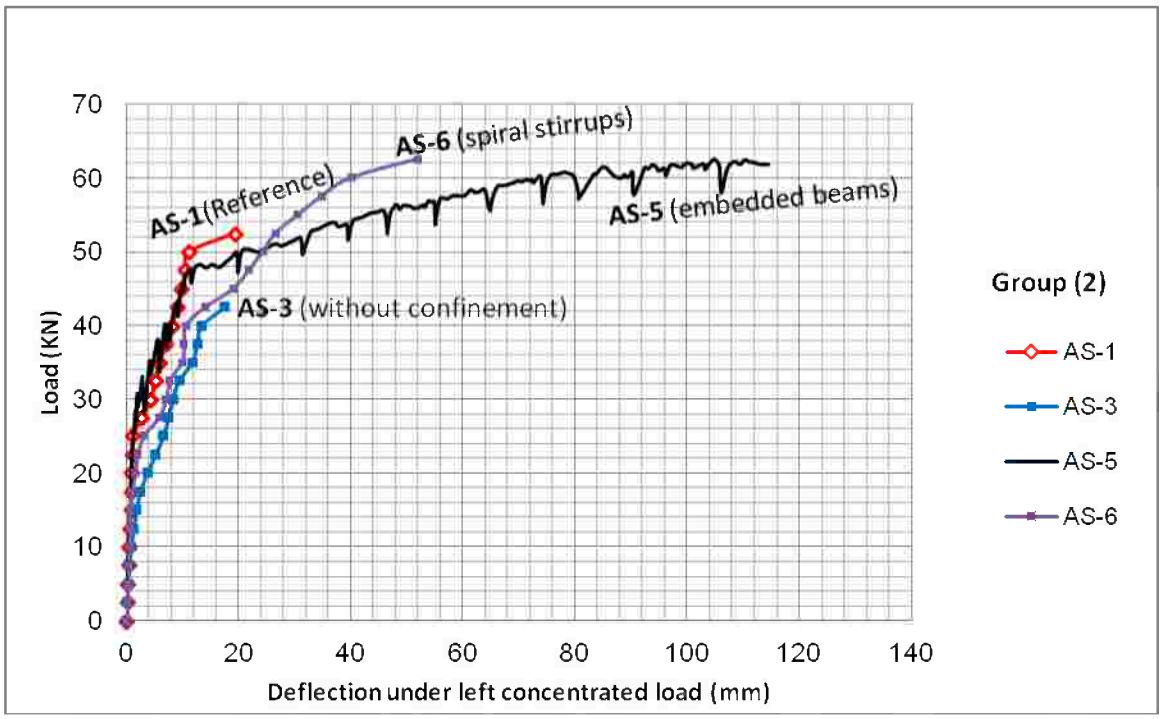

Figure (4-32): Relation between load and deflection under left concentrated load of Group (2) (dial No.1).

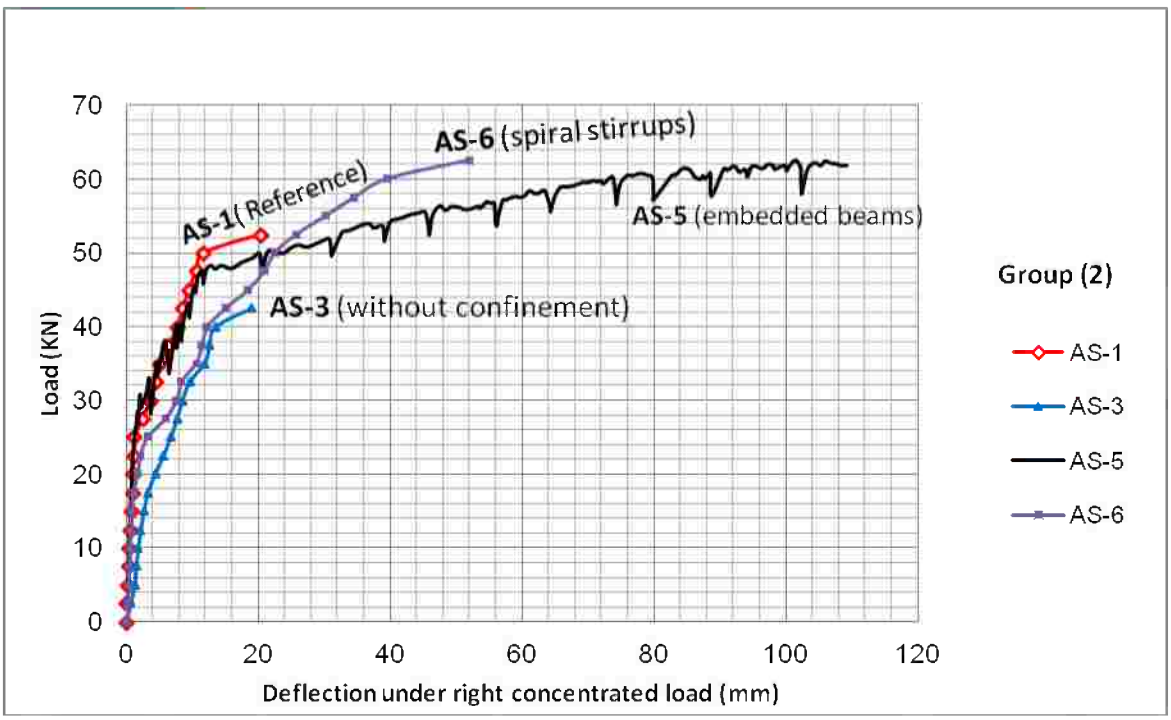

Figure (4-33): Relation between load and deflection under right concentrated load of Group (2) (dial No.3).

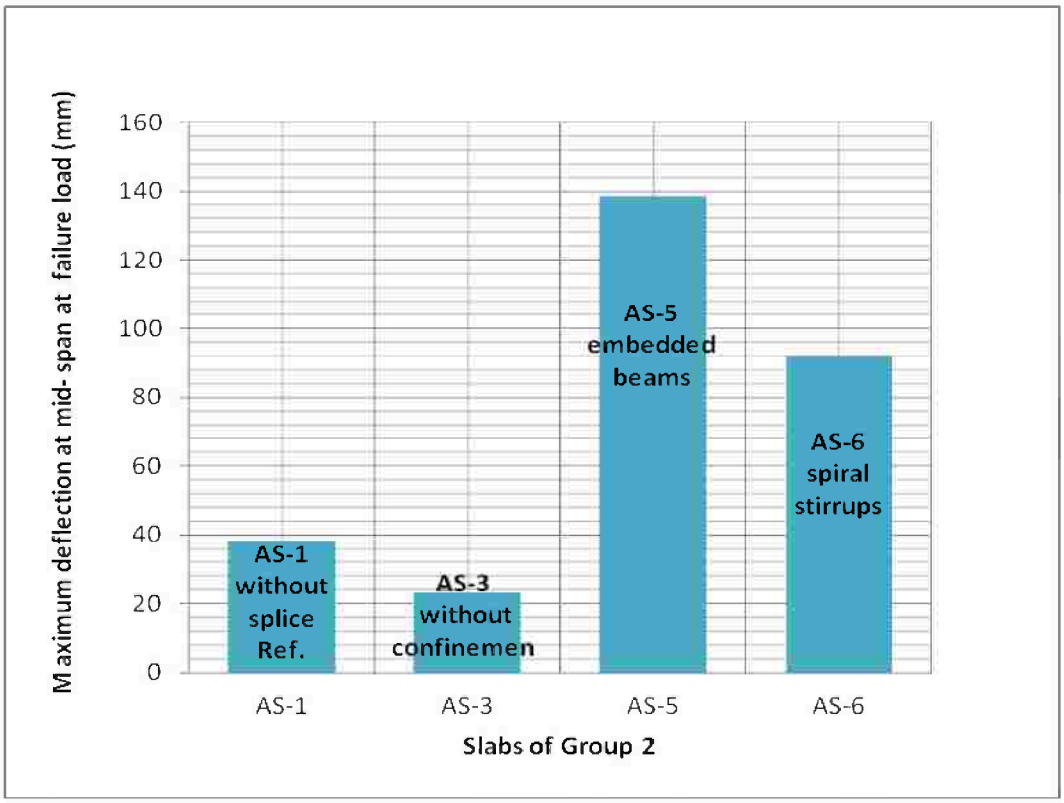

Figure (4-34): Maximum deflection at mid-span at failure load for slabs of Group (2).

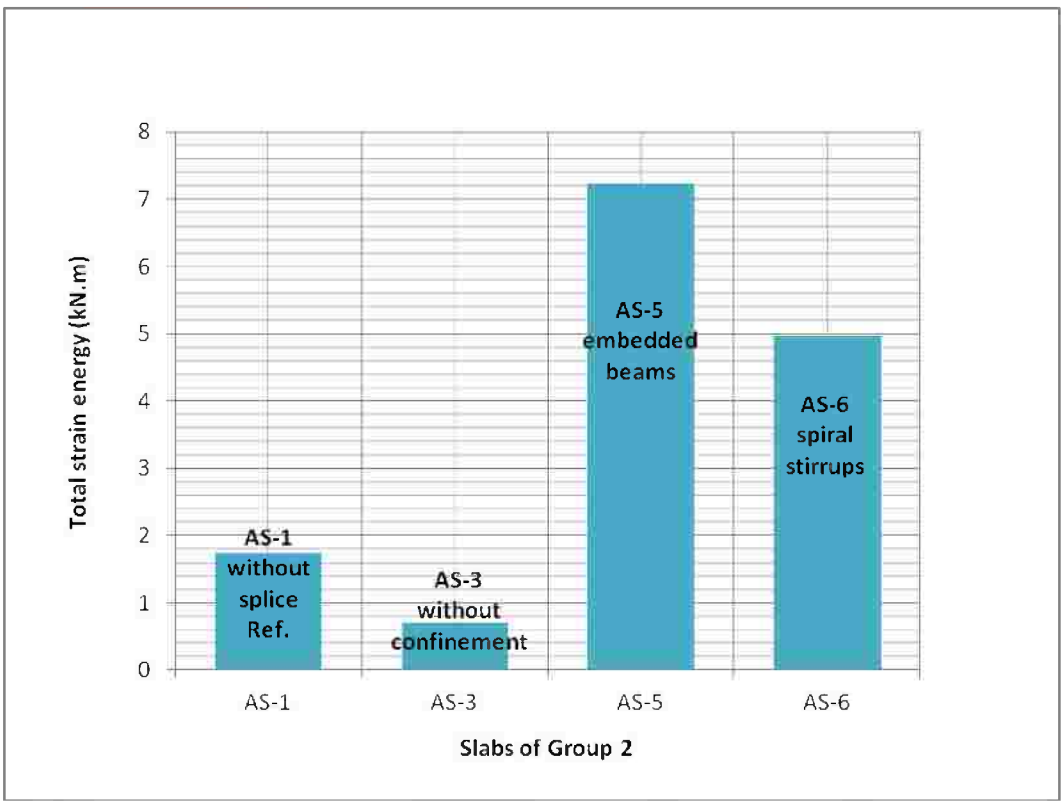

Figure (4-35): Total strain energy for slabs of Group (2).

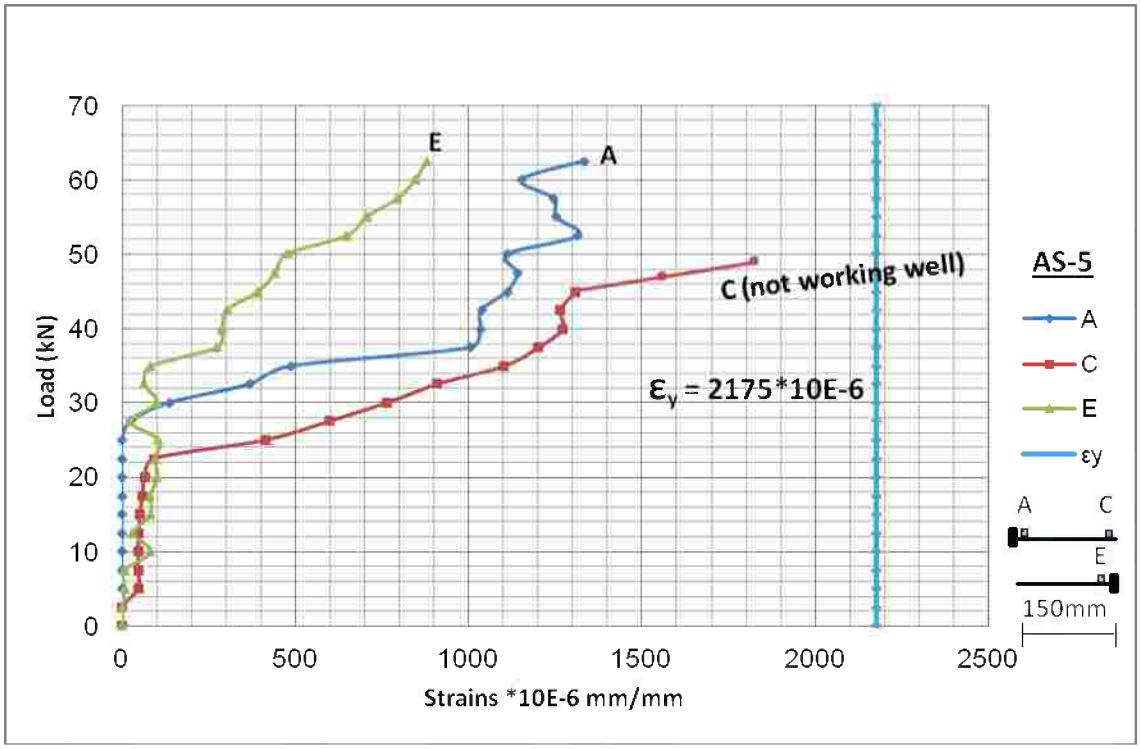

Figure (4-36): Relation between steel strain and load of slab **AS-5** (15 d_b), Group (2).

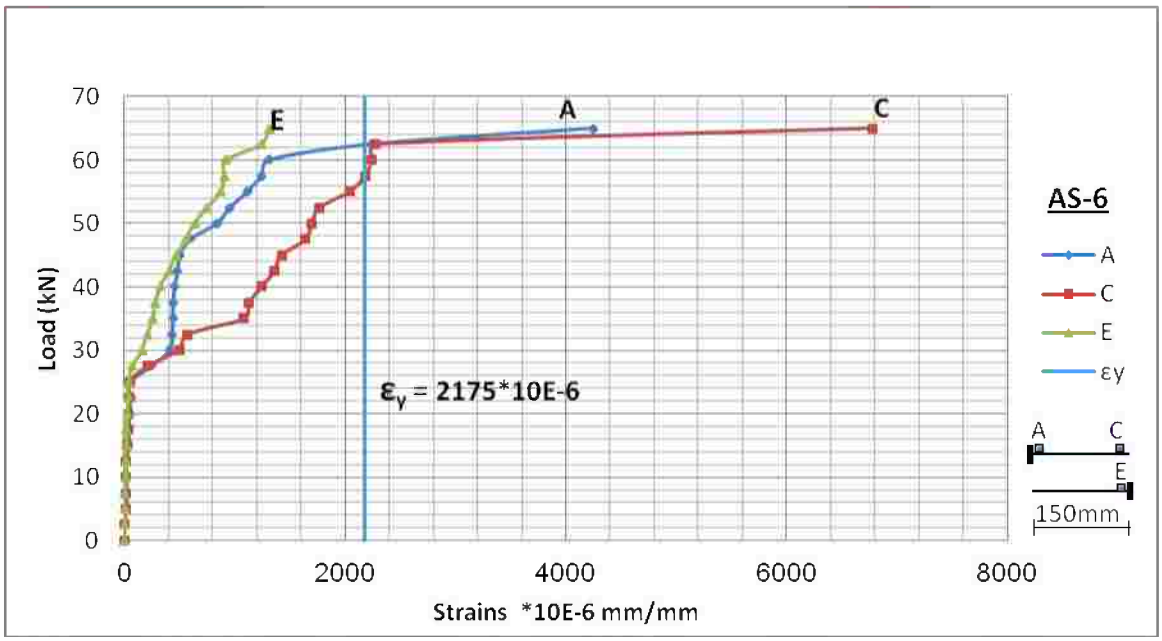

Figure (4-37): Relation between steel strain and load of slab **AS-6** (15 d_b), Group (2).

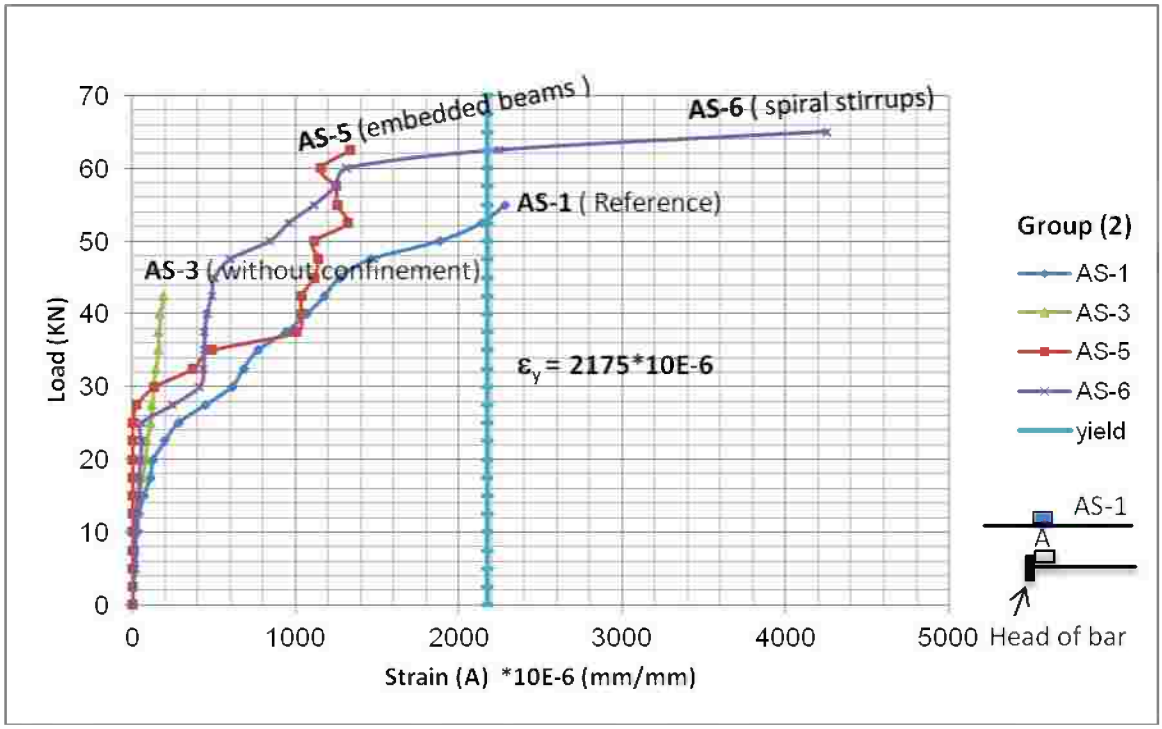

Figure (4-38): Relation between Strain (A) and load for slabs of Group (2).

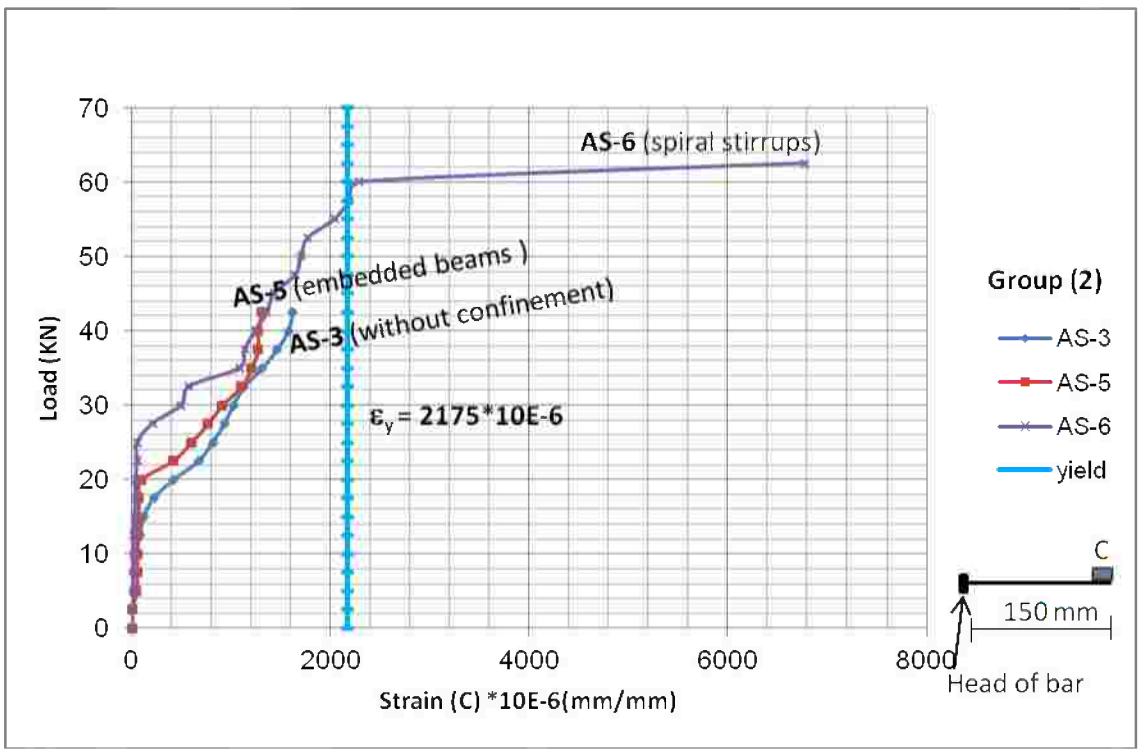

Figure (4-39): Relation between Strain (C) and load for slabs of Group (2).

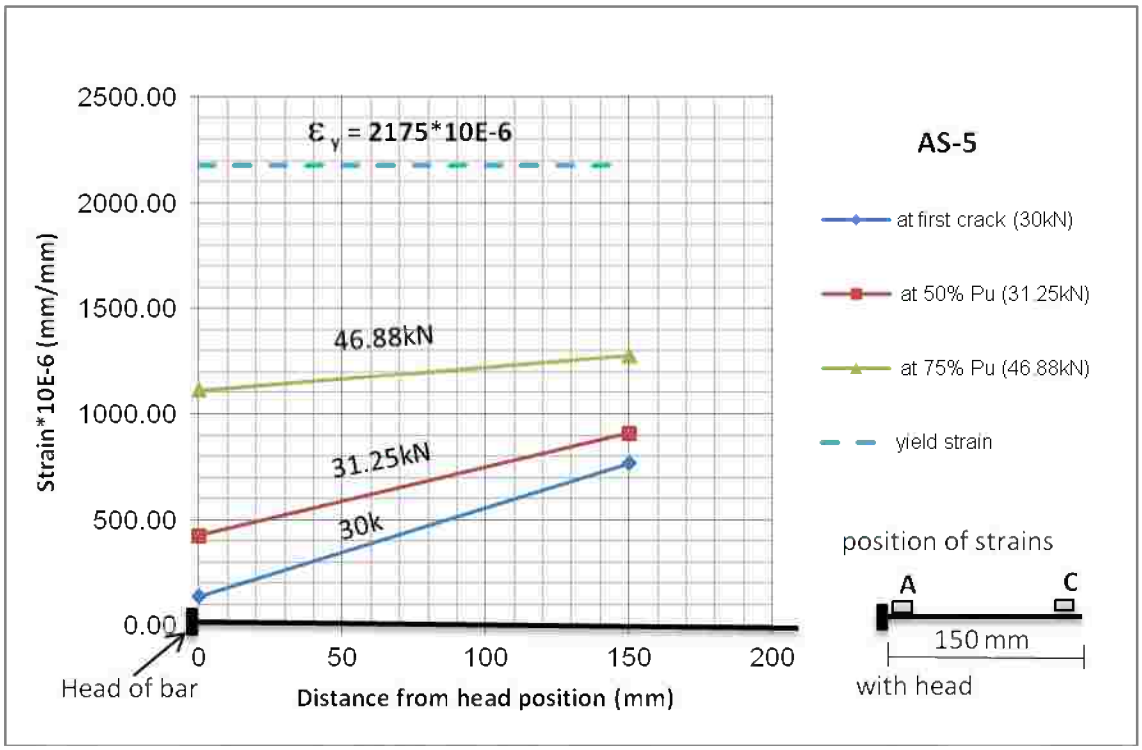

Figure (4-40): Strain distribution along the splice zone of slab **AS-5** at different loads.

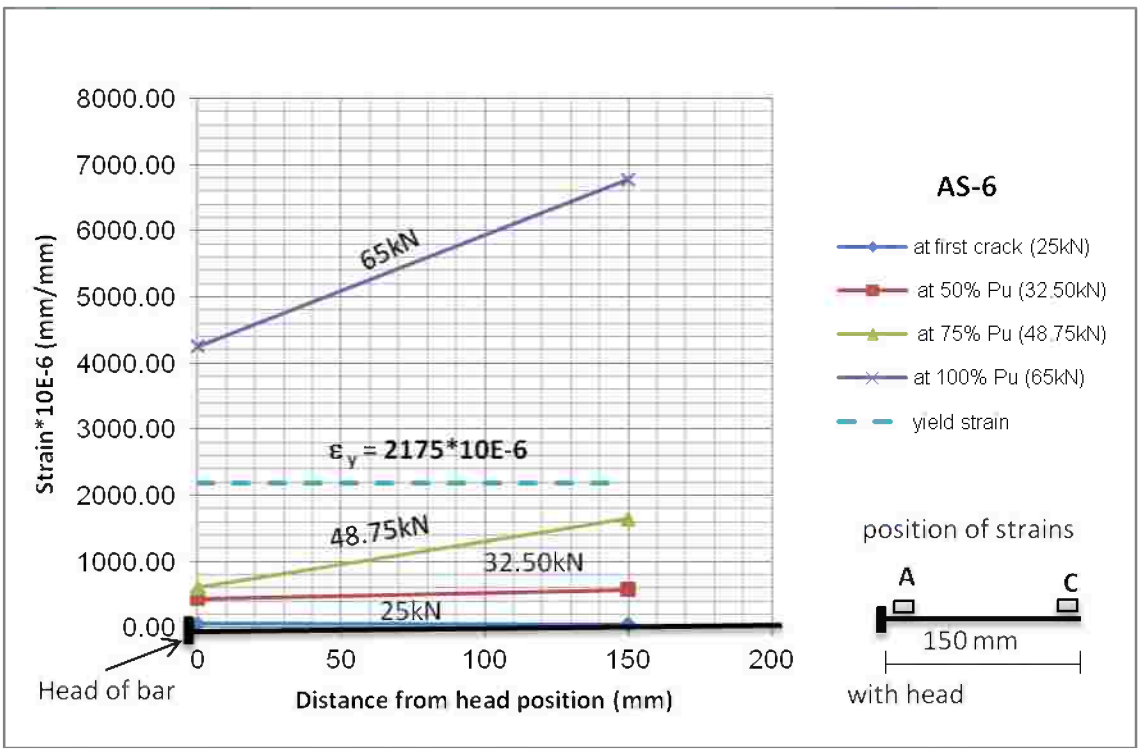

Figure (4-41): Strain distribution along the splice zone of slab **AS-6** at different loads.

(a): Cracks on the side face.

(b): Cracks close to the end of the lap zone.

(c): Cracks on the bottom surface close to lap zone before failure.

Figure (4-42): The crack pattern of **AS-4**.

(a): Bottom cover spalling in lap zone just before failure.

(b): Specimen just after the failure.

(c): The concrete around the debonded lap zone just after failure.

Figure (4-43): Failure of the lap splice of slab **AS-4**.

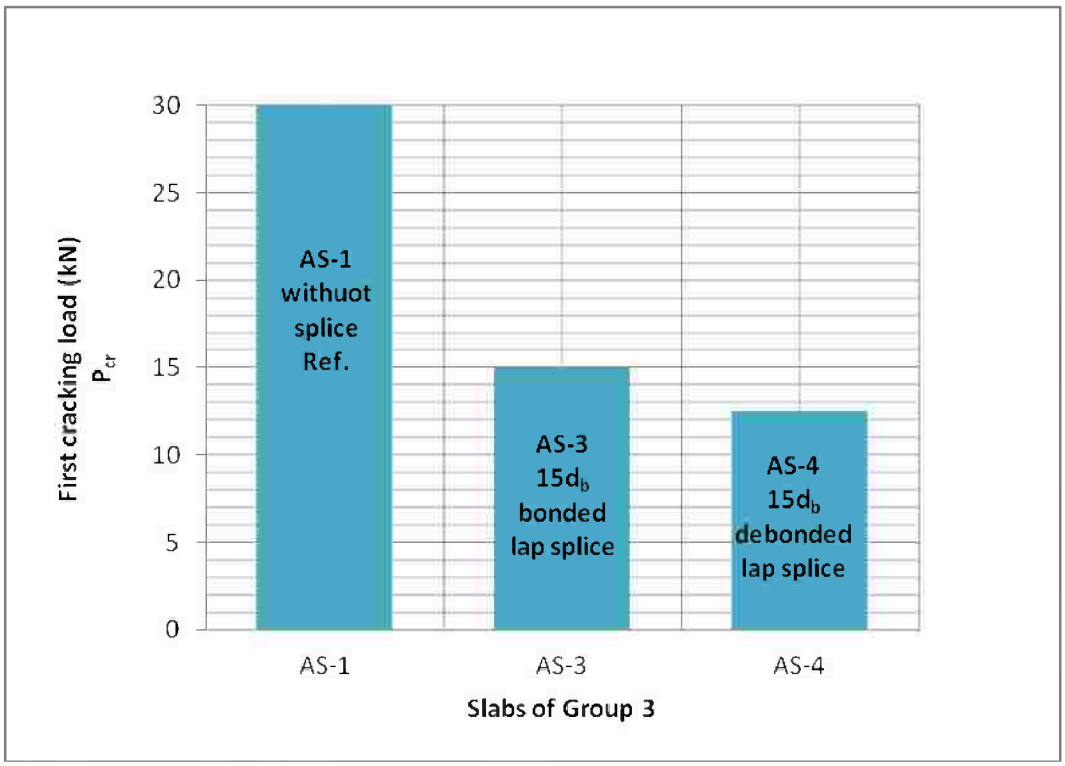

Figure (4-44): First cracking loads for slabs of Group (3).

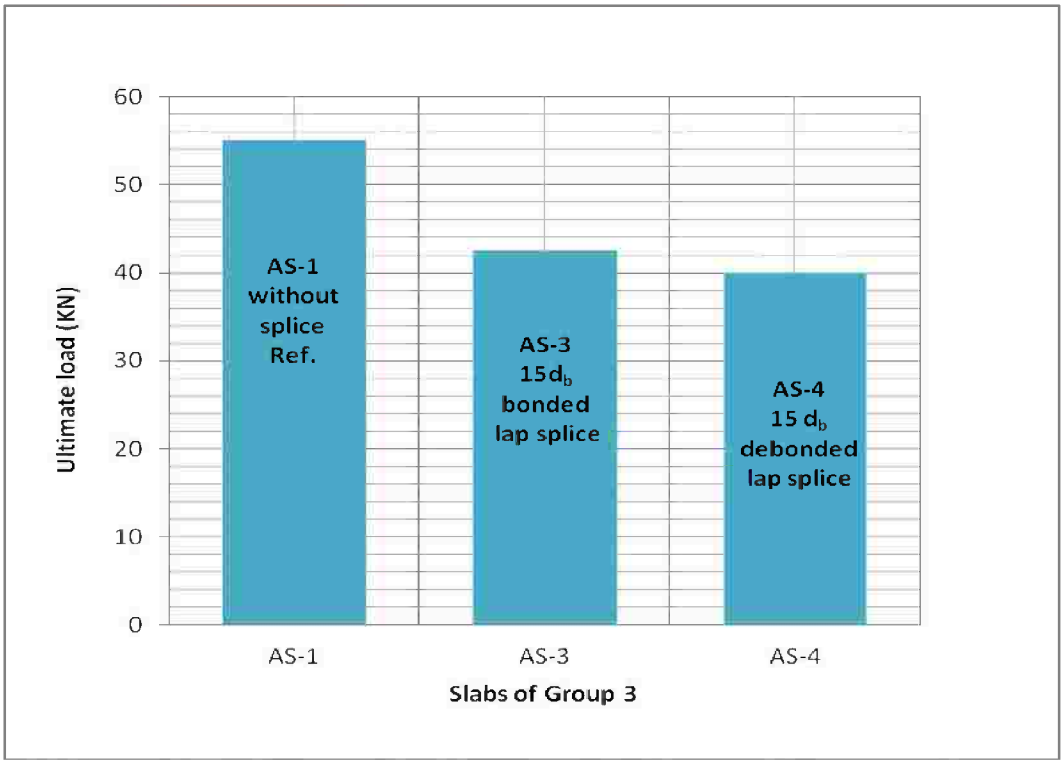

Figure (4-45): Failure loads for slabs of Group (3).

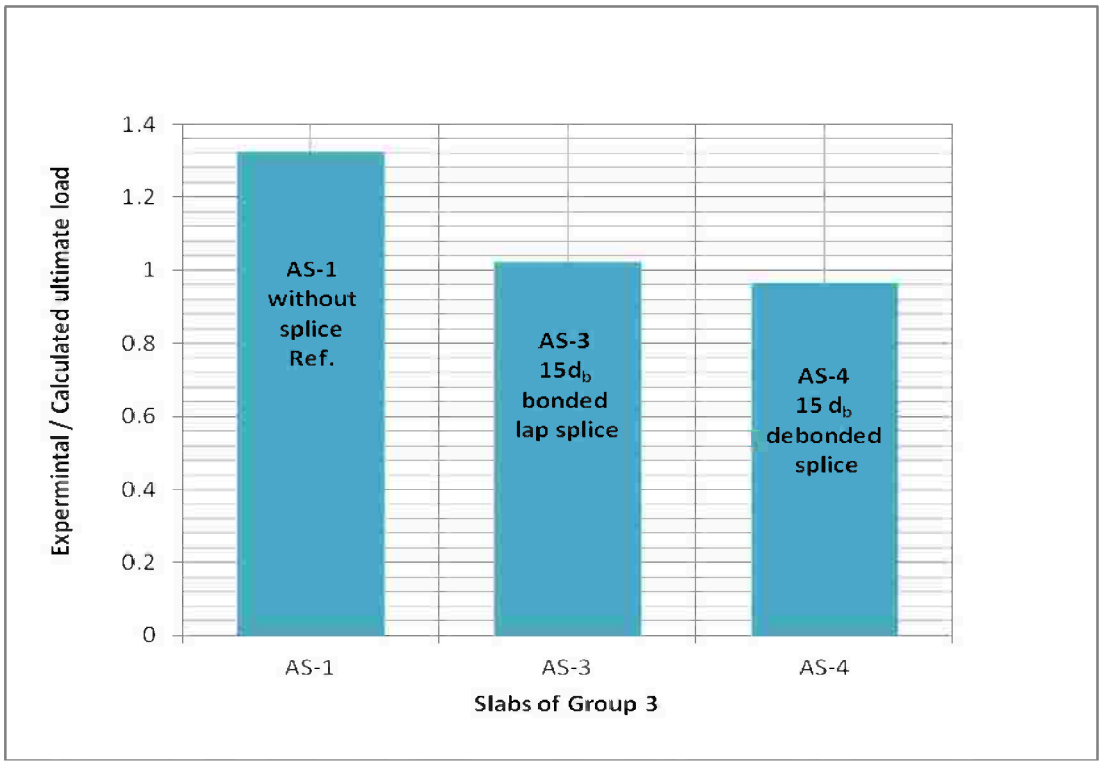

Figure (4-46): (Experimental / Calculated) ultimate loads for slabs of Group (3)

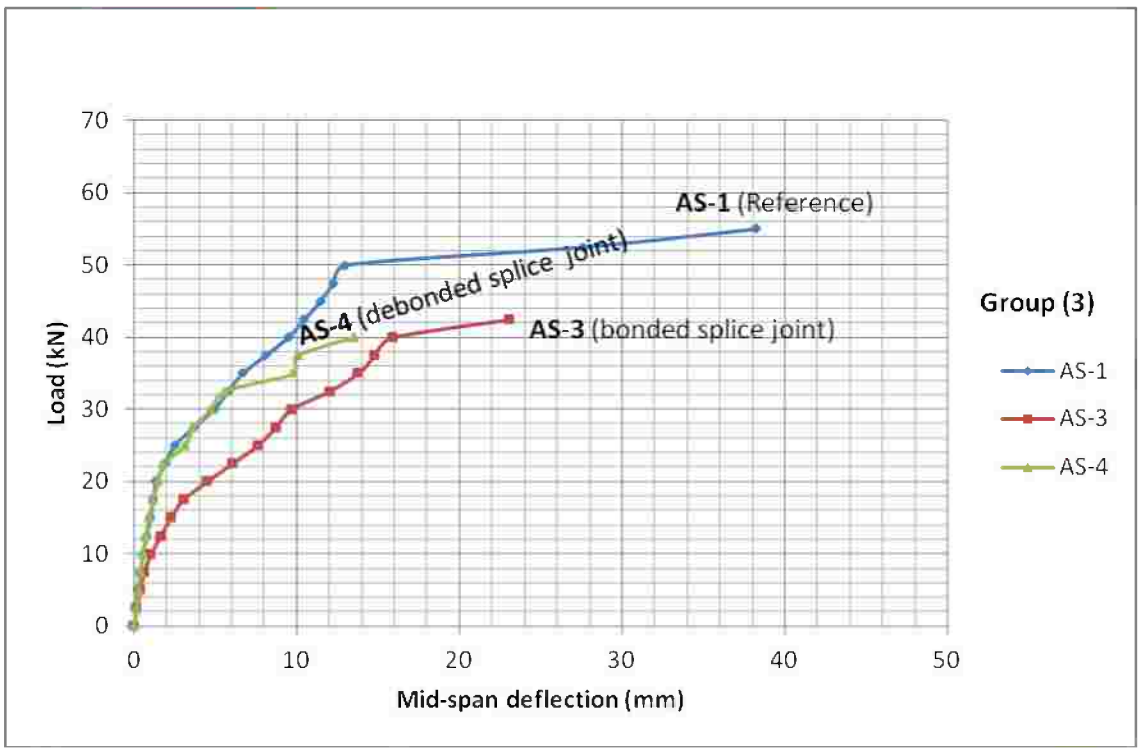

Figure (4-47): Relation between mid-span deflection and load for slabs of Group (3) (dial No.2).

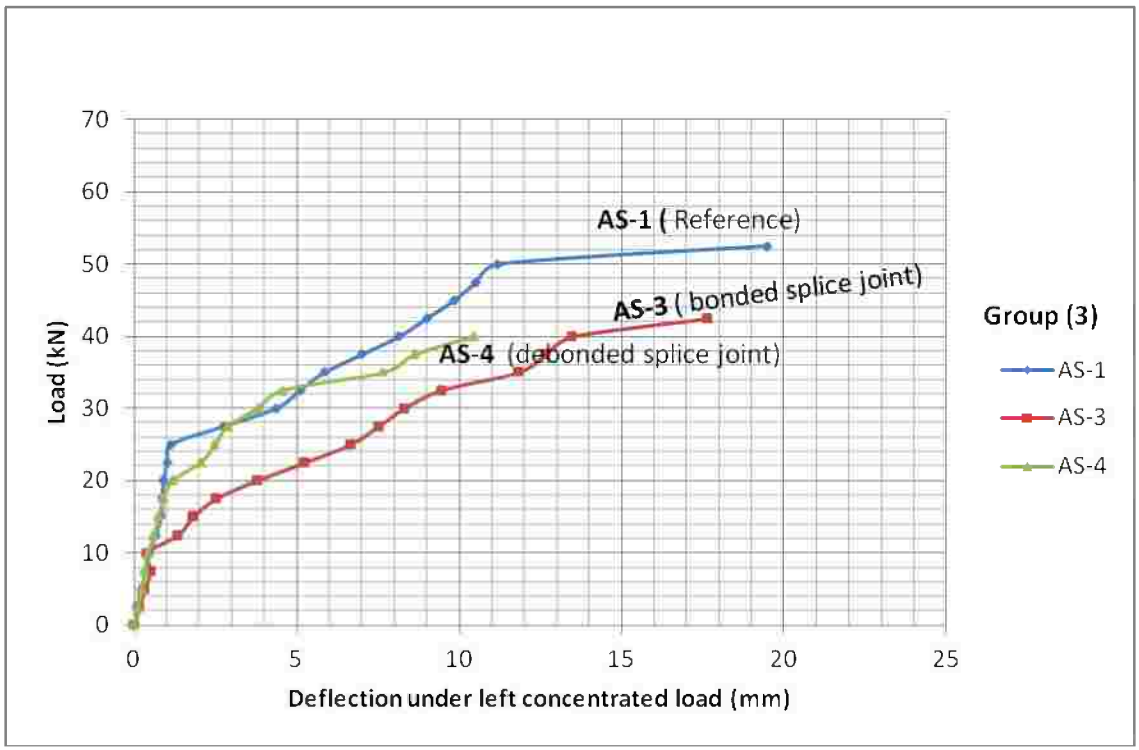

Figure (4-48): Relation between load and deflection under left concentrated load of Group (3) (dial No.1).

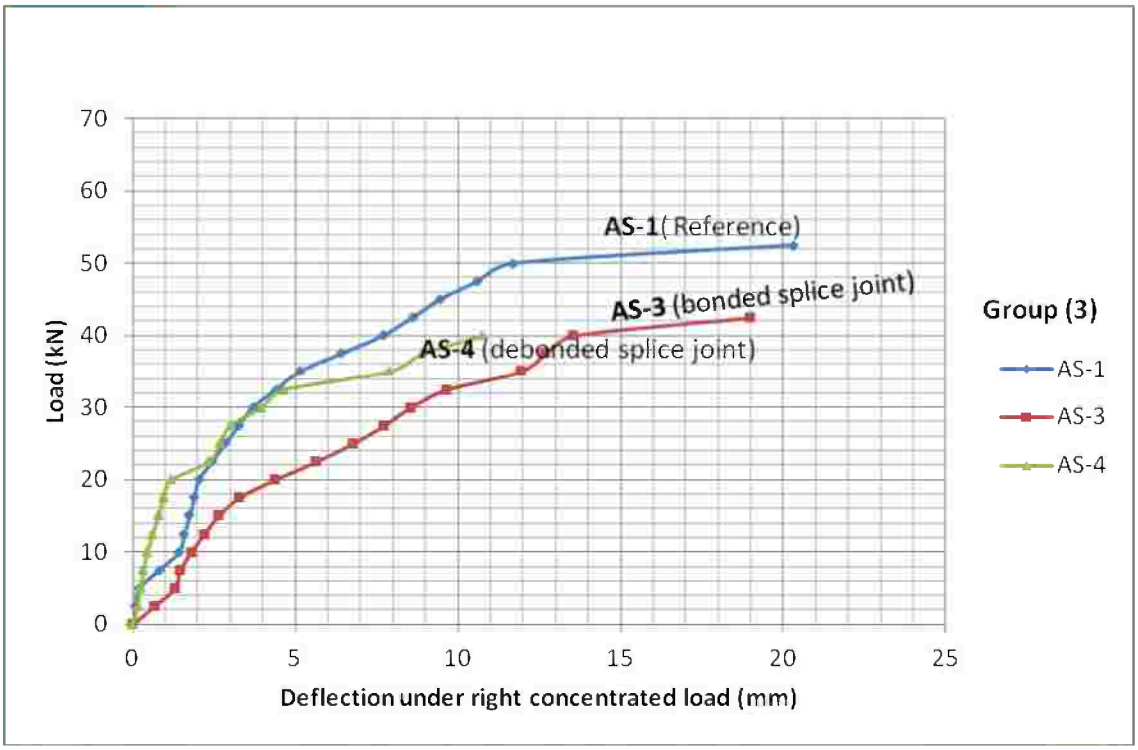

Figure (4-49): Relation between load and deflection under right concentrated load of Group (3) (dial No.3).

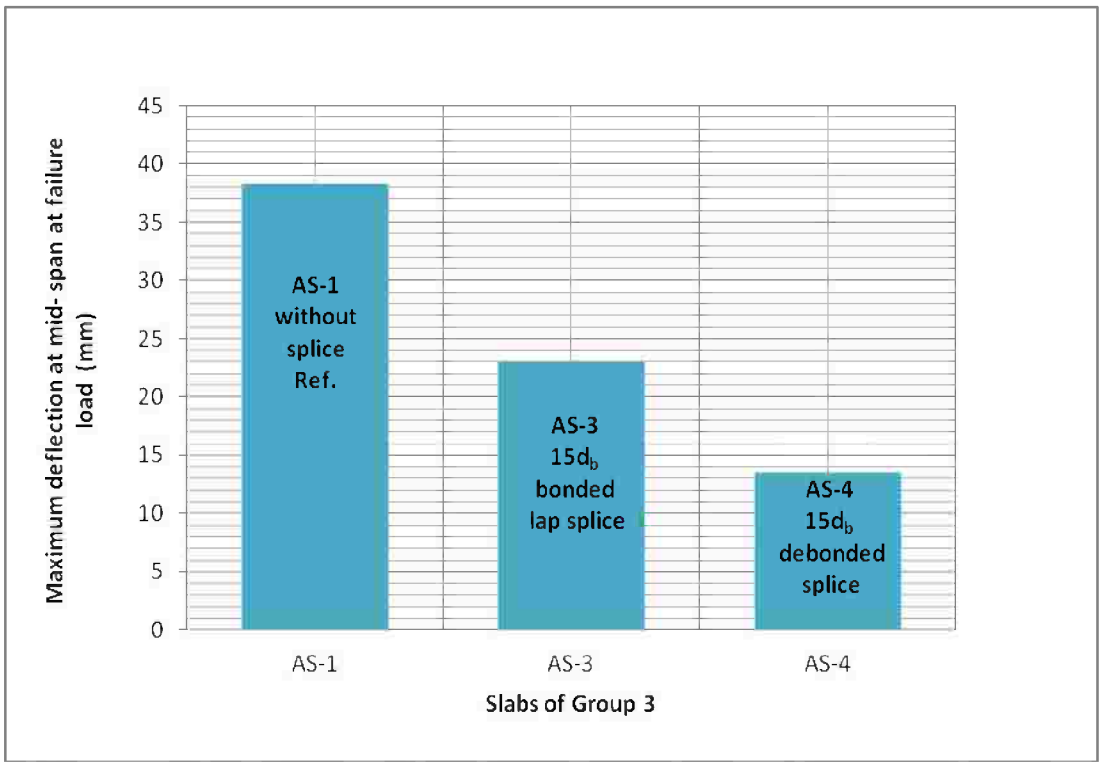

Figure (4-50): Maximum deflection at mid-span at failure load for slabs of Group (3).

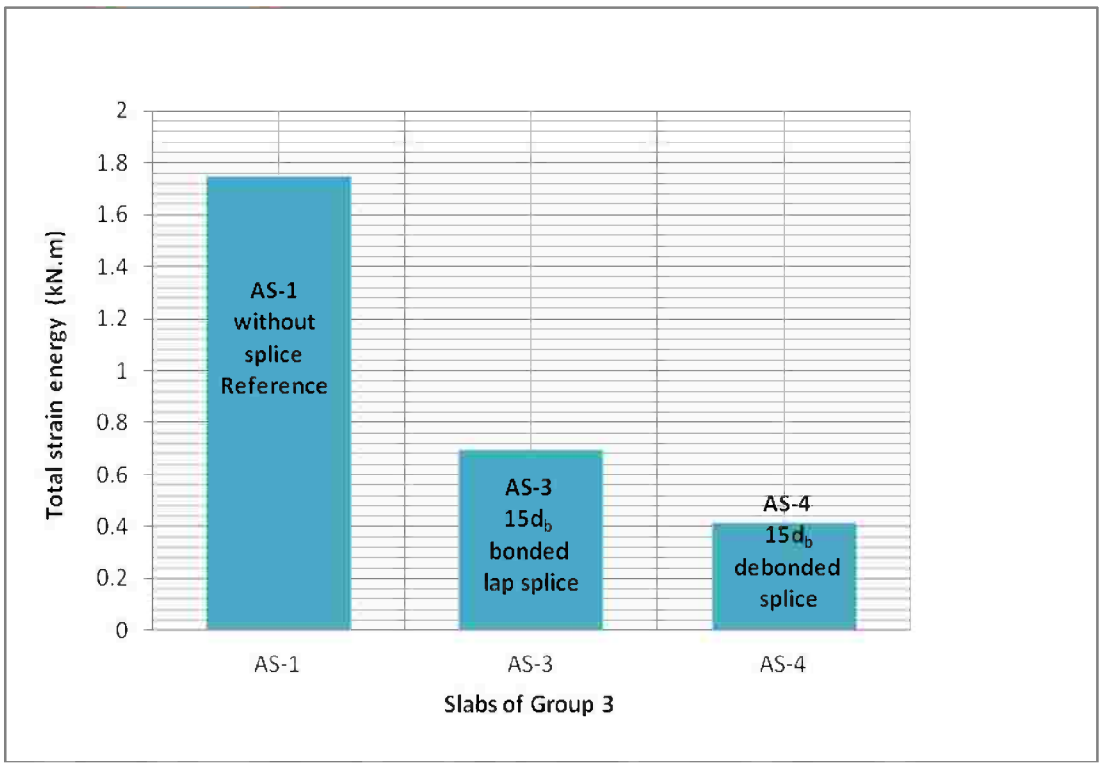

Figure (4-51): Total strain energy for slabs of Group (3).

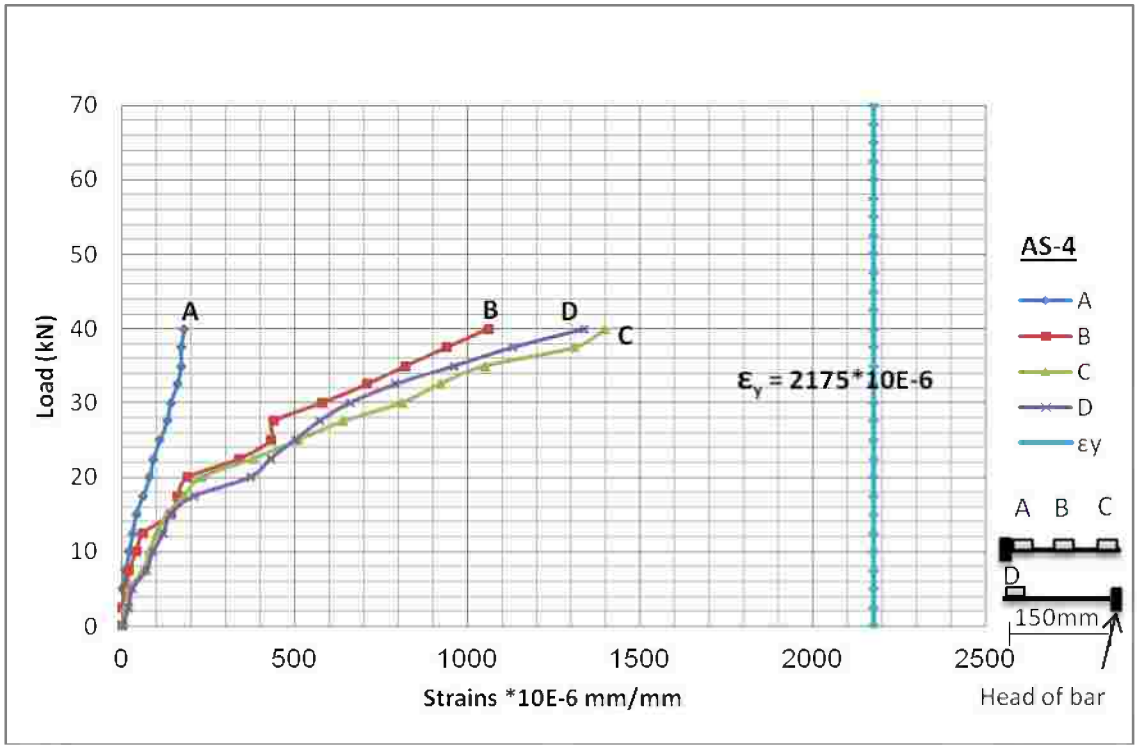

Figure (4-52): Relation between steel strain and load of slab **AS-4** (15 d_b), Group (3).

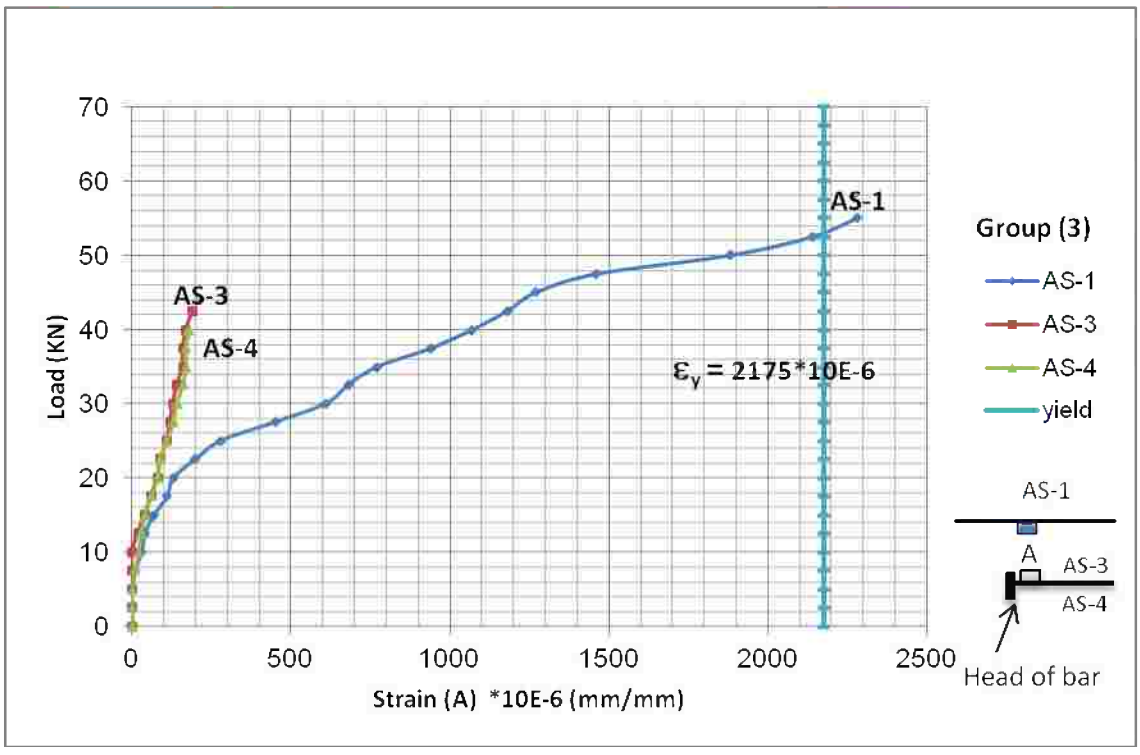

Figure (4-53): Relation between Strain (A) and load for slabs of Group (3).

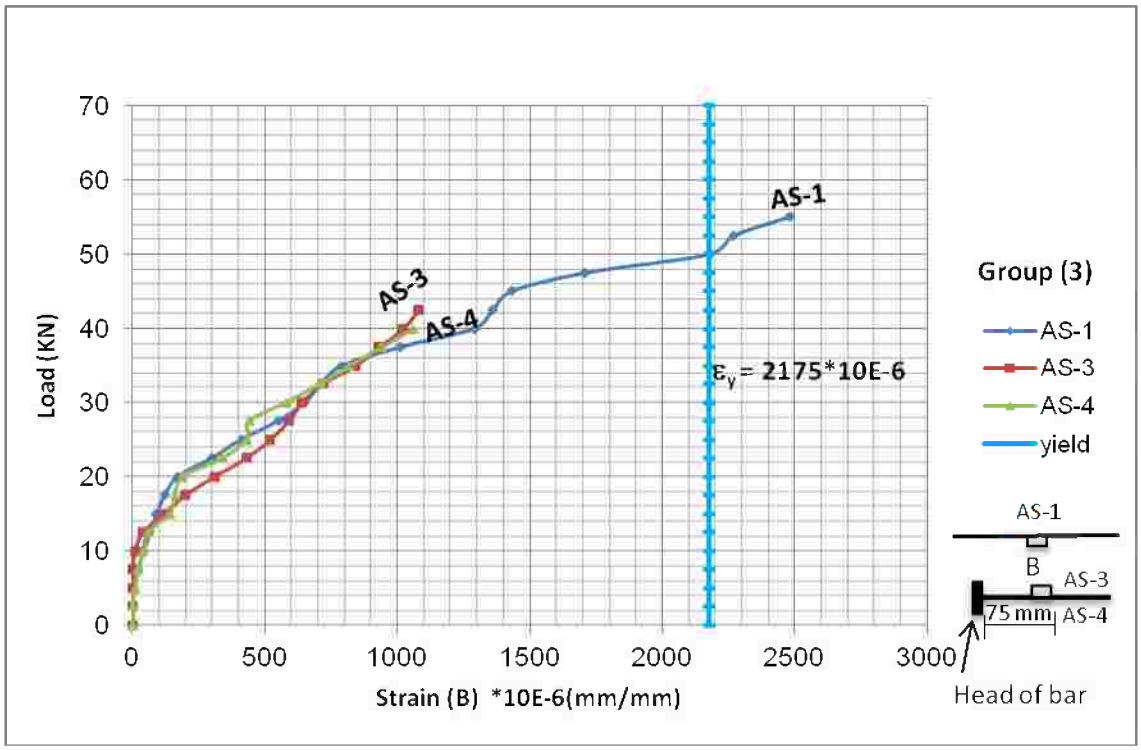

Figure (4-54): Relation between Strain (B) and load for slabs of Group (3).

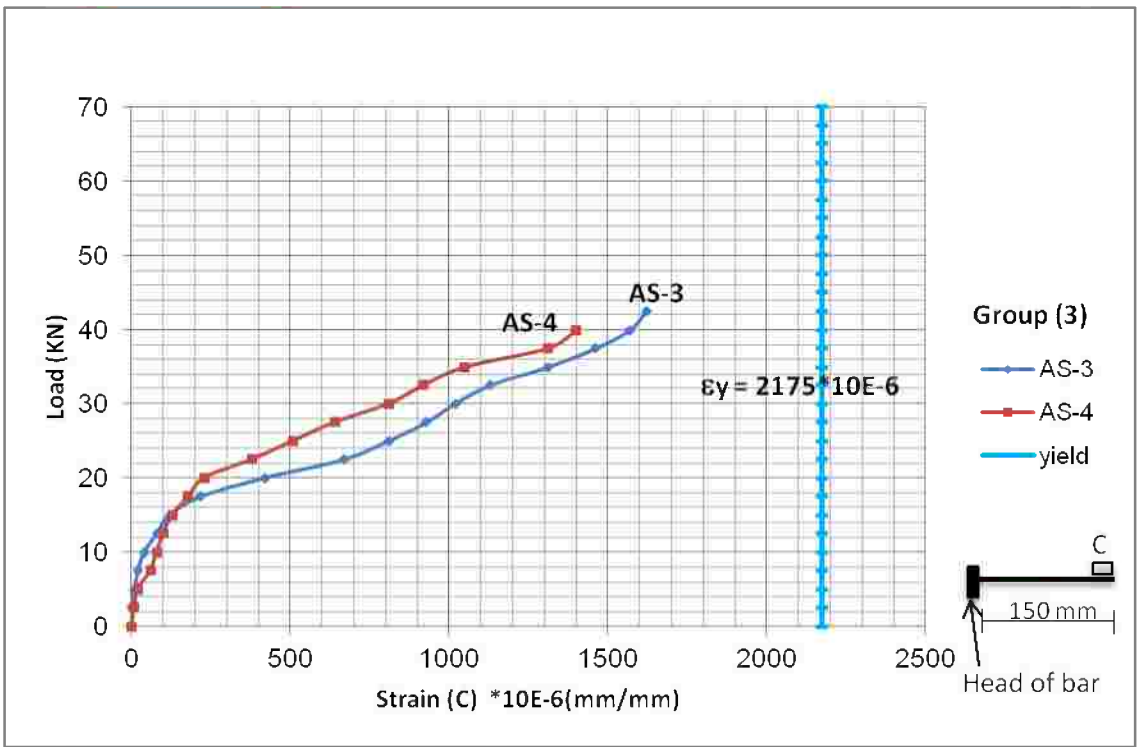

Figure (4-55): Relation between Strain (C) and load for slabs of Group (3).

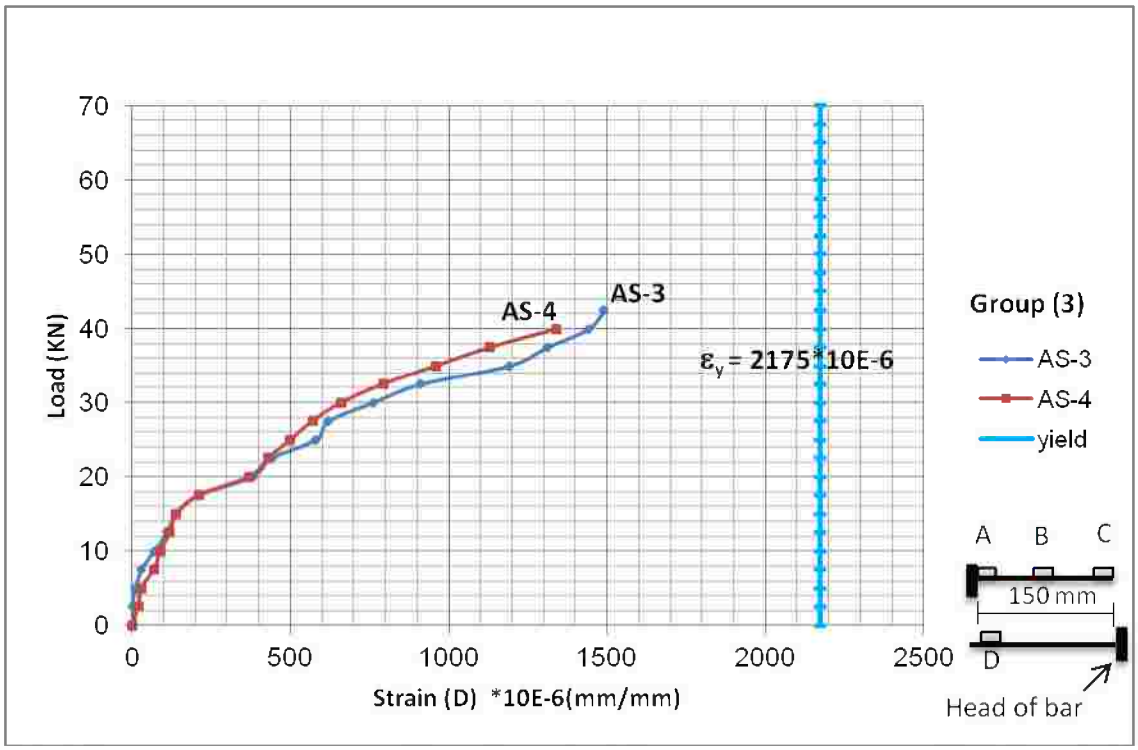

Figure (4-56): Relation between Strain (D) and load for slabs of Group (3).

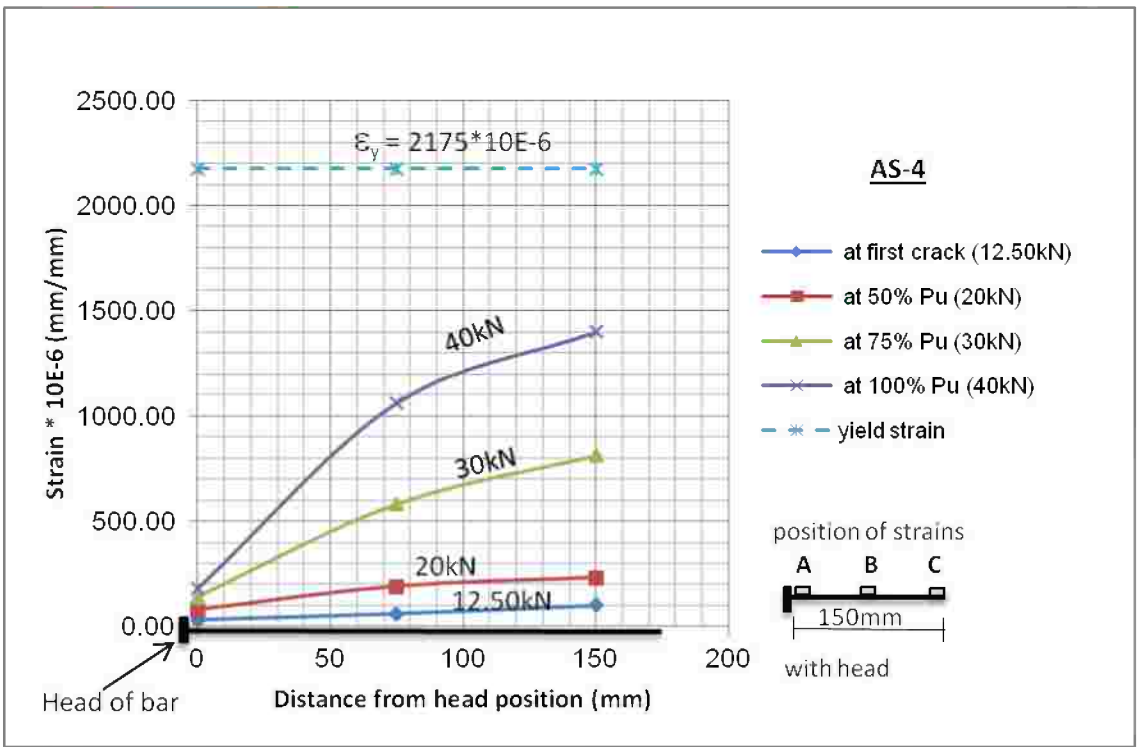

Figure (4-57): Strain distribution along the splice zone of slab **AS-4** at different loads.

(a): Cracks on the side face at failure.

(b): Cracks close to confined lap zone.

(c): Cracks on the bottom surface of slab **AS-8** confined with embedded beams around bar heads at failure.

Figure (4-58): The crack pattern of **AS-8**.

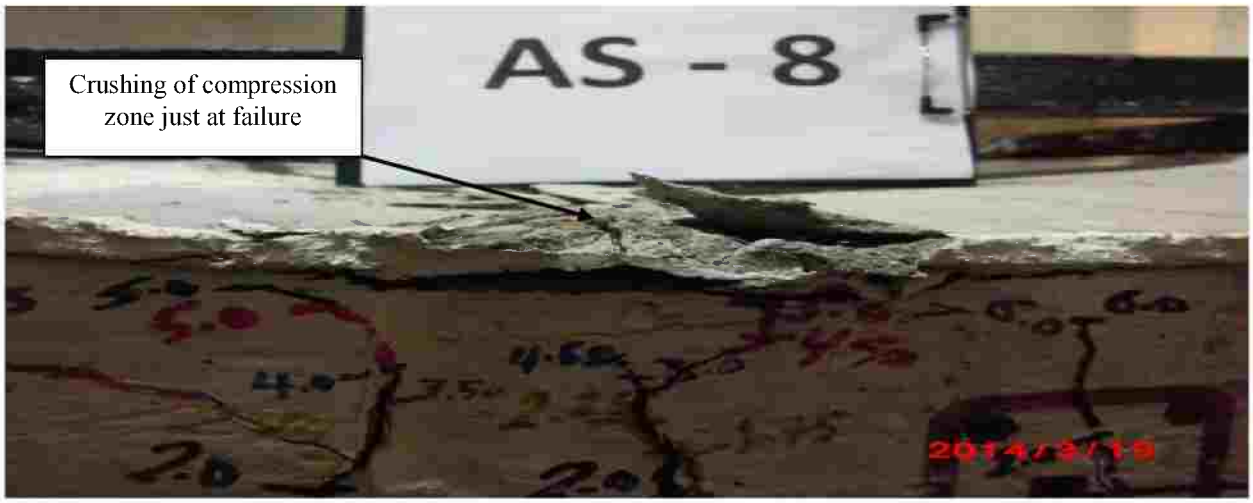

(a): Splitting and crushing compression zone just at failure.

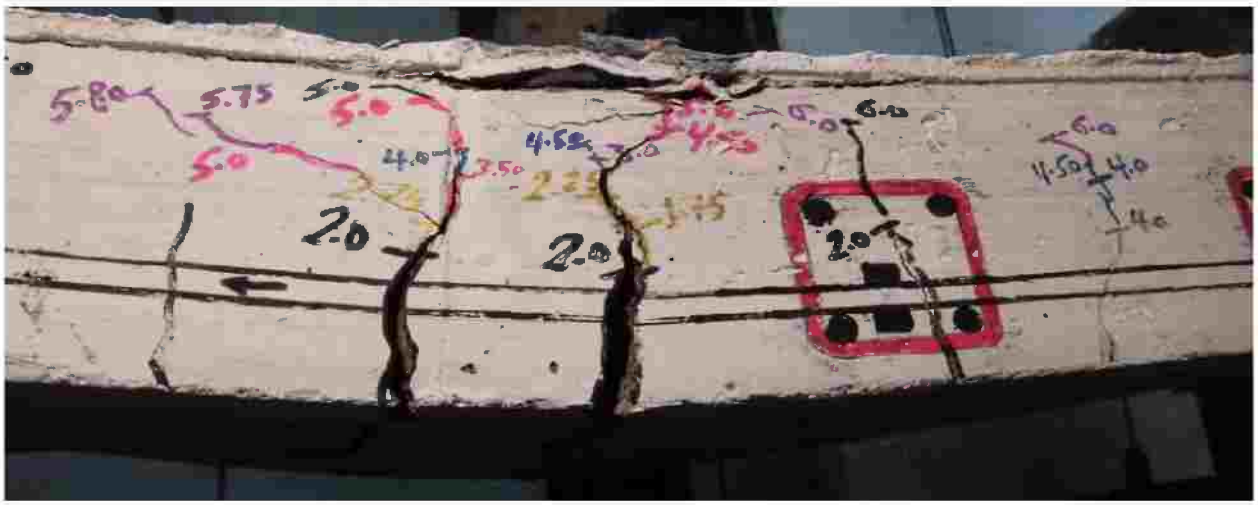

(b) :Cracks became wider and extensive outside of confined lap zone just at failure.

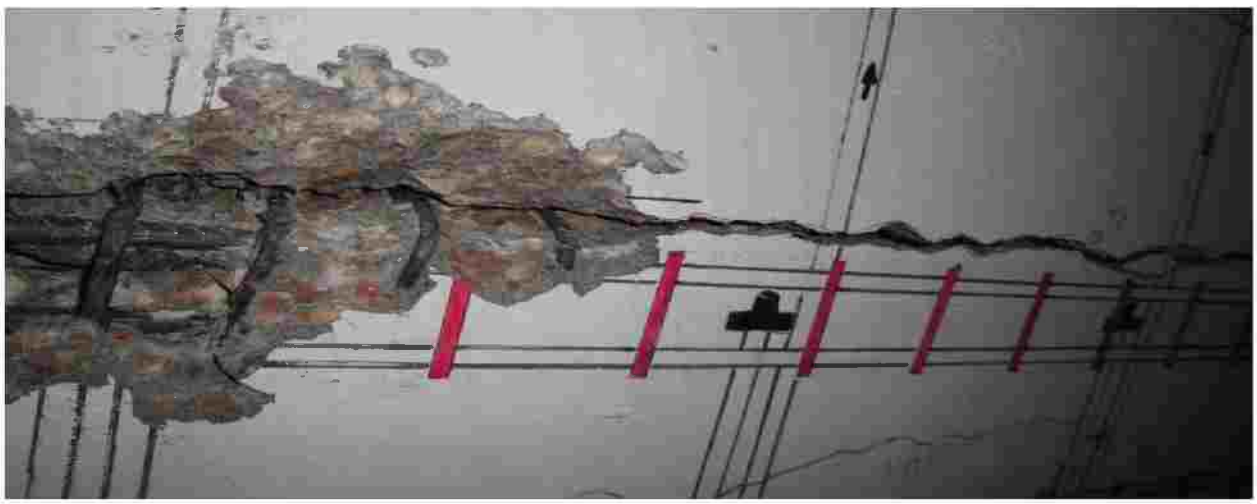

(c): The concrete around confined zone after cover removed over confined lap zone.

Figure (4-59): Failure of the confined splice slab **AS-8**.

(a): Cracks on the side face.

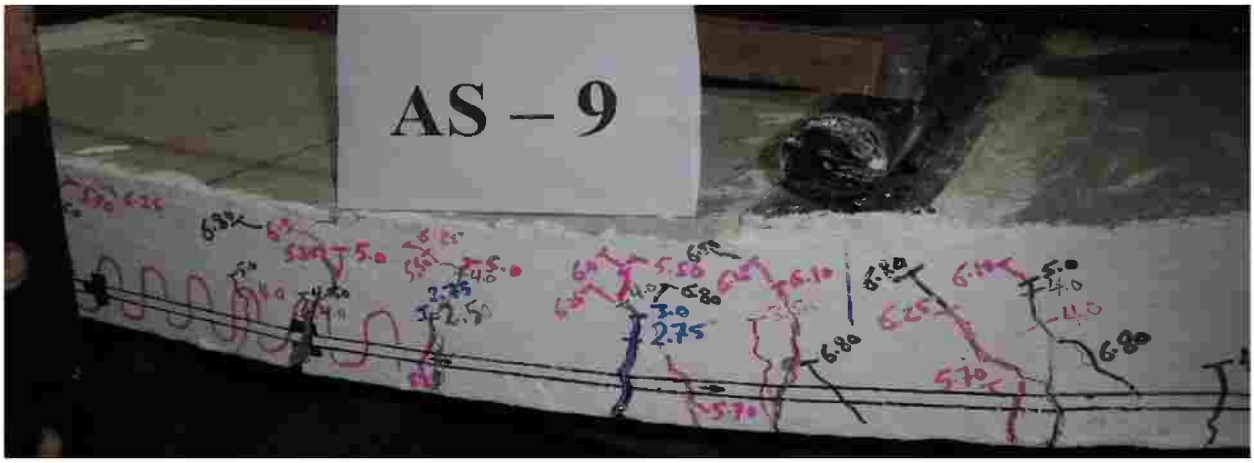

(b): Cracks close to the bar head.

(c): Cracks on the bottom surface of the slab confined by circular spiral stirrups in lap zone at failure.

Figure (4-60): The crack pattern of **AS-9**.

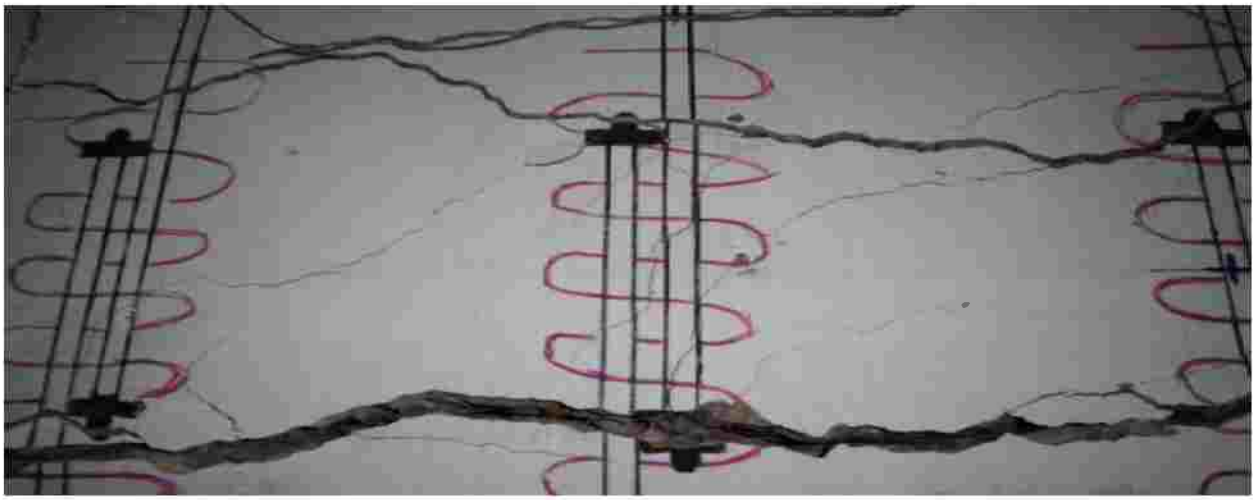

(a) :Cracks became wider and extensive around of confined lap zone at failure.

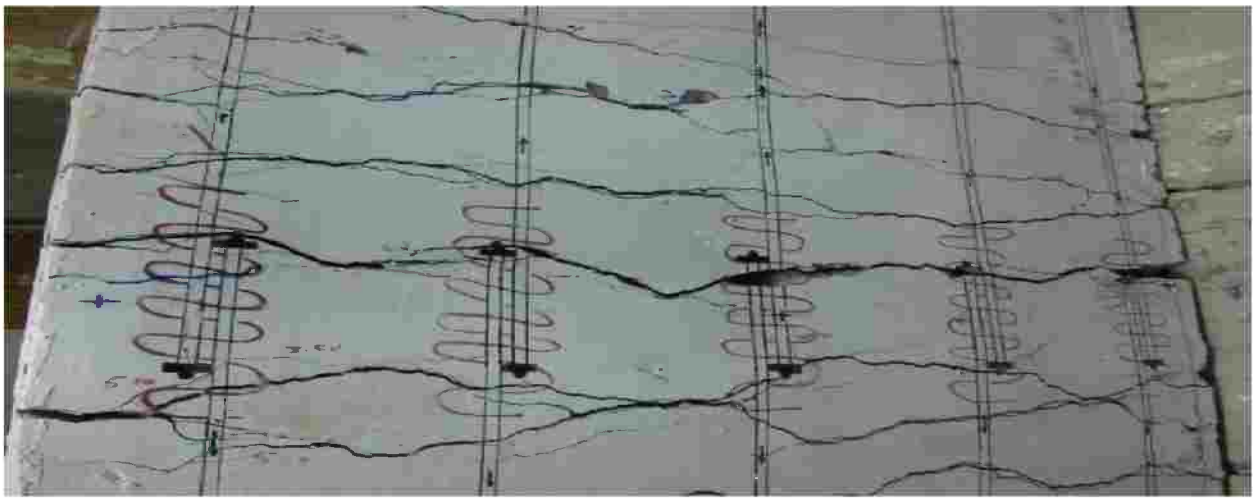

(b) :Lap zone after finished test and before removed cover.

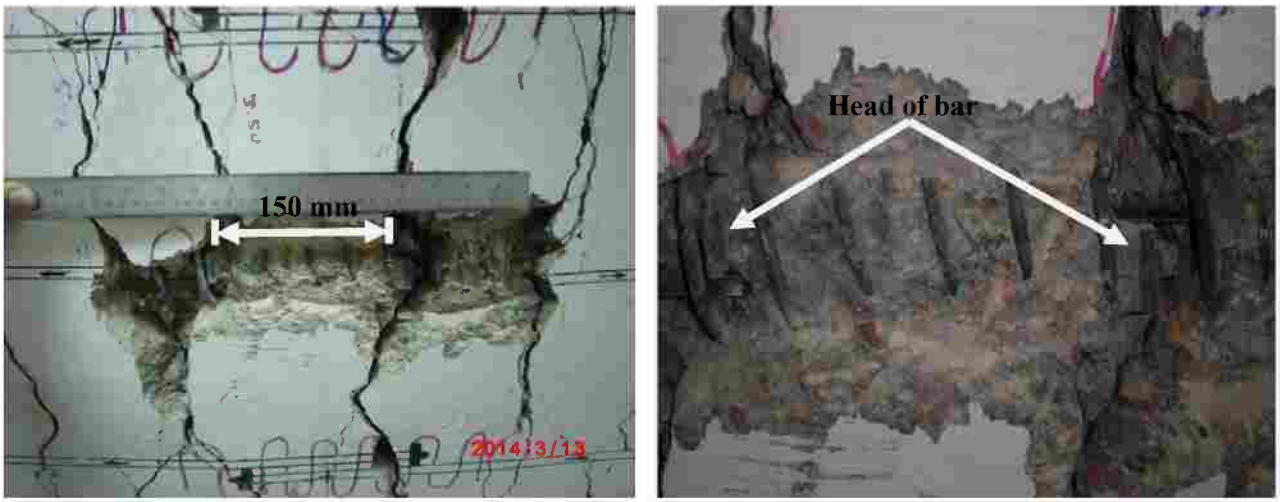

(c): The concrete around confined zone after removal cover in confined lap zone.

Figure (4-61): Failure of the confined splice slab **AS-9**.

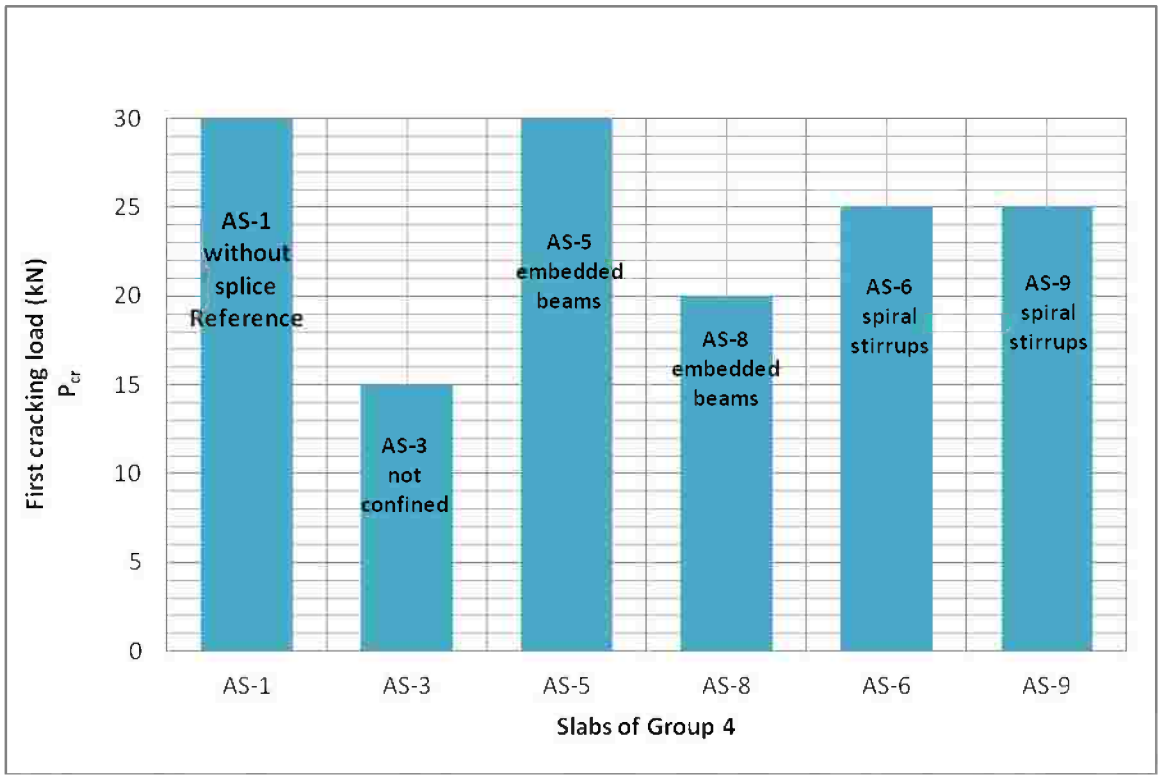

Figure (4-62): First cracking loads for slabs of Group (4).

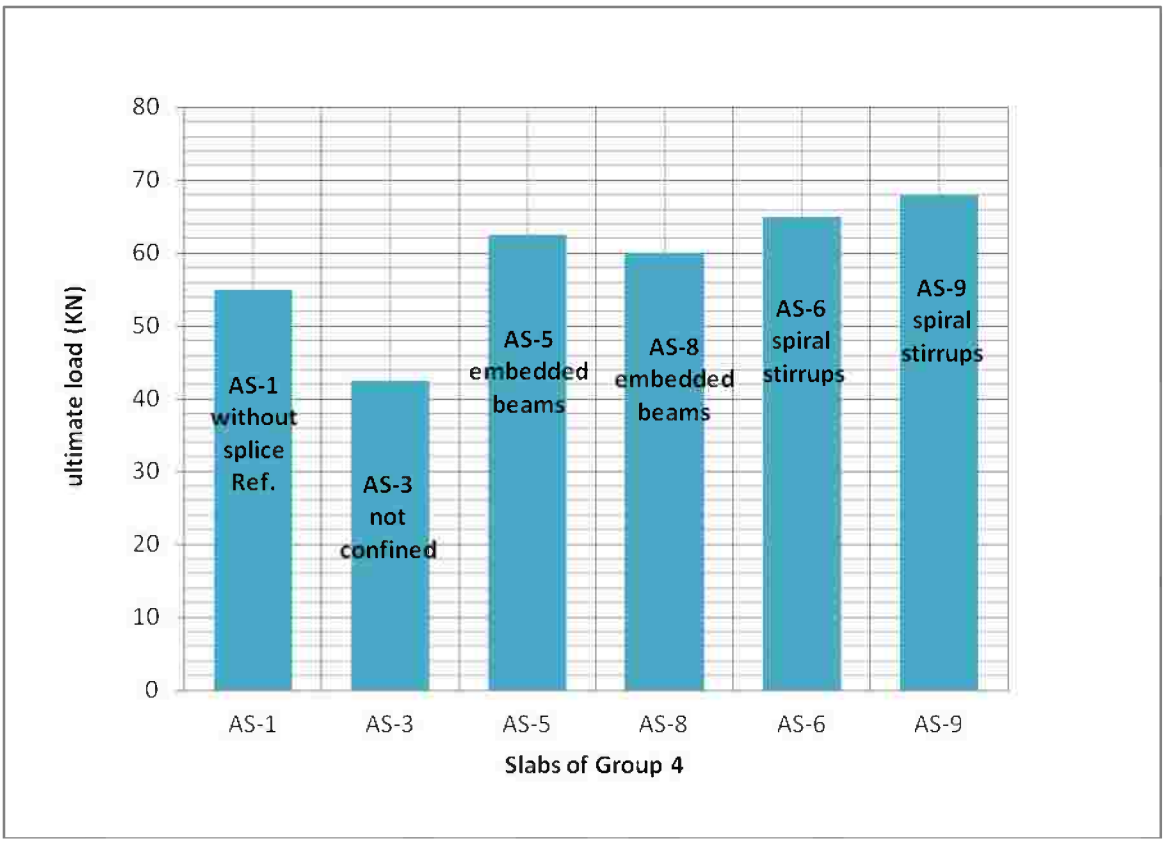

Figure (4-63): Failure loads for slabs of Group (4).

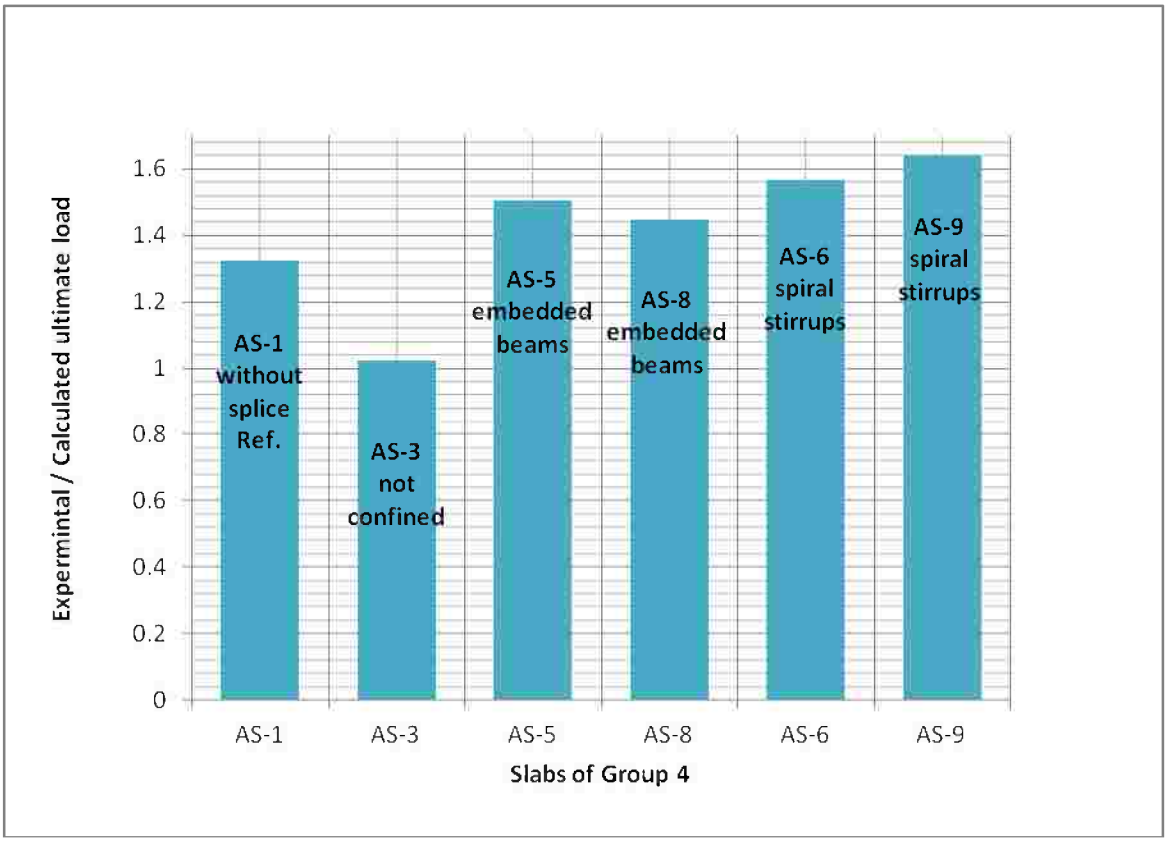

Figure (4-64): (Experimental / Calculated) ultimate loads for slabs of Group (4).

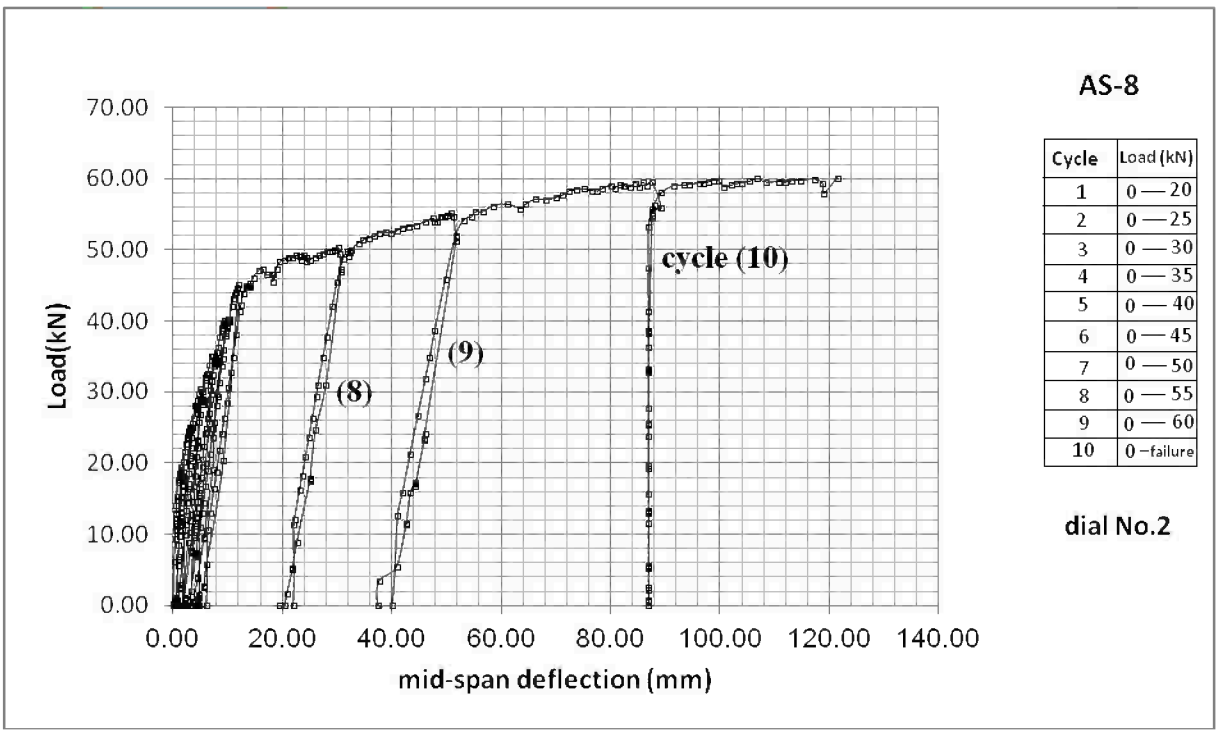

Figure (4-65): Repeated loading on slab **AS-8**, 10 cycles of loading.

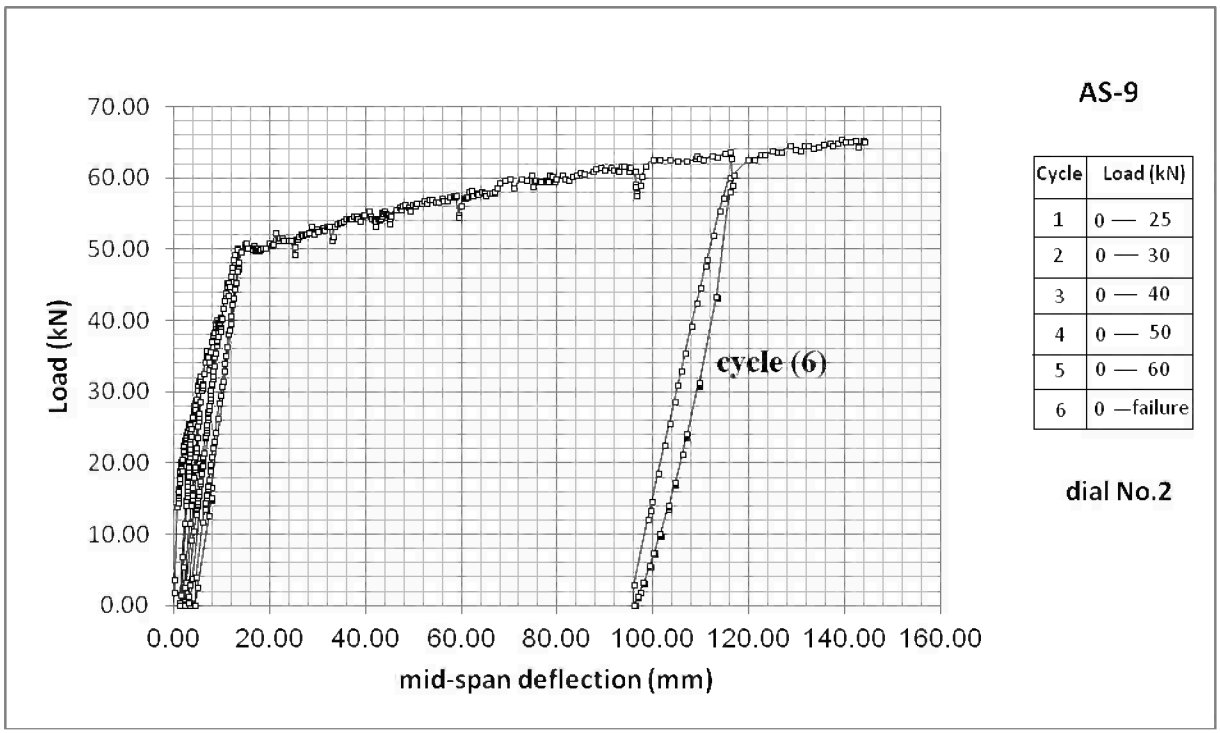

Figure (4-66): Repeated loading on slab **AS-9**, 6 cycles of loading.

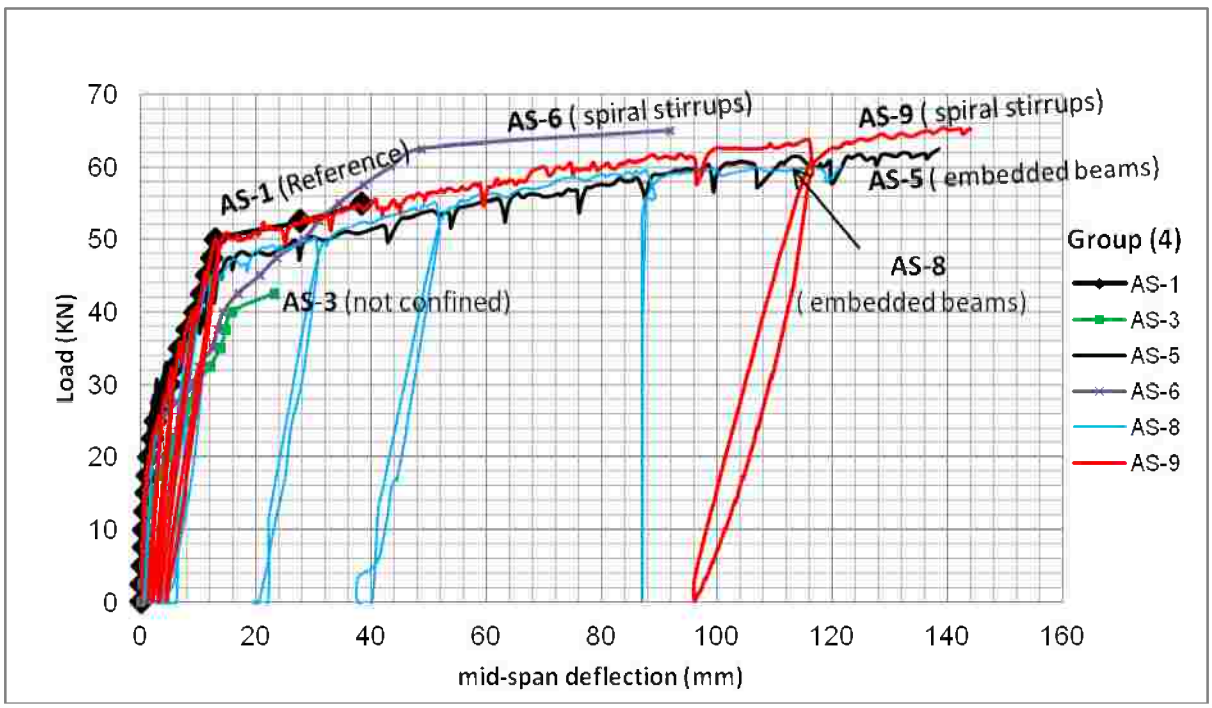

Figure (4-67): Relation between mid-span deflection and load for slabs of Group (4) (dial No.2)

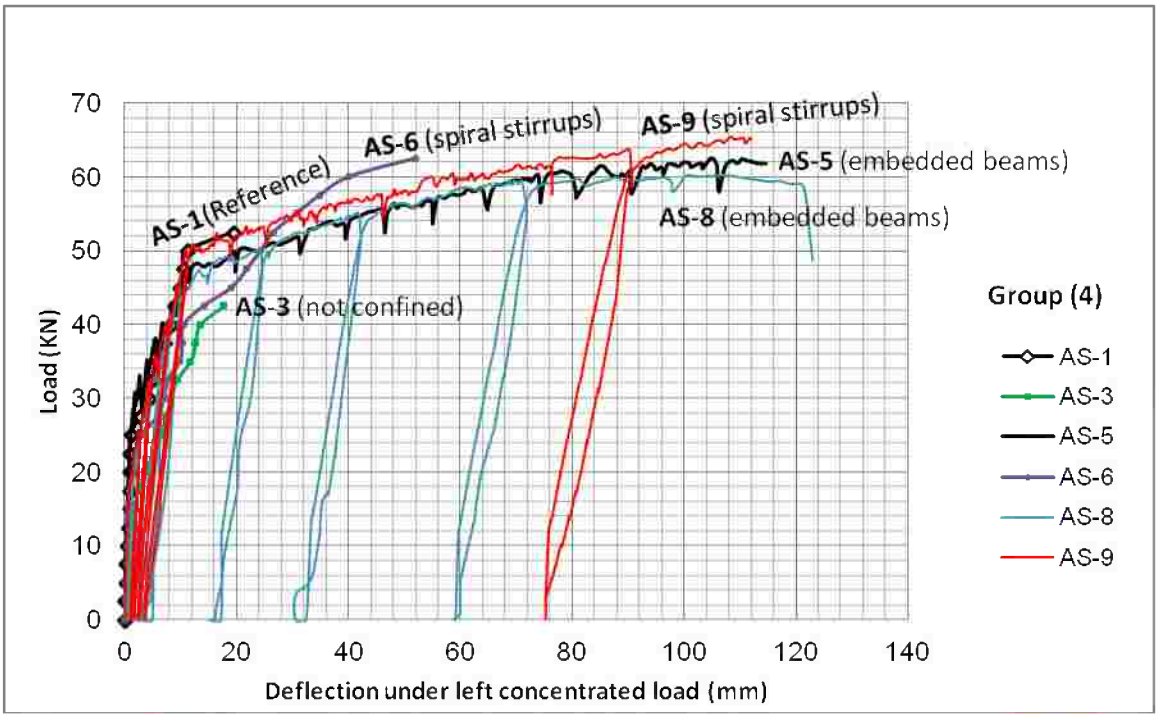

Figure (4-68): Relation between load and deflection under left concentrated load of Group (4) (dial No.1).

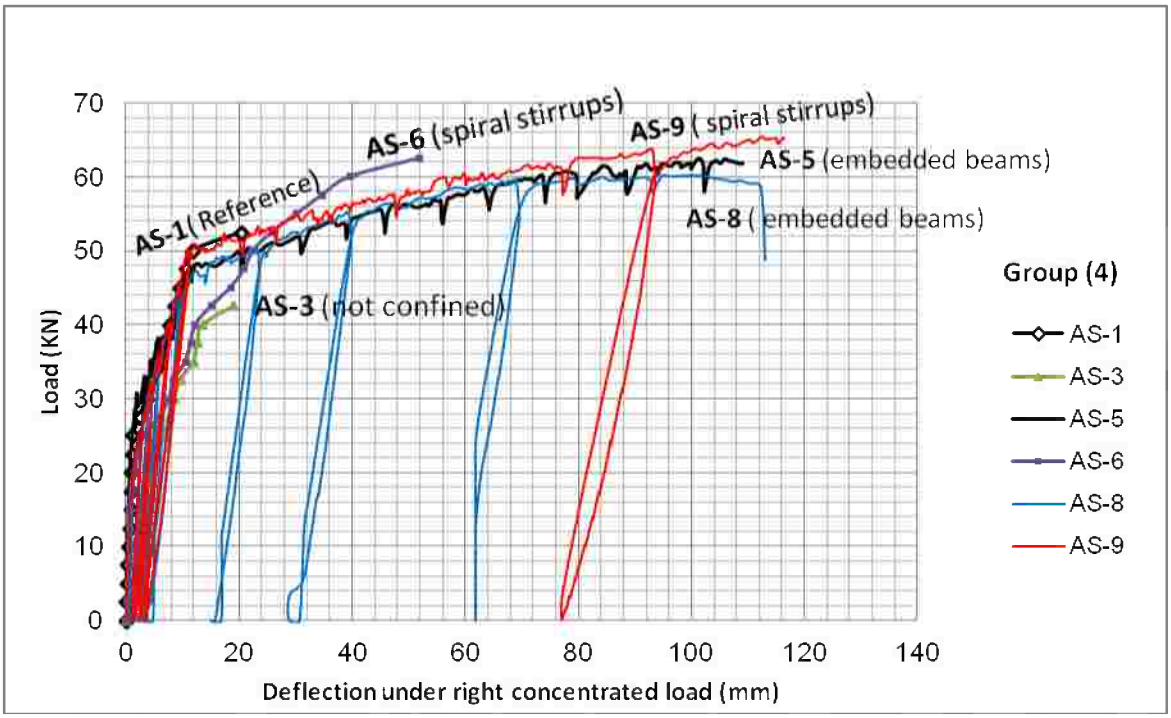

Figure (4-69): Relation between load and deflection under right concentrated load of Group (4) (dial No.3).

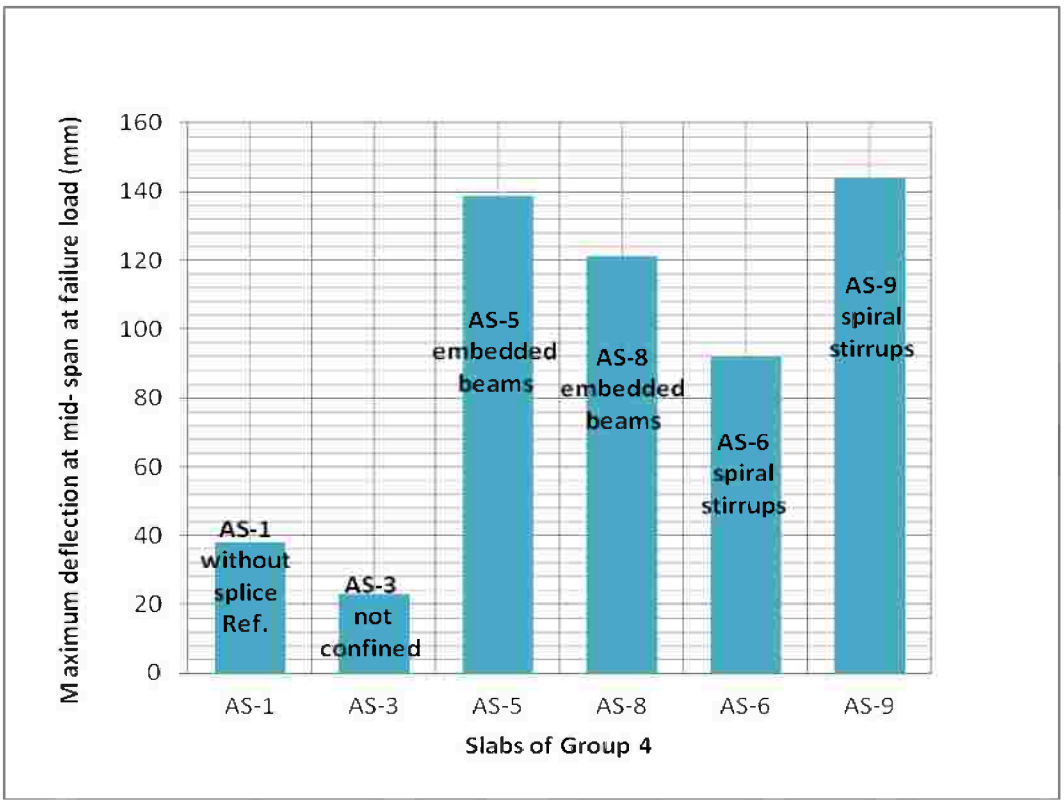

Figure (4-70): Maximum deflection at mid-span at failure load for slabs of Group (4).

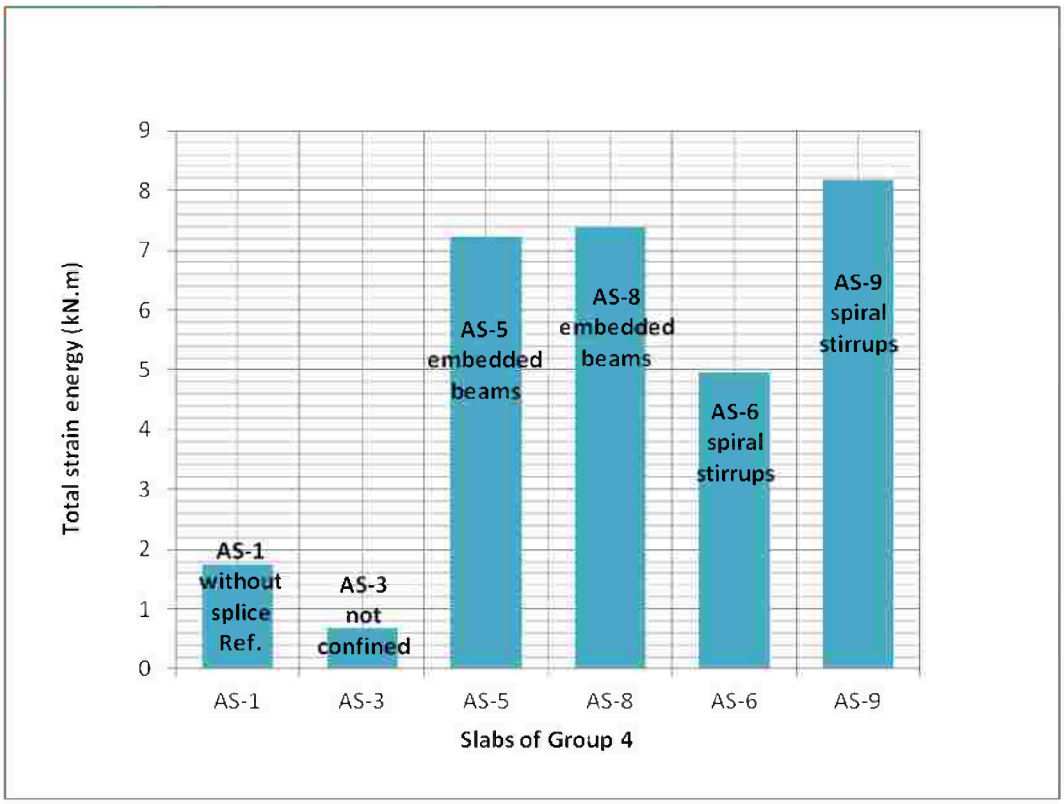

Figure (4-71): Total strain energy for slabs of Group (4).

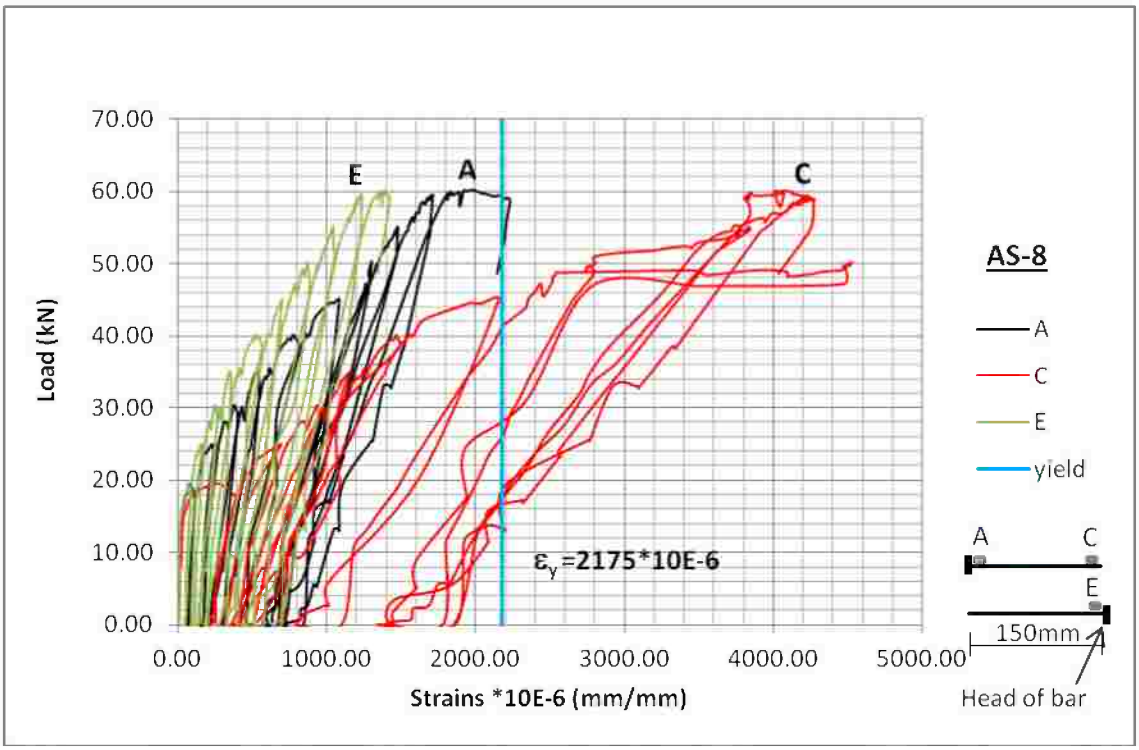

Figure (4-72): Relation between steel strain and load of slab **AS-8** (15 d_b), Group (4).

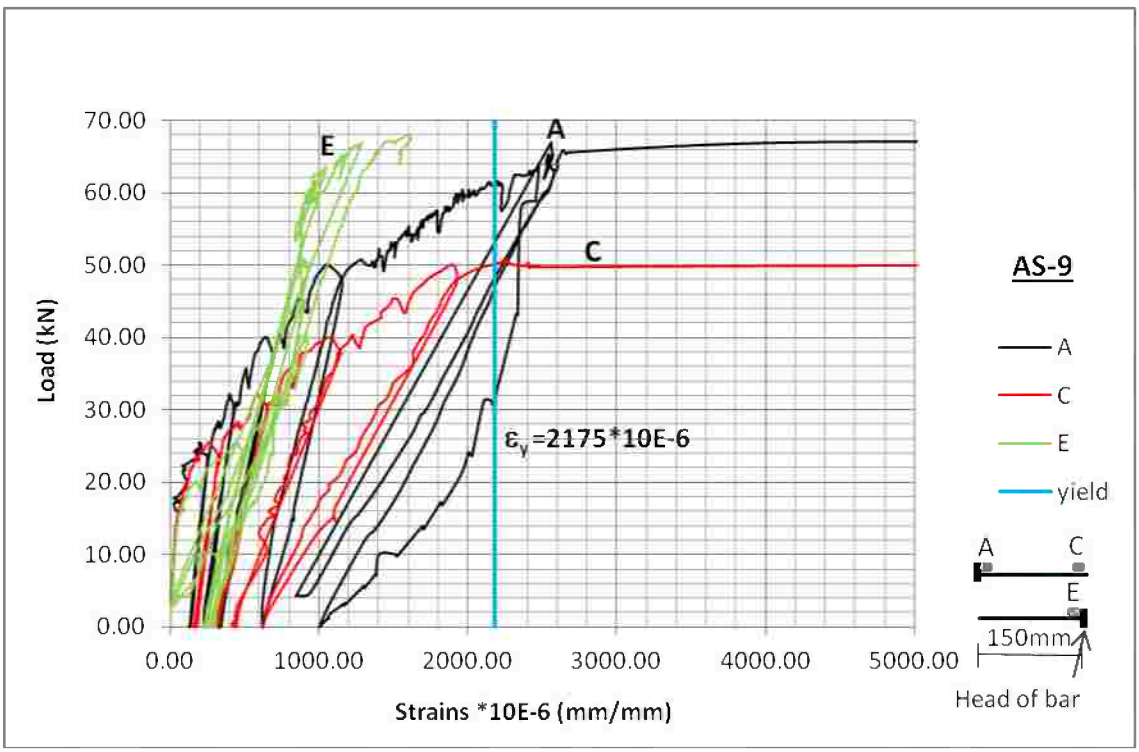

Figure (4-73): Relation between steel strain and load of slab **AS-9** (15 d_b), Group (4).

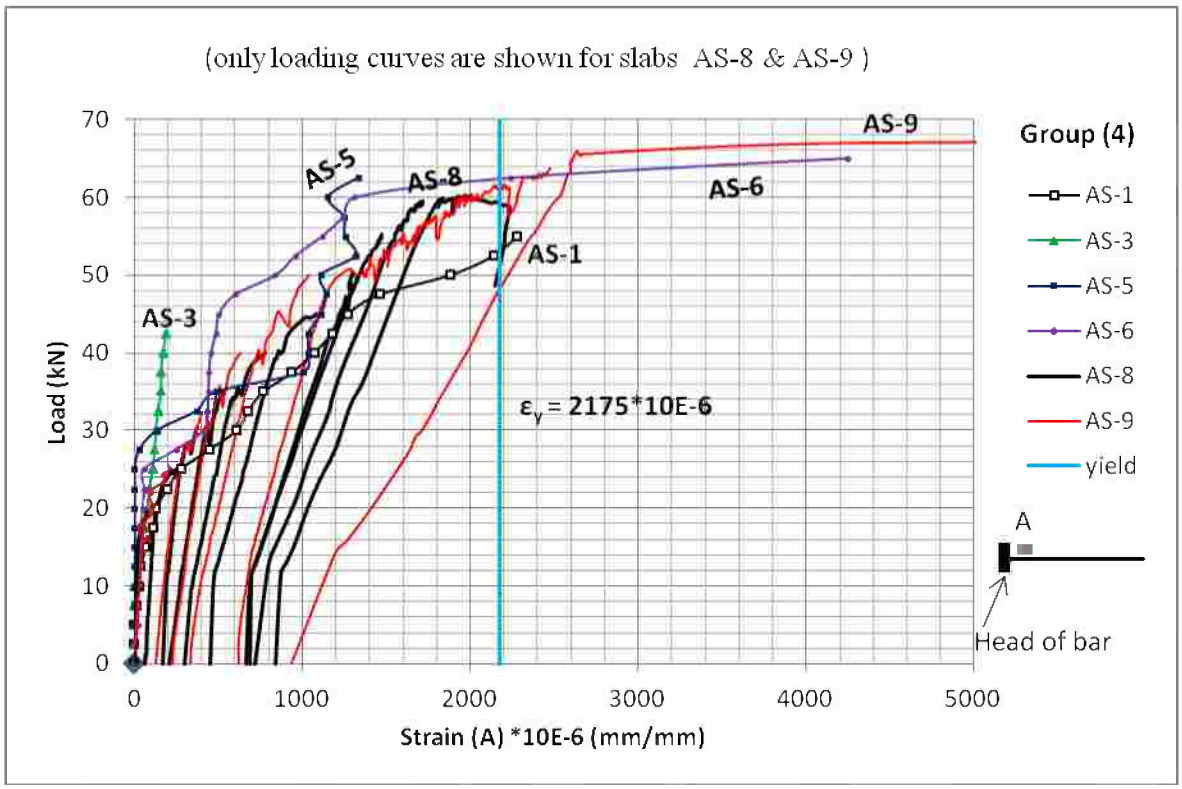

Figure (4-74): Relation between Strain (A) and load for slabs of Group (4).

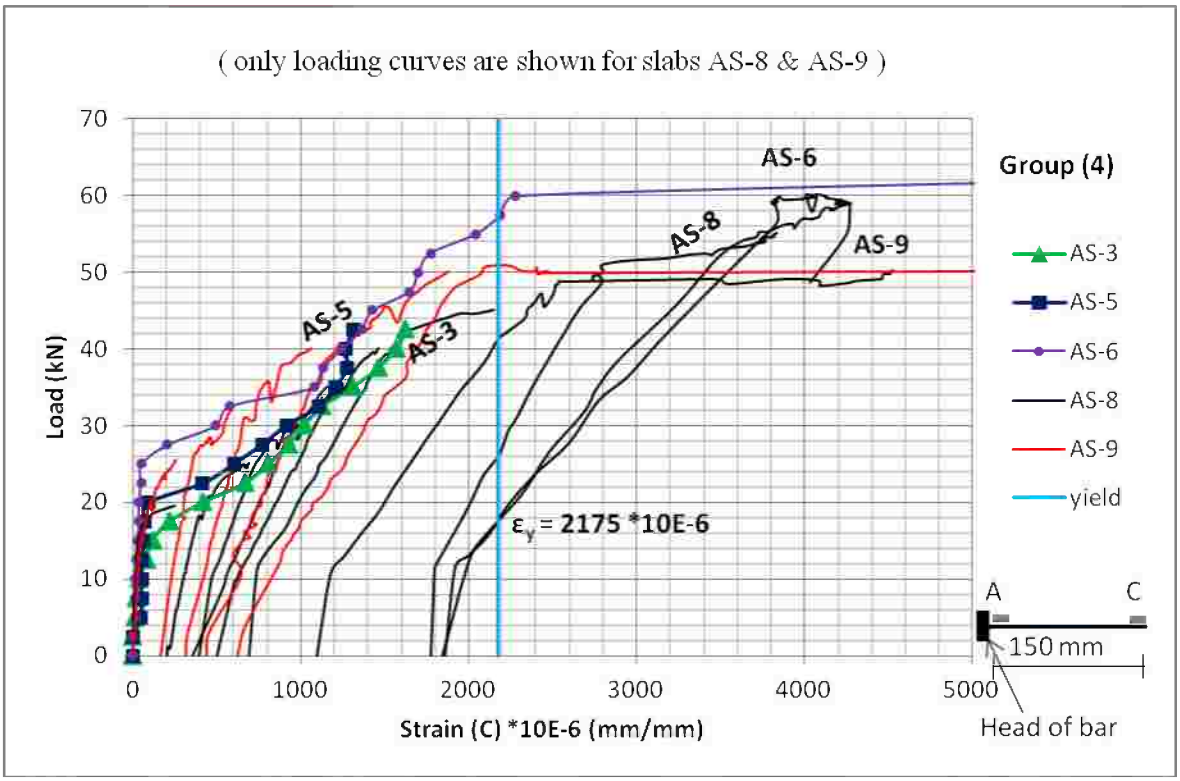

Figure (4-75): Relation between Strain (C) and load for slabs of Group (4).

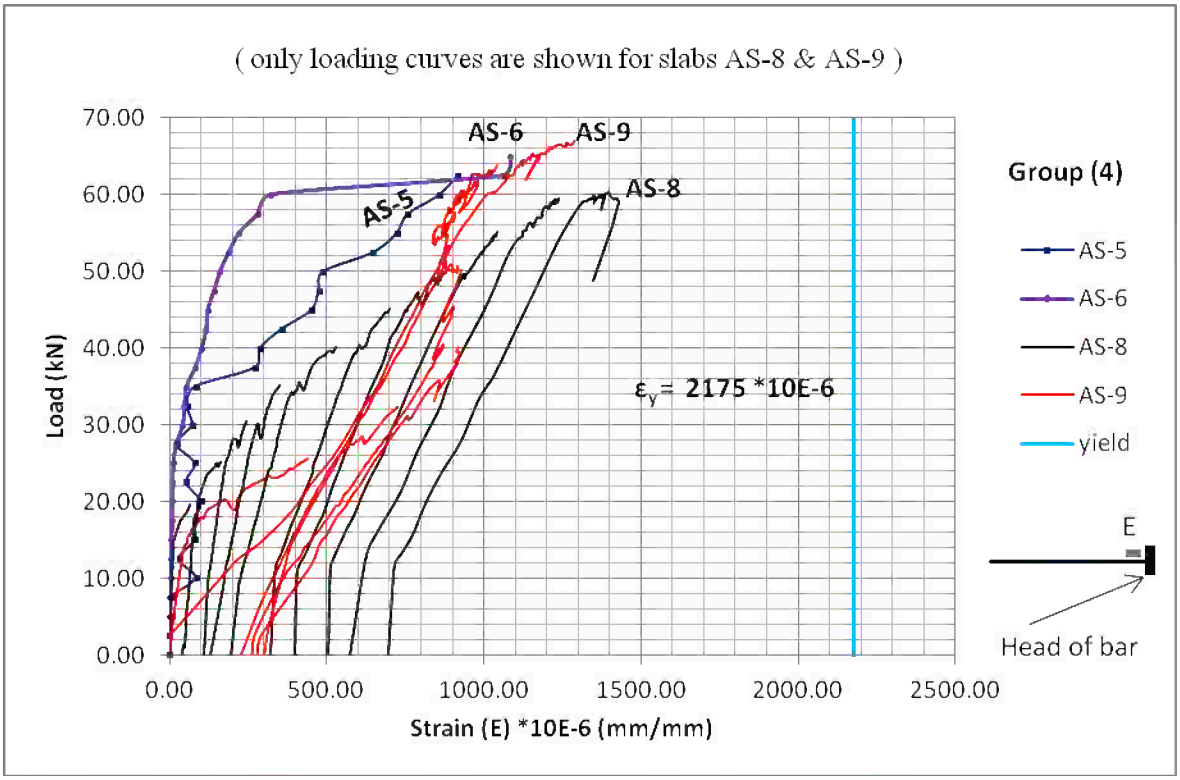

Figure (4-76): Relation between Strain (E) and load for slabs of Group (4).

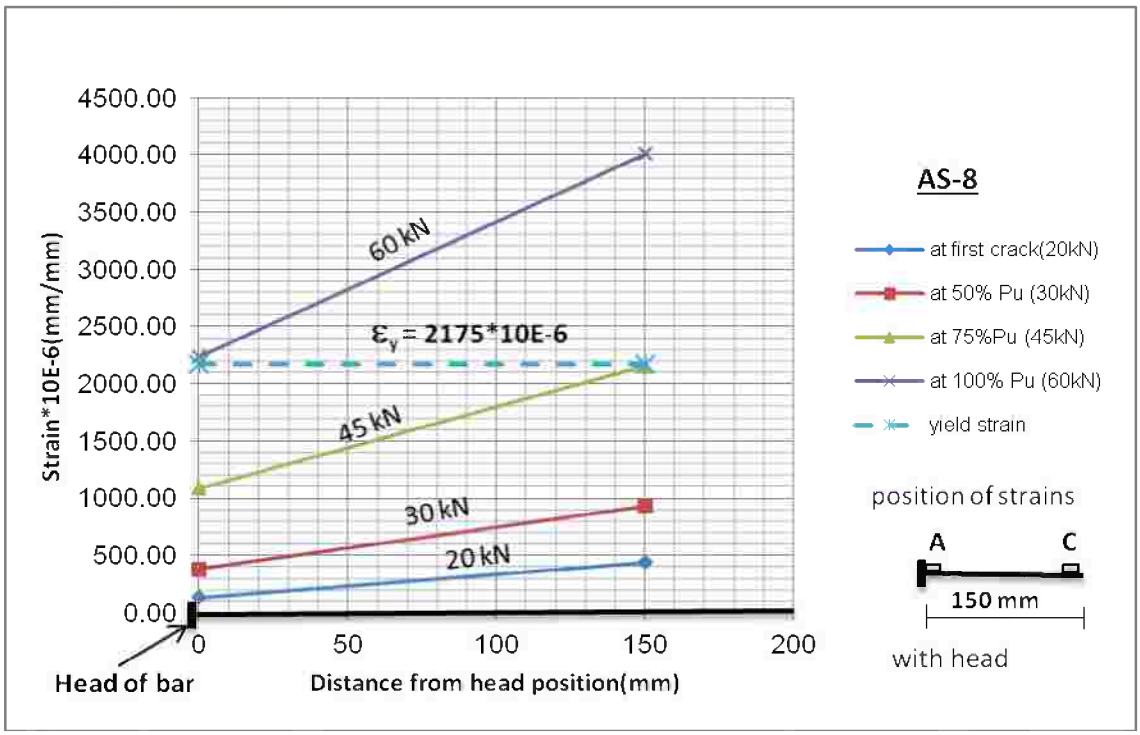

Figure (4-77): Strain distribution along the splice zone of slab **AS-8** at different loads.

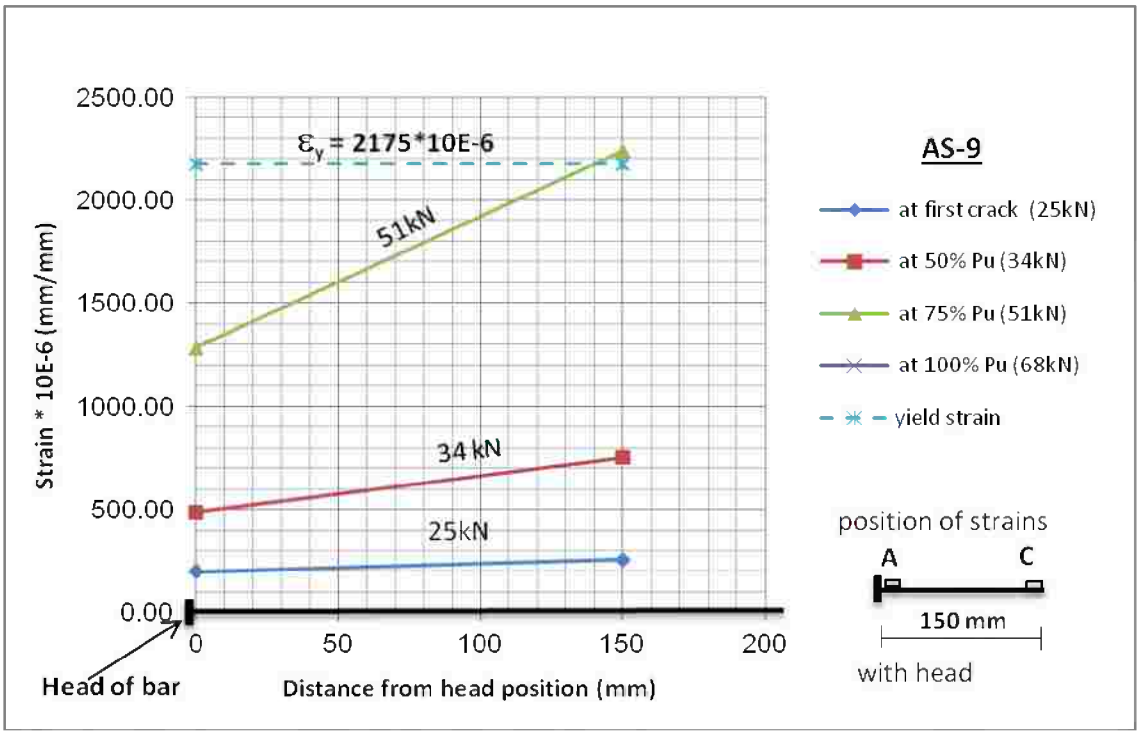

Figure (4-78): Strain distribution along the splice zone of slab **AS-9** at different loads.